

Measurements of Association and Partition Equilibria of n-Alkylbenzenes with Fulvic Acid, Humic Acid, Sodium Dodecylbenzenesulfonate, n-Dodecane, and 1-Octanol in Aqueous Media by Headspace Gas Chromatography

by

Mahmoud Eljack
A Dissertation
Submitted to the
Graduate Faculty
of
George Mason University
in Partial Fulfillment of
The Requirements for the Degree
of
Doctor of Philosophy
Chemistry

Committee:

_____	Dr. Abul Hussam, Dissertation director
_____	Dr. Shahamat U. Khan, Committee Member
_____	Dr. Paul Cooper, Committee Member
_____	Dr. Robert Honeychuck, Committee Member
_____	Dr. Richard Diecchio, Interim Associate Dean for Student and Academic Affairs, College of Science
_____	Dr. Peggy Agouris, Interim Dean, College of Science
Date: _____	Fall Semester 2013 George Mason University Fairfax, VA

Measurements of Association and partition Equilibria of n-Alkylbenzenes with Fulvic Acid, Humic Acid, Sodium Dodecylbenzenesulfonate, n-Dodecane, and 1-Octanol in Aqueous Media by Headspace Gas Chromatography

A Dissertation submitted in partial fulfillment of the requirements for the degree of Doctor of Philosophy at George Mason University

by

Mahmoud Eljack
Master of Science
George Mason University, 2011

Director: Abul Hussam, Professor
Department of Chemistry

Fall Semester 2013
George Mason University
Fairfax, VA



THIS WORK IS LICENSED UNDER A [CREATIVE COMMONS
ATTRIBUTION-NONCOMMERCIAL 3.0 UNPORTED LICENSE](https://creativecommons.org/licenses/by-nc/3.0/).

DEDICATION

This work is dedicated to my grandfather Alshareef Alnoor Alshreef , mother, Zakia Alshareef Alnoor , and father, Daffalah Eljack Almansouri.

أهدي هذه الرسالة حباً وطاعة وبرا إلي

أمي ذكية الشريف النور الشريف محمد الأمين

والذي دفع الله الجاك المنصوري

جدي الشريف النور الشريف محمد الأمين الشريف الخاتم

There is no god but He: that is the witness of Allah His angels and those endued with knowledge, standing firm on justice. There is no god but He, the Exalted in Power, the Wise.

(The holy Quran 3:18)

ACKNOWLEDGEMENTS

I would like to gratefully and sincerely thank Professor Abul Hussam for his guidance, understanding, patience, and most importantly, his friendship during my graduate studies at George Mason University. My sincere and true thanks to my dissertation committee members; Dr. Shahamat U. Khan, Professor Robert Honeychuck, and Professor Paul Cooper for their guidance and support throughout this work. Also, I would like to thank the Chemistry and Biochemistry Department for being a nice family and home. Finally, and most importantly, I would like to thank my fiancée Diala for her tolerance of my busy schedule, encouragement, and support.

TABLE OF CONTENTS

	Page
List of Tables	viii
List of Figures	xi
List of Equations	xiv
Abstract	xvi
INTRODUCTION.....	19
1.1. Introduction	19
1.2. Humic substances and their importance in nature: A Literature survey	19
1.3. Properties of humic and fulvic acids	22
1.4. Origin of humic and fulvic acids.....	25
1.5. Motivation and statement of the problem	26
THEORETICAL SECTION	29
2.1. Introduction	29
2.2. Theory of vapor-liquid equilibria and HSGC	29
2.3. A General theory of association equilibria and HSGC	32
EXPERIMENTAL SECTION	41
3.1. Introduction	41
3.2. Apparatus	41
3.3. A general protocol for HSGC measurement	44
3.4. Chemicals	47
3.5. B-BB stock solution	48
3.6. Surfactant and humic substances stock solution	50
3.7. HSGC sampling procedure	51
3.8. Gas chromatography–mass spectrometry procedure.....	52
STUDY OF ASSOCIATION OF ALKYL BENZENES WITH SDBS, FULVIC ACID, AND HUMIC ACID.....	53
4.1. Surfactant sodium dodecylbenzene sulphonate- n-alkylbenzenes system	53

4.1.1.	Solute-SDBS association constant, K_{11}	55
4.1.2.	Critical micelle concentration (cmc).....	58
4.1.3.	Solute-micelle association constant, K_{n1}	60
4.1.4.	Solute- micelles partition coefficient, K_x	61
4.1.5.	Intra-micellar activity coefficient	63
4.1.6.	Transfer free energies of functional groups	64
4.2.	Fulvic acid- n-alkylbenzene system	65
4.2.1.	Solute-fulvic acid association constant, K_{11}	67
4.2.2.	Critical fulvic acid aggregation concentration (cfc)	70
4.2.3.	Solute-aggregation association constant, K_{n1}	71
4.2.4.	Solute-aggregate partition coefficient, K_x	72
4.2.5.	Intra-aggregate activity coefficient	75
4.2.6.	Transfer free energies of functional groups	77
4.3.	Humic acid-n- alkylbenzene system	78
4.3.1.	Solute-humic acid association constant, K_{11}	80
4.3.2.	Critical humic acid aggregation concentration (<i>chc</i>)	82
4.3.3.	Solute-aggregation association constant, K_{n1}	83
4.3.4.	Solute-aggregate partition coefficient, K_x	85
4.3.5.	Intra-aggregate activity coefficient of n-alkylbenzene in HA	87
4.3.6.	Transfer free energies of functional groups	89
4.4.	Effect of pH on the association of n-alkylbenzenes with FA.....	90
4.4.1.	Solute-fulvic acid association constant, K_{11} : Effect of pH	92
4.4.2.	Critical fulvic acid aggregation concentration (cfc): Effect of pH	93
4.4.3.	Solute-aggregation association constant, K_{n1} , at different pH.....	94
4.4.4.	Effect of pH on solute-aggregate partition coefficient, K_x	95
4.4.5.	Effect of pH on intra-aggregate activity coefficient	97
4.4.6.	Effect of pH on the transfer free energies of functional groups	98
4.4.7.	pH profile during addition of FA	99
4.5.	Effect of temperature on the association of n-alkylbenzenes with FA	101
4.5.1.	Solute-fulvic acid association constant and thermodynamic parameters: Effect of temperature on K_{11}	103
4.5.2.	Critical fulvic acid aggregation concentration (cfc): Effect of temperature	
	105	

4.5.3.	Effect of temperature on solute-aggregation association constant, K_{n1}	106
4.5.4.	Effect of temperature on solute-aggregate partition coefficient, K_x	107
4.5.5.	Effect of temperature on intra-aggregate activity coefficient	108
4.5.6.	Effect of temperature on the transfer free energies of functional groups .	110
APPLICATION OF AQUEOUS SDBS, HA, AND FA TO SOLUBILIZE AND EXTRACT PETROLUEM HYDROCARBONS.....		111
5.1.	Introduction	111
5.2.	Results and Discussion.....	112
5.3.	Solubilization and extraction of gasoline hydrocarbons with aqueous FA.....	121
STUDIES OF LIQUID-LIQUID EXTRACTION BY HSGC		124
6.1.	Principle of liquid-liquid extraction (LLE)	124
6.2.	Theory of liquid-liquid extraction (LLE) with HSGC	125
6.3.	Results and discussion.....	130
6.3.1.	Liquid-liquid extraction, LLE with n-Dodecane (S) –water (W) system .	130
6.3.2.	Liquid-liquid extraction, LLE with 1-Octanol (S) –water (W) system	136
CONCLUSION AND FUTURE OUTLOOK.....		142
APPENDIX		148
REFERENCES		152

LIST OF TABLES

Table	Page
Table 1. Analytical Characteristics of a Haploboroll humic acid and a Spodosol fulvic acid ⁶¹	26
Table 2. Preparation of alkylbenzenes stock standard along with their densities. The activity coefficients are calculated from UNIFAC by using the mole fractions in the mixture.	49
Table 3. Preparation of dilute solution of alkylbenzenes in water. The table shows mole fractions of alkylbenzenes present in the water.	50
Table 4. Table shows peak area ratio for the addition of SDBS in aqueous solution of n-alkylbenzenes at 25.0 ⁰ C. Given the A ⁰ one can calculate A _i for each entry.....	55
Table 5. Values of K ₁₁ from linear least-squares regression of A ⁰ /A _i vs. [SDBS] _t in the pre-micellar region at 25.0 ⁰ C	58
Table 6. Values of K _{n1} from linear least-squares regression of A ⁰ /A _i vs. [SDBS] _t in the post-micellar region at 25.0 ⁰ C.	61
Table 7. Table shows peak area ratio for the addition of FA in aqueous solution of n-alkylbenzenes at pH 5.5 and 25.0 ⁰ C. Given the A ⁰ one can calculate A _i for each entry. 67	67
Table 8. Values of K ₁₁ from linear least-squares regression of A ⁰ / A _i vs. [FA] _t in the pre-aggregation region at 25.0 ⁰ C. Literature K ₁₁ for SDS-solutes are listed in the last column.....	69
Table 9. Values of K _{n1} from linear least-squares regression of A ⁰ / A _i vs. [FA] _t in the post-aggregation region at 25.0 ⁰ °C.....	72
Table 10. Partition coefficients of n-alkylbenzenes in FA compared to other surfactants at 25.0 ⁰ C.....	74
Table 11. Activity coefficients of n-alkylbenzenes in FA compared to synthetic surfactants at 25.0 ⁰ C. The molar volumes, mL/mol, are shown in parenthesis.	76
Table 12. Thermodynamic transfer free energy of n-alkylbenzenes in various surfactants at 25.0 ⁰ C.....	78
Table 13. Table shows peak area ratio for the addition of HA in aqueous solution of n-alkylbenzenes at pH 7.5 and 25.0 ⁰ C. Given the A ⁰ one can calculate A _i for each entry. 79	79
Table 14. Values of K ₁₁ from linear least-squares regression of A ⁰ / A _i vs. [HA] _t in the pre-aggregation region at pH 7.5 and 25.0 ⁰ C. Literature K ₁₁ for SDS-solute, our FA-, and SDBS-solute values are listed in the table. The values for FA, SDBS, and SDS are converted to L/g from L/mol described earlier.	81
Table 15. Values of K _{n1} from linear least-squares regression of A ⁰ / A _i vs. [HA] _t in the post-aggregation region at pH 7.5 and 25.0 ⁰ C. The aggregation number n is also shown	

for the surfactants. The values for FA, SDBS, and SDS are converted to L/g from L/mol.	84
Table 16. Partition coefficients of n-alkylbenzenes in HA compared to other surfactants at 25.0 ⁰ C.....	86
Table 17. Activity coefficient of humic acid compared to other surfactants at pH 7.5 and 25.0 ⁰ C.....	88
Table 18. Thermodynamic transfer free energy of n-alkylbenzenes in various surfactants at pH 7.50 and 25.0 ⁰ C.	90
Table 19. Table shows peak area ratio for the addition of FA in aqueous solution of n- alkylbenzenes at 25.0 ⁰ C and pH 7.6. Given the A ⁰ one can calculate A _i for each entry. 91	
Table 20. Values of K ₁₁ from linear least-squares regression of A ⁰ / A _i vs. [FA] _t in the pre-aggregation region at 25.0 ⁰ C and three different pH values.	93
Table 21. Values of K _{n1} from linear least-squares regression of A ⁰ / A _i vs. [FA] _t in the post-aggregation region at 25.0 ⁰ C and different pH values.	94
Table 22. Partition coefficients of n-alkylbenzenes in FA at 25.0 ⁰ C and different pH values.	96
Table 23. Intra-aggregate activity coefficients of n-alkylbenzene in FA at 25.0 ⁰ C and different pH values.....	98
Table 24. Thermodynamic transfer energy of alkylbenzenes 25.0 ⁰ C and different pH values.	99
Table 25. Table shows peak area ratio for the addition of FA in aqueous solution of n- alkylbenzenes at pH 5.5 and 30.0 ⁰ C. Given the A ⁰ one can calculate A _i for each entry.	102
Table 26. Table shows peak area ratio for the addition of FA in aqueous solution of n- alkylbenzenes at pH 5.5 and 40.0 ⁰ C. Given the A ⁰ one can calculate A _i for each entry.	103
Table 27. The solute-FA association constant, K ₁₁ and the thermodynamic parameters for n-alkylbenzenes-FA system at pH 5.5 and different temperatures. ^a	105
Table 28. Values of K _{n1} from linear least-squares regression of A ⁰ / A _i vs. [FA] _t in the post-aggregation region at pH 5.5 and different temperatures.	106
Table 29. Partition coefficients of n-alkylbenzenes in FA at pH 5.5 and different temperatures.....	107
Table 30. Intra-aggregate activity coefficients of n-alkylbenzene at pH 5.5 and different temperatures.....	109
Table 31. Thermodynamic transfer free energy of n-alkylbenzenes at pH 5.5 and different temperatures.	110
Table 32. Removal efficiency extracted from the sand after sand washing with HA, FA, SDBS and water at different pH and at ambient conditions.	115
Table 33. Table shows peak area ratio for the addition of n-dodecane in aqueous solution of n-alkylbenzenes at 25.0 ⁰ C. The n-dodecane peak area is also shown. Given the A ⁰ one can calculate A _i for each entry.	131
Table 34. Values of K ₁₁ from linear least-squares regression of A ⁰ /A _i vs. [n-dodecane] _t in the pre-phase separation at 25.0 ⁰ C.....	133
Table 35. Partitioning of n-alkylbenzenes in n-dodecane / water at 25.0 ⁰ C.....	135

Table 36. Infinite Dilution Activity Coefficients of n-alkylbenzenes in n-dodecane at 25.0 ⁰ C. UNIFAC activity coefficient calculator by Bruce Choy & Danny Reible, University of Sydney, Australia.....	136
Table 37. Table shows peak area ratio for the addition of 1-octanol in aqueous solution of n-alkylbenzenes at 25.0 ⁰ C. The 1-octanol peak area is also shown. Given the A ⁰ one can calculate A _i for each entry.	138
Table 38. Values of K ₁₁ from linear least-squares regression of A ⁰ /A _i vs. [1-octanol] _t in the pre-aggregation region at 25.0 ⁰ C.	139
Table 39. Partition coefficient for n-alkylbenzene in 1-octanol/ water system at 25.0 ⁰ C.	140
Table 40. Infinite Dilution Activity Coefficients in 1-octanol at 25.0 ⁰ C.....	141
Table 41. Analysis of crude oil from Fula field, Sudan using wellhead sampling	148

LIST OF FIGURES

Figure	Page
Figure 1. Structures of Fulvic acid (a) Buffle's model ⁵⁸ , (b) Khan and Schnitzer's model ⁵⁹ , and humic acid (c) Schulten and Schnitzer's model ⁶⁰	24
Figure 2. Sketch showing the solute (n-butylbenzene) in vapor / liquid equilibrium in a thermostated sample cell. The partial pressure shown is due to the distribution of the solute in vapor phase, which is sampled and measured by the headspace GC as peak area, A_i , proportional to P_i	31
Figure 3. Schematic depiction of association and partitioning process of n-butylbenzene in water- FA aggregate pseudo-phase and its distribution during vapor/ liquid equilibrium. This representation is also true for any hydrophobic solute.....	34
Figure 4. Block diagram of the headspace gas chromatograph. PC, personal computer; IC, interface controller; WB, water bath; GC, gas chromatograph; I, integrator; MS, magnetic stirrer; C, cell; AB, autoburet; HVB, heated valve box (thermostated to 165 0C); CT, cold trap; VP, vacuum pump; L, sampling loop; V_1 , six-port gas sampling valve; V_2 and V_3 sample selection valves	43
Figure 5. Photograph shows the experimental setup of the HSGC. The valves are inside the valve box insulated with fiberglass and aluminum foil. The thermostated sample cell is placed on the magnetic stirrer and the autosyringe next to it.....	45
Figure 6 a. Diagram shows valve positioning, internal plumbing connections and the valve sequence: SEQ1: sample is isolated, the sample and the ballast are under vacuum, and the He is flowing through the sampling valve; SEQ2: the sample cell is opened; the headspace vapor fills the sampling loop and the ballast for 10s. Another 10s was allowed for the vapor to equilibrate inside the tubing and then injected into the GC in SEQ3: the sample cell is disconnected and the injection valve is turned on for 100s for flash transfer of samples into the GC. The two GC integrator are activated at the same time	46
Figure 7. Structure of (a). Sodium dodecyl sulfate (SDS), and (b). Sodium dodecylbenzene sulfonates (SDBS).....	54
Figure 8. Proposed low energy interactions between benzene rings of SDBS and n-butylbenzene.	57
Figure 9. (a) Peak area ratio A^0 / A_i vs. $[SDBS]_t$ for alkylbenzenes(benzene, toluene, ethylbenzene, n-propylbenzene and n-butylbenzene) at 25.0 ⁰ C. (b) Figure shows the intersection of two lines outlined in the theory section. Typical experimental errors are shown for ethylbenzene and the straight line. The error bars indicate larger error at lower vapor phase concentration.....	57
Figure 10. Sketch shows the water surface is covered by SDBS surfactants at low concentration of SDBS. As the concentration of SDBS starts to increase, the surfactant	

aggregates into micelles. The partitioning of n-butylbenzene in SDBS micelles (pseudophase) is shown.	59
Figure 11. Effect of total SDBS concentration on water-micelles partition coefficient of n-alkylbenzenes at 25.0 ⁰ C.....	62
Figure 12. Effect of total SDBS concentration on intra-micellar activity coefficients of n-alkylbenzenes at 25.0 ⁰ C.....	64
Figure 13. Changes in peak areas as the concentration of FA increases at 25.0 ⁰ C.	66
Figure 14. (a) Peak area ratio A^0/A_i vs. $[FA]_t$ for n-alkylbenzenes 25.0 ⁰ C. (b) Figure shows the intersection of two lines outlined in the theory section. Typical experimental errors are shown for ethylbenzene and the straight line. The error bars indicate larger error at lower vapor phase concentration.....	69
Figure 15. Effect of total FA concentration on water-aggregate pseudophase partition coefficient of n-alkylbenzene at 25.0 ⁰ C.....	74
Figure 16. Effect of total FA concentration on intra-aggregate activity coefficients of n-alkylbenzene at 25.0 ⁰ C.....	77
Figure 17. (a) Peak area ratio A^0/A_i vs. $[HA]_t$ for n-alkylbenzenes at 25.0 ⁰ C. (b) Figure shows the intersection of two lines outlined in the theory section. Typical experimental errors are shown for benzene and the straight line. The error bars indicate larger error at lower vapor phase concentration.	81
Figure 18. Effect of total HA concentration on water-aggregate pseudo-phase partition coefficient of n-alkylbenzene at pH 7.5 and 25.0 ⁰ C.....	86
Figure 19. Effect of total HA concentration on intra-aggregate activity coefficients of n-alkylbenzene at pH 7.5 and 25.0 ⁰ C.....	89
Figure 20. Peak area ratio A^0/A_i vs. $[FA]_t$ for n-alkylbenzenes at 25.0 ⁰ C and pH (a) 5.5 (b) 7.6.....	93
Figure 21. Proposed microenvironment of n-alkylbenzenes in the pseudo-phase of FA aggregate. It shows the inner core is of aromatic nature and the outer layer H-bonded carboxylic groups.....	96
Figure 22. Effect of total FA concentration on water-aggregate pseudo-phase partition coefficient of n-alkylbenzene at 25.0 ⁰ C and pH (a) 5.5 and (b) 7.6.	97
Figure 23. Effect of total FA concentration on intra-aggregate activity coefficients of n-alkylbenzene at 25.0 ⁰ C and pH (a) 5.5 and (b) 7.6.....	98
Figure 24. Figures show pH change during addition of FA stock solution at 25.0 ⁰ C and initial pH of (a) 2.35 and (b) 11.92.	101
Figure 25. Peak area ratio A_o/A_i vs. $[FA]_t$ for n-alkylbenzenes at pH 5.5 and (a) 30.0 C and (b) 40.0 C.	104
Figure 26. Effect of total FA concentration on water-aggregate pseudo-phase partition coefficient of n-alkylbenzenes at pH 5.5 and (a) 30.0 ⁰ C (b) 40.0 ⁰ C.....	108
Figure 27. Effect of total FA concentration on intra-aggregate activity coefficients of n-alkylbenzene at pH 5.5 and (a) 30.0 ⁰ C and (b) 40.0 ⁰ C.....	109
Figure 28. GC–MS of diesel fuel extracted from contaminated sand. Top: total ion chromatogram of diesel fuel and mass spectrum of hexadecane, m/e 226 (bottom). It shows the peaks caused by n-alkanes consecutively marked as 1-12 for C ₁₀ - C ₂₂ with carbon increments. (a) the control without FA and (b) after washing with FA at pH 11.9.	

The typical peak area was about 15 times smaller than the control showing extraction capability of FA.	112
Figure 29. Percent retention of diesel hydrocarbons using fulvic acid at different pH and 22.0 ⁰ C.....	115
Figure 30. Removal efficiency of diesel hydrocarbons using humic acid at different pH values and 22.0 ⁰ C.....	116
Figure 31. Removal efficiency of diesel hydrocarbons using fulvic acid, humic acid, SDBS and water at 22.0 ⁰ C.....	117
Figure 32. Picture shows water (control) did not solubilize the crude oil, SDBS showed some solubility, FA and the mixture (FA/HA) show moderate solubility, and HA showed the highest solubility. Clearly, crude oil is very stable and hard to solubilize using high concentration of conventional surfactants.	119
Figure 33. Picture shows FA color change with changing pH. The color becomes darker with decreasing pH.	120
Figure 34. Changes in the UV-VIS spectra of aqueous FA solutions in the pH interval 2.4 - 11.92. The samples were darker at lower pH and lighter in color at higher pH correlates with relative magnitude of the absorbance.	121
Figure 35. A typical HSGC experiment run shows peaks for gasoline (Shell 87) in (a) absence and in (b) presence of 13.9 μ M FA. HSGC was recorded for 24 addition of 0.534 μ M FA each.	123
Figure 36. A plot of percent solubilization of (a) <i>o</i> -xylene, <i>p</i> -xylene, isopropylbenzene, and <i>p</i> -ethyltoluene and (b) B, T, and EB in FA and. About 35-60% of the compounds are extracted in FA as 1:1 or n:1 complex at 25.0 ⁰ C.	123
Figure 37. Peak area ratio as a function of n-dodecane/water phase ratio at 25.0 ⁰ C.....	133
Figure 38. Peak area ratio as a function of 1-octanol /water phase ratio at 25.0 ⁰ C.	139
Figure 39. Matrix-assisted laser desorption/ionization time-of-flight mass spectrometry, MALDI-TOF-MS. The following spectra are taken for HA sample used in this work..	149

LIST OF EQUATIONS

Equation	Page
$\mu_{i,L} = \mu_{i,G}$	1..... 30
$\mu_{i,L} = \mu_{i,L}^0 + RT \ln (\gamma_{i,L} \chi_{i,L})$	2..... 30
$\mu_{i,G} = \mu_{i,G}^0 + RT \ln (\gamma_{i,G} \chi_{i,G})$	3..... 30
$\mu_{i,G}^0 = \mu_{i,L}^0$	4..... 31
$\gamma_{i,G} \chi_{i,G} = \gamma_{i,L} \chi_{i,L}$	5..... 31
$\gamma_{i,L}^\infty = (p_i / p^0) (1 / \chi_{i,L})$	6..... 31
$A_i = R^* p_i$	7..... 32
$A^0 = R^* p^0$	8..... 32
$\gamma_{i,L}^\infty = (A_i / A^0) (1 / \chi_{i,L})$	9..... 32
$FA + B \leftrightarrow FA-B \quad K_{11} = [FA-B] / [FA] [B]$	10..... 33
$FA_n + B \leftrightarrow FA_n-B \quad K_{n1} = [FA_n-B] / [FA_n][B]$	11..... 33
$FA_n = [FA_t-cfc] / n$	12..... 33
$B_t = [B] + K_{11}[FA][B] + (K_{n1}/n) [FA_t-cfc][B]$	13..... 34
$A_i = R_i [B]_g$	14..... 35
$K_w = [B]/[B]_g$	15..... 35
$[B] = (K_w/R_i)A_i$	16..... 35
$A^0/A_i = 1 + K_{11}[FA] + (K_{n1}/n)[FA_t-cfc]$	17..... 36
$F_w = A_i / A^0$	18..... 37
$F_m = 1 - F_w$	19..... 37
$X_w = F_w t / 55.555$	20..... 37
$X_m = F_m t / [(FA_t-cfc) + F_m t]$	21..... 38
$K_x = \chi_m / \chi_w = 55.555 F_m / [F_w (FA_t-cfc)]$	22..... 38
$K_c = K_x (M_w / M_m)$	23..... 38
$\chi_m \gamma_m = \chi_w \gamma_w$	24..... 39
$\gamma_m = \gamma_w / K_x$	25..... 39
$(n_w + n_v)_0 = n_w + n_s + n_v$	26..... 126
$K_{wv} = (n_w / n_v)_0 = n_w / n_v$	27..... 126
$(n_{v0}/n_v) + K_{wv} = 1 + K_{wv} + n_s/n_v$	28..... 126
$A^0 / A_i = (1 + n_s / n_v)$	29..... 126
$n_s/n_v = C_s^* V_s / C_v^* V_v = K_{sv} (V_s / V_v)$	30..... 127
$A^0 / A_i = (1 + K_{sv} (V_s / V_v))$	31..... 127
$A^0 / A_i = 1 + K_{sw} (V_s / V_w)$	32..... 127
$S + B \rightarrow SB \quad K_{11} = [SB] / ([S]^* [B])$	33..... 127
$K_{wv} = (B / B_v)_0 = B / B_v$	34..... 127
$B_o = B + SB$	35..... 128

$B_{vo} * K_{wv} = (K_{wv} + K_{11} * S * K_{wv}) B_v$	36	128
$A^0 / A_i = 1 + S K_{11}$	37	128
$X_s \gamma_s = X_w \gamma_w$	38	129
$\gamma_s = \gamma_w / K_x$	39	129

ABSTRACT

MEASUREMENTS OF ASSOCIATION AND PARTITION EQUILIBRIA OF N-ALKYLBENZENES WITH FULVIC ACID, HUMIC ACID, SODIUM DODECYLBENZENESULFONATE, N-DODECANE, AND 1-OCTANOL IN AQUEOUS MEDIA BY HEADSPACE GAS CHROMATOGRAPHY

Mahmoud Eljack, PhD

George Mason University, 2013

Dissertation Director: Dr. Abul Hussam

Natural organic matter (NOM) such as humic acids (HA), fulvic acids (FA), and humin in soils and sediments plays an important role in partitioning, binding, and transport of organics and metal ions in nature. We have developed an equilibrium headspace gas chromatographic (HSGC) technique and the theory to study the association and partitioning of n-alkylbenzenes (benzene, toluene, ethylbenzene, n-propylbenzene, and n-butylbenzene) with aqueous FA, HA, and sodium dodecylbenzenesulfonate (SDBS). The alkylbenzenes were chosen because they are the major constituents of gasoline and also toxic to human health and the environment. The precise measurement of n-alkylbenzenes in the vapor phase in equilibrium with the liquid phase allowed determination of solute - monomer surfactant (S), association constants (K_{11}), solute- aggregate, S_n , association constant (K_{n1}), critical aggregation constants for

FA, HA, and SDBS. It also allowed measurements of the mole fraction based partition coefficients (K_x), infinite dilution activity coefficients of solute inside the aggregate pseudo-phase (γ_m), and the transfer free energies of alkyl chain $-CH_2-$ and benzene from aqueous to aggregate pseudo-phase. Theory shows that the parameters can be calculated without the concentration of the solute. All measurements were made at infinite dilution ($<10^{-6}$ mole fraction) where solute-solute interactions are nonexistent. Almost no such studies could be found in the literature and, therefore, constitute a fundamental contribution in this field.

This study shows that there is strong binding and partitioning of n-alkylbenzenes with FA and HA present as single molecule or as aggregates. We show that FA and HA forms aggregates containing hydrophobic pseudo-phase at 4- 8 μ M concentrations. Both K_{11} and K_{n1} values were of the order of at least 10^5 M^{-1} and 2-3 orders of magnitude higher than that of synthetic surfactants. The pseudo-phase partition coefficient, K_x values are also of the order of 10^7 . The n-alkylbenzenes in FA pseudo-phase shows the lowest γ_m (0.0001) among the three systems studied and one of the lowest known values. Most importantly, the transfer free energy of partitioning of a $-CH_2-$ group -155 cal/mol compared to that of benzene, -9722 cal/mol, indicates that the aggregate pseudo-phase is polarizable benzene-like and less n-alkane aliphatic-like. This is also true for HA and SDBS, but not for SDS. The high solubilization efficiencies of FA and HA for hydrocarbons was used to extract 30-60% of hydrocarbons from diesel contaminated sand. Also, FA was used to study the solubilization efficiency of aromatic hydrocarbons from gasoline contaminated water. Finally, the theory of association equilibria was

successfully applied to liquid-liquid extraction of n-alkylbenzenes from water into n-dodecane and 1-octanol. This experiment allowed pre-extraction and post-extraction calculation of molecular association constant, K_{11} , and critical phase ratio (cpr) for extraction, solute partition coefficient, K_x (organic/ water), and infinite dilution activity coefficient of solute in organic phase, γ_s .

INTRODUCTION

1.1. Introduction

This work involves primarily the study of solubilization and association equilibria of hydrocarbons in natural and synthetic surfactants by headspace gas chromatography (HSGC). While the synthetic surfactants are well understood and studied by many instrumental techniques the natural surfactants such as humic materials are not so at concentrations where solute-solute interactions are negligible. The novel methodology, HSGC, used in this study were compared and validated with synthetic surfactants. Here, we review the nature of humic materials as described in the literature with special reference for the study in question.

1.2. Humic substances and their importance in nature: A Literature survey

Natural organic matter (NOM) in soils and sediments plays an important role in transportation of substances between soil and water¹. NOM consists of both humic and non-humic fractions. The non-humic substances include carbohydrates, proteins, peptides, amino acids, low molecular weight organic acids, wax and others. The humic fraction includes humic acids (HA), fulvic acids (FA), and humin which are the major fraction of dissolved organic matters (DOMs) in water. They are natural amphiphilic molecules with hydrophilic part composed of ionic and nonionic domains while the

hydrophobic part is made of aliphatic and aromatic rings^{2,3,4,5}. The importance of NOM comes from their ability to complex metal ions to form covalent bonds and coordination complexes⁶ with organic molecules for their transport in the environment. DOMs have been used to enhance hydrophobic organic compounds' (HOCs) solubility in remediation of contaminated soils and found to exhibit surfactant properties^{7,8}.

These studies are preliminary and there are still some disputes in the literatures in their abilities to form micelles⁹. It was reported that humic substances form aggregates consists of approximately 20 molecules¹⁰. A proposed polymer like model of DOMs consist of coil at high concentration, high ionic strength, and low acidity, but uncoiled taking extended shapes in low ionic strength or basic solutions. But the idea "polymer model" has shown to be not true by later studies using nuclear magnetic resonance (NMR), electron spin resonance (ESR), and transmission electron microscopy^{11, 12, 13, 14}. HA solutions containing the herbicide atrazine labeled with ¹⁹F were studied by Chien *et al*¹⁵ using the paramagnetic relaxation of the ¹⁹F NMR signal in which they were able to determine the hydrophobic domain of humic substances, and this finding was in line with a proposed micellar structure. Another study by Simpson *et al* using high-resolution magic angle spinning (HR-MAS) NMR solution-state spectra of a soil sample containing partial water soluble humic materials confirmed the presence of hydrophobic region¹². Dissolved organic matter (DOM) studies by transmission electron microscopy revealed the formation of 400-800 nm micelle-like colloids¹³. Wandruszka *et al* and Simpson *et al* showed that DOMs form micelle-like clusters connected via H-bonds and hydrophobic interactions^{14,16}. Traditionally, research on DOMs (specifically humic and fulvic acids)

were studied for the complexation of Zn^{2+} , Fe^{2+} , Mn^{2+} , and Cu^{2+} because they bind to the acidic group of the DOM and the speciation of some of the toxic metal species are controlled by the presence of DOM in the aquatic environment ¹⁷. Also studied were the non-polar molecules such as polycyclic aromatic hydrocarbons (PAHs) or polychlorinated biphenyls (PCBs) for their solubilization and consequent transport in nature ¹⁸.

The presence of dissolved organic matter (DOM) in water, particularly fulvic acids (FAs) and humic acids (HAs), increases the solubility ^{19,20}, bioavailability ^{21, 22}, environmental fate and transport process ^{23,24} of aromatic hydrophobic organic compounds by the virtue of non-covalent interactions with these HOCs. These noncovalent interactions were shown to be significant as shown by studying the effect of DOM on HOC adsorption to activated carbon ^{25, 26, 27, 28, 29}. Mixing HOC, activated carbons and dissolved FA and HA resulted in lowered removal efficiency of HOC by activated carbon due to the competition between activated carbon and HA and FA for HOC,s ^{25, 26, 27, 28, 29}.

There are mixed results regarding the effect of dissolved HA and FA on the bioavailability of HOCs. The rate of the bioavailability and biodegradation of chlorobenzuron, diazinon, ³⁰ and benzo[a]- pyrene ³¹ were slowed by the presence of dissolved HA and FA. Also, the same effect or no effect were observed in the biodegradation rate of dichloro-diphenyl-trichloroethane, DDT in the presence of HA and FA respectively³². On the other hand, great biodegradation of PCB was observed in the presence of dissolved soil HA, and the conclusion was that dissolved humic acids

increase HOC solubility³³. There were many attempts to study the association constants of HOC–DOM interactions, and the results varied and failed to be correlated to K_{ow} and the structures of FA and HA^{34, 35, 36,37, 38, 39, 40}. This is because the mechanism of noncovalent interactions between HOC and dissolved DOM is not fully understood. Some studies explained this mechanism as sorption,⁴¹ others involving fluorescence measurements thought of it as entrapment of HOC in a pocket formed by HA^{42, 43, 44, 45}. Recent studies using static and time-resolved fluorescence quenching studies^{46,47,48, 49, 50, 51} and NMR^{52, 53} proposed that dissolved humic substances, namely FA and HA, form micelle-like domains of these monomers connected together via H-bonding, π - π interactions and polar-nonpolar interactions.

The amphiphilicity of humic substances gives them a surface active character related to the water solubility enhancement of hydrophobic organic pollutants⁵⁴. It was shown that HSs possess micelle-like aggregates at a specific concentration causing a great increase of the water solubility of PAHs^{55, 56}. Chiou *et al* showed the water solubility of pesticides has increased by the presence of humic substances, HSs⁵⁷.

1.3. Properties of humic and fulvic acids

We focused this work on fulvic acid more than humic acid, because of the lack of such studies in the literature for FA. The choice of FA is prompted by its purity and proven chemical structure as shown in **Figure 1**. The structure of fulvic acid (Buffle's model) shown in **Figure 1a** is the simplest structure of fulvic acid⁵⁸. It shows that fulvic acid consists of naphthalene rings substituted with carboxyl, hydroxyl, and short aliphatic

chains containing alcohol, methyl, carboxyl and carbonyl groups. **Figure 1b** shows the structure of fulvic acids that consists of benzene carboxylic acids and phenolic H- bonded together forming a very stable aggregate as proposed by Schnitzer and Khan⁵⁹.

The fulvic acids are light yellow to yellow-brown in color. Fulvic acids contain more functional groups of an acidic nature, particularly -COOH than the rest of humic substances. The total acidities of fulvic acid in general are 900 - 1400 meq/100g depending on the origin, but the one we are using has one of 1030 meq/100g. They are that fraction of humic substances that is soluble in water under all pH conditions. They remain in solution after removal of humic acid by acidification. Humic acid is more complicated showing different bonding structures and functional groups ranging from salicylic, phthalate, to many nitrogen containing groups as proposed by Schulten and Schnitzer⁶⁰. This model was based on several physical and chemical studies involving electron microscopy, X-rays analysis, viscosity measurements.

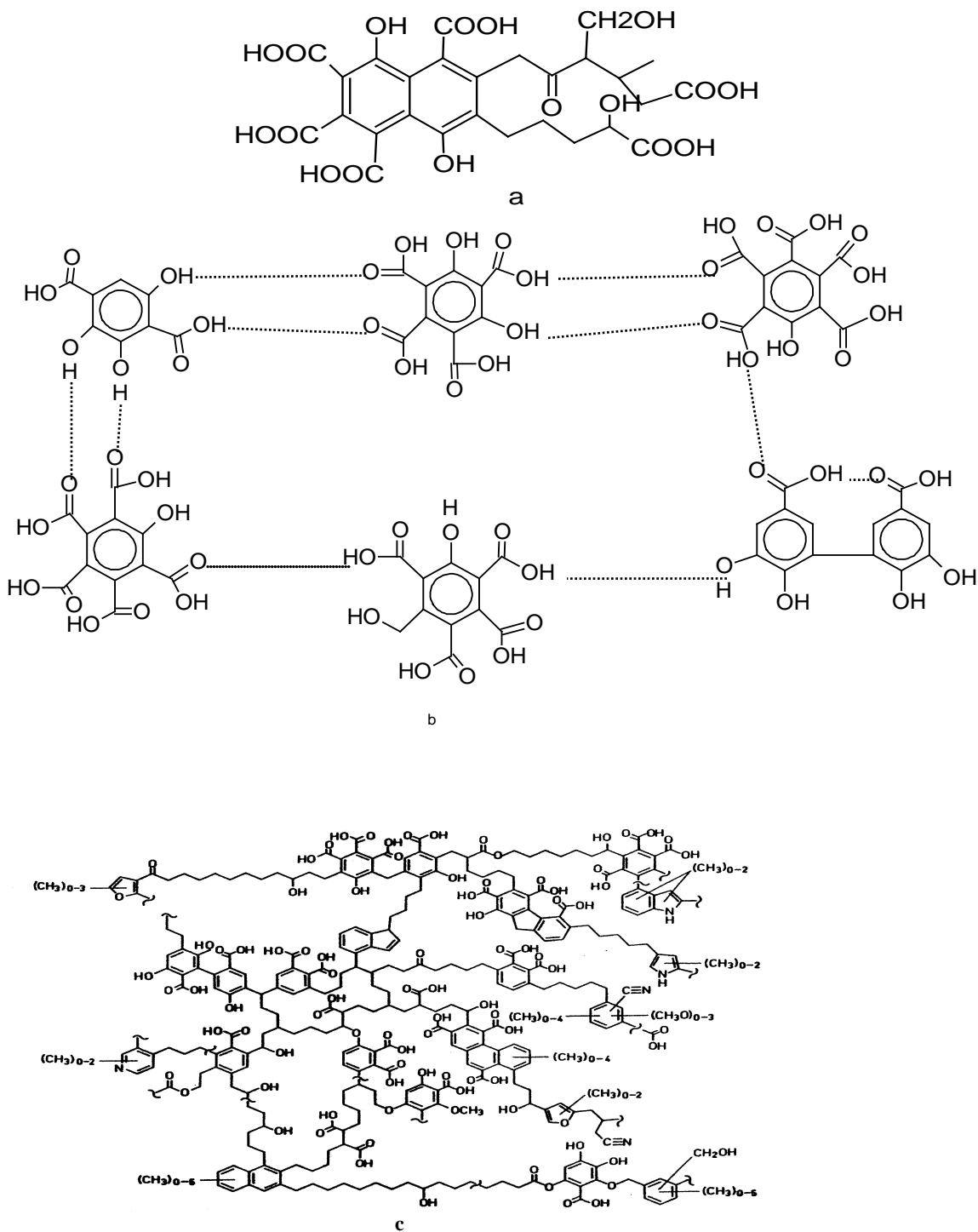


Figure 1. Structures of Fulvic acid (a) Buffle's model⁵⁸, (b) Khan and Schnitzer's model⁵⁹, and humic acid (c) Schulten and Schnitzer's model⁶⁰.

1.4. Origin of humic and fulvic acids

The humic acid and fulvic acid chosen for this study were extracted from A horizon of Haploboroll and Bh horizon of a Spodosol. **Table 1** shows a detailed analysis for these humic substances which show that humic acids contain more C, but less O than fulvic acids; that both humic acids and fulvic acids might contain N, O, and S and their contents of these elements are approximately similar, that total acidity and CO₂H content of fulvic acids are much higher than those of the humic acids; both contain phenolic -OH, total -C=O, and -OCH₃ groups, but humic acids lack alcoholic -OH compared to fulvic acids.

The E₄/E₆ ratio of humic acids is almost half as low as that of fulvic acids which means that humic acids are much larger molecular weight than fulvic acids^{61, 62}. The E₄/E₆ ratio is an indication of the molecular size⁶³ and is used also to characterize HA and FA. The E₄/E₆ ratio is an index of light absorption in the visible range. If E₄/E₆ ratio is high that means the molecule has a relatively low molecular weight, and if it is low then it has a relatively high molecular weight. Fulvic and humic acid have a wide range of molecular weights and sizes, ranging from a couple of hundred to as much as several hundred thousand atomic mass units. In general, FA are lower molecular weight than HA, and soil-derived materials are larger than aquatic materials. For example the molecular weights of aquatic fulvic acids range from 200 to 2000⁶⁴.

Table 1. Analytical Characteristics of a Haploboroll humic acid and a Spodosol fulvic acid ⁶¹.

	Humic acid	Fulvic acid
	Elements (g kg ⁻¹)	
C	564	509
H	55	33
N	41	7
S	11	3
O	329	448
	Functional groups (cmol kg ⁻¹)	
Total acidity	660	1240
COOH	450	910
Phenolic OH	210	330
Alcoholic OH	280	360
Quinonoid C=O	250	60
Ketonic C=O	190	250
OCH ₃	30	10
E ₄ /E ₆	4.3	7.1

1.5. Motivation and statement of the problem

There are two main underlying questions that this work raises: how efficiently do humic substances solubilize various organic pollutants and how differently might they contribute to the environment compared to synthetic ones? To answer these questions requires accurate binding and association equilibrium constants between a solute and the humic substance in a thermodynamic sense. Very little work has been reported on this aspect as described in the above section. The importance of this work lies in the fact that natural surfactants generally exhibit greater environmental compatibility, better surface activity, lower toxicity, and higher biodegradability than synthetic surfactants. Therefore,

natural surfactants have greater advantages for using in the remediation of soils and subsurface environments contaminated with alkylbenzenes, PCB, PAH, etc.

First, we find no studies reported on the association of humics with small nonpolar molecules such as n-alkylbenzenes at low concentrations (environmentally relevant) to the extent that a meaningful binding and partitioning information could be obtained, even though alkylbenzenes are the major constituents of gasoline and also very toxic to the environment. Second, we find almost no binding constants for these small molecules. Third, there is no reliable aggregation number or critical aggregation constants at low DOM concentrations available. These were due to the insensitivity of most spectrometric techniques to discern small changes in the signal from the weak interactions between molecule and the DOM. It is, therefore, obvious that if one can get such information with small n-alkylbenzenes such as molecules with FA over a range of FA concentrations, one could test some of the findings in the literature on perceived structure and association equilibria. Here, we show that a very precise HSGC technique can be used to measure the activity change of alkylbenzene due to its interactions with FA. No such studies have been reported in the literature. Change in vapor pressure measurements can be used to directly calculate the transfer energies, enthalpies and entropies due to molecular association^{65, 66, 67}. With small volatile molecules containing functional groups, one can calculate the transfer free energies of functional groups, which can be used to estimate free energies for large organic molecules⁶⁸ by the principle of linear free energies of functional groups. Here, we plan, for the first time, the use of a very precise HSGC technique to measure the activity change due to the interactions of

benzene homologs with fulvic and humic acids. The technique was extensively used earlier to study solubilization of small molecules in micelles and microemulsions^{69, 70, 71}. We have chosen fulvic over humic acids as the dominant NOM and its availability in purest form. These NOMs are extremely well characterized by a host of other techniques⁶¹. Also, one of the reasons we chose FAs is the fact that FAs have not been studied as much as humic acids, particularly, with hydrophobic compounds. Most studies which involved FAs were limited to FAs association with cationic species.

THEORETICAL SECTION

2.1. Introduction

In this section we discuss the basic principles of vapor-liquid equilibria and the application of HSGC to obtain reliable thermodynamic information. The basic principles were describe elsewhere⁷². However, the HSGC technique we used here is known as the equilibrium HSGC, because the gas sampling process does not perturb the vapor-liquid equilibria⁷³.

2.2. Theory of vapor-liquid equilibria and HSGC

The basis of HSGC is the sampling of the vapor in equilibrium with liquid in a reproducible manner. The presence of solute and its concentration is determined by the gas chromatography equipped with a suitable detector such as flame ionization detector (FID). The signal from the detector (peak area) allows the determination of several physicochemical properties of liquid- vapor phase distribution systems such as activity, activity coefficient, and partition coefficient. Here, we describe the basic thermodynamics from which such information is obtained. For a solute, *i* in a vapor-liquid equilibrium, as shown in **Figure 2**, the chemical potential of solute, *i* is given by:

$$\mu_{i,L} = \mu_{i,G} \quad 1$$

$$\mu_{i,L} = \mu_{i,L}^0 + RT \ln (\gamma_{i,L} \chi_{i,L}) \quad 2$$

$$\mu_{i,G} = \mu_{i,G}^0 + RT \ln (\gamma_{i,G} \chi_{i,G}) \quad 3$$

Where μ_i the chemical potential of I in the mixture is, μ^0 is the chemical potential of i in the pure state, γ_i is the activity coefficient, and χ_i mole fraction in the solution. The subscripts G and L represent the vapor, G and liquid, L phases.

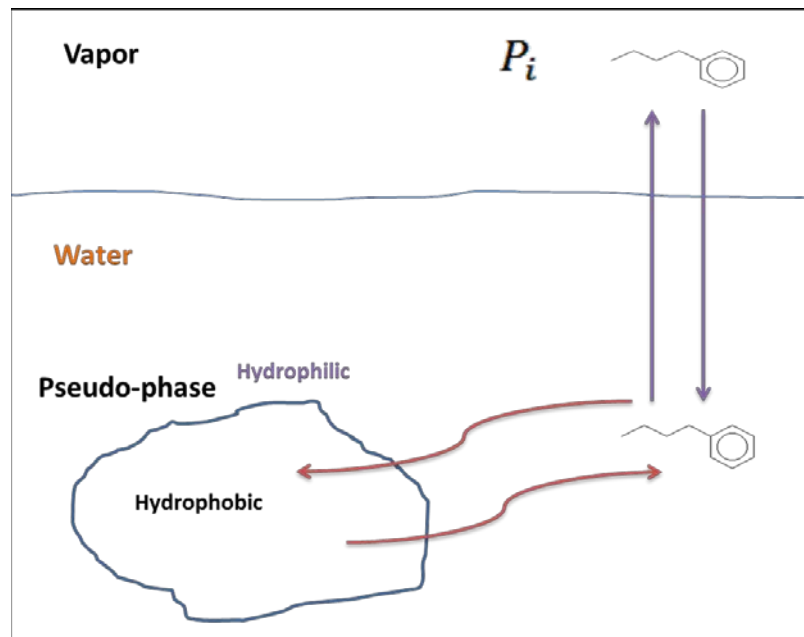


Figure 2. Sketch showing the solute (n-butylbenzene) in vapor / liquid equilibrium in a thermostated sample cell. The partial pressure shown is due to the distribution of the solute in vapor phase, which is sampled and measured by the headspace GC as peak area, A_i , proportional to P_i .

And for pure phase

$$\mu_{i,G}^0 = \mu_{i,L}^0 \quad 4$$

And that gives

$$\gamma_{i,G} \chi_{i,G} = \gamma_{i,L} \gamma_{i,L} \quad 5$$

In our work, the solute (benzene, toluene, ethylbenzene, n-propylbenzene, and n-butylbenzene) is more volatile than the solvent (water). However, the solution is very dilute and the vapor is also very dilute. Therefore, we assume both are ideal dilute solutions. Given $\chi_{i,G} = p_i / p^0$, and for a dilute solution $\gamma_{i,G} = 1$, therefore $\gamma_{i,L} \rightarrow \gamma_{i,L}^\infty$. So equation 5 becomes:

$$\gamma_{i,L}^\infty = (p_i / p^0) (1 / \chi_{i,L}) \quad 6$$

It is known that the partial vapor pressure and the corresponding peak area values are directly proportional to the concentration, and similarly, the vapor pressure of the pure analyte is related to the corresponding peak area.

$$A_i = R^* p_i \quad 7$$

$$A^0 = R^* p^0 \quad 8$$

R is the calibration or response factor (area/ partial pressure or area/ mols), combining eq. 6, 7 and 8.

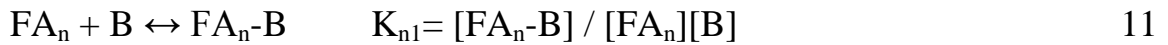
$$\gamma_{i,L}^\infty = (A_i / A^0) (1/ \chi_{i,L}) \quad 9$$

Since we know the exact mole fraction of i in the solvent, we can calculate the infinite activity coefficient $\gamma_{i,L}^\infty$ precisely using HSGC. Later, we show that the knowledge of solute concentration is not necessary to obtain any of the thermodynamic properties.

2.3. A General theory of association equilibria and HSGC

This general theory applies to any system where volatile hydrocarbon solutes solubilize in substance (FA) such as synthetic surfactants and natural surfactants and it is based on previous work⁷¹. For the sake of completeness we restate the theory with FA as

the DOM which solubilizes n-alkylbenzene as solute. Experimentally, the solution equilibria are established by adding aqueous FA into a very dilute aqueous solution of alkylbenzene solute, B, where solute-solute interactions are negligible. The equilibria are:



$$\text{FA}_n = [\text{FA}_t\text{-cfc}] / n \quad 12$$

Where, (FA-B) is the monomeric fulvic acid-solute complex with a binding constant K_{11} . $\text{FA}_n\text{-B}$ is the predominant complex in the post-aggregation region, which is present after the aggregation of n FA molecules with a binding constant K_{n1} . FA_t is the total concentration of fulvic acid added and cfc is the critical fulvic acid concentration (cfc). This process is depicted in **Figure 3**.

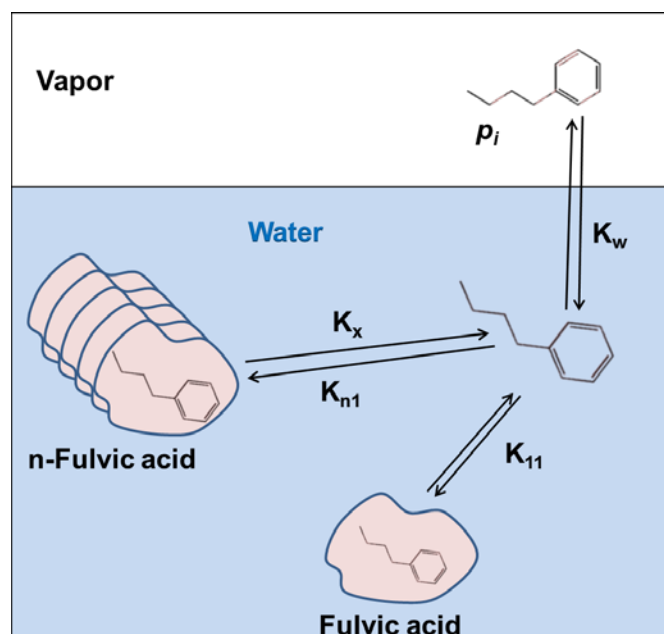


Figure 3. Schematic depiction of association and partitioning process of n-butylbenzene in water- FA aggregate pseudo-phase and its distribution during vapor/ liquid equilibrium. This representation is also true for any hydrophobic solute.

For simplicity we assume that only one type of complex, FA-B, is present in the pre-aggregation region. Theoretical studies show that a system containing two FA molecules did not form aggregates due to its low concentration ⁷⁴. We also assume that FA_n is monodispersed with an aggregation number, n , and the solute, B , is monomeric. For a very dilute solution these assumptions are valid. Equation 12 relates to the total concentration of the fulvic acid, c_{fc} , and n . Combining equations 10-12, the total concentration of solute, B_t is obtained,

$$B_t = [B] + K_{11}[FA][B] + (K_{n1}/n) [FA_t - c_{fc}][B] \quad 13$$

In equilibrium HSGC, the peak area due to the gas phase hydrocarbon in equilibrium with its aqueous phase is measured. The solute peak area, A_i , is proportional to the gas-phase concentration of the solute, $[B]_g$,

$$A_i = R_i [B]_g \quad 14$$

Where, R_i is the gas chromatographic response factor of the solute (peak area /concentration). The solute concentration in the gas phase is also related to the concentration of the free monomeric solute in the aqueous phase, $[B]$ by the distribution constant, K_w .

$$K_w = [B]/[B]_g \quad 15$$

Combining equations 14 and 15, the free solute concentration can be related to the peak area due to the solute by the following equation,

$$[B] = (K_w/R_i)A_i \quad 16$$

Assuming a negligible amount of solute partition in the gas phase compared to the total concentration of solute and K_w is independent of the presence of FA, equations 13 and 16 yield

$$A^0/A_i = 1 + K_{11}[FA] + (K_{n1}/n)[FA_t - cfc] \quad 17$$

Where A^0 and A_i are the peak areas due to the solute in the absence and in the presence of fulvic acid, respectively. The first two terms of eq 17 shows 1: 1 interaction between the monomer solute and the fulvic acid in the pre-aggregation region. After the onset of FA aggregation, if the pre-aggregation complex becomes very weak compared to the aggregation-solute complex, the second term can be neglected. Therefore, a plot of A^0/ A_i vs. FA_t is linear with a slope of K_{11} in the pre-aggregation region and yields another straight line with a slope of K_{n1}/n in the post-aggregation region. The intersection point of the straight lines corresponds to the cfc. Equation 17 shows that solute concentration is not needed to obtain K_{11} , K_{n1}/n , and cfc. It is applicable to all solutes for which A^0 and A_i can be reliably measured. However, if a reliable measurement of A_i is not possible due to the limited solubility of solute in neat aqueous solution, then the experiment can be done with aggregations solubilized in solute of known FA_t . In this case, a series of A_i values are measured after successive dilution of the solution with the solvent, in which case the FA aggregation could dissociate into pre-aggregation region. If the solution remains in the postaggregation region throughout the dilution and if $K_{n1} \gg K_{11}$, then eq 17 can be rewritten as:

$$1/A_i = [1 - (K_{n1}/n) cfc]/A^0 + (1/A^0)(K_{n1}/ n) FA_t \quad 17a$$

Equation 17a shows that the plot of $1/A_i$ vs. FA_t is a straight line with $(1/A^0) (K_n / n)$ as the slope and $[1 - (K_{n1} / n) cfc] / A^0$ as the intercept. If the cfc is known, then K_{n1} / n can be calculated from the ratio of the intercept and the slope. Thus, the value of A^0 can be calculated from the slope. In the case of $FA_t \gg cfc$, eq 17a can be further simplified:

$$1/A_i = 1/A^0 + (1/A^0)(K_{n1}/n) FA_t \quad 17b$$

Once A_i and A^0 are obtained, the fraction of solute in the aqueous phase, F_w and in the aggregation pseudo-phase, F_m can also be calculated:

$$F_w = A_i / A^0 \quad 18$$

$$F_m = 1 - F_w \quad 19$$

The aggregation pseudo-phase is a domain distinct from the bulk aqueous phase in that it consists of hydrocarbon tail form, e.g., synthetic surfactant or hydrophobic force induced conformation of fulvic acid containing an aggregation of benzene like substituents. In both cases these are hydrophobic in nature, which may contain some water.

Given the total moles of solute, t , the mole fractions of solute in the aqueous and aggregation pseudo-phases are respectively.

$$X_w = F_w t / 55.555 \quad 20$$

$$X_m = F_{mt} / [(FA_t - cfc) + F_{mt}] \quad 21$$

The above equations assume that the total moles of all solutes present are extremely small (generally, 6-7 orders of magnitude smaller) compared to that in the bulk water or solvent. This condition is easily met by sample preparation and the sensitivity of FID detector for hydrocarbons. We calculated that a partial pressure of 3.7×10^{-6} torr for benzene is easily measured with the HSGC. This is at least 3 orders of magnitude lower than the most sensitive fused quartz pressure transducer⁷⁵. If the total concentration of solute is negligible in comparison to the aggregations concentration, then the mole fraction based solute partition coefficient between aggregations and the aqueous phase is given by:

$$K_x = \chi_m / \chi_w = 55.555 F_m / [F_w (FA_t - cfc)] \quad 22$$

K_x can be considered as a quantitative measure of solubilization of hydrocarbons in presence of NOMs or surfactants. It can be shown that the molar concentration-based partition coefficient can be calculated by:

$$K_c = K_x (M_w / M_m) \quad 23$$

Where M_w is the molar volume of water and M_m is the molar volume of aggregations. It is clear from eqs 22 and 23 that aggregations- water partition coefficients can be

calculated without knowing solute concentration. Given that a pseudo-phase model of solute partitioning in the aggregate microenvironment⁷⁶ is accepted, then under equilibrium condition, the thermodynamic activities of the solute are the same in two phases, i.e.

$$\chi_m \gamma_m = \chi_w \gamma_w \quad 24$$

Where γ_w is the activity coefficient of solute in the water phase and γ_m is the activity coefficient of solute in the aggregation phase. Based on pure solute as the standard state, γ_m is also known as the intra-aggregation activity coefficient. Combining eqs 22 and 24, we get:

$$\gamma_m = \gamma_w / K_x \quad 25$$

If the solute concentration is in the Henry's law region, then γ_w can be replaced by its infinite dilution activity coefficient, which can be obtained from the literature, or can be measured by the same HSGC technique. Equation 25 shows that measurements of γ_m can be obtained without a standard solute concentration. The excess thermodynamic free energy of transfer of solute from aqueous bulk into aggregate domain (hydrophobic or hydrophilic) can be computed from $\Delta G_{ex,t} = -RT \ln (\gamma_m \text{ or } \gamma_x)$. The ΔH_t and ΔS_t can be calculated from the temperature dependence of ΔG . These values will be compared with known values from aqueous to hydrocarbon or hydrophobic domains of synthetic

surfactants. We should also be able to calculate the contributions of functional groups to the free energies by comparing two compounds.

EXPERIMENTAL SECTION

3.1. Introduction

One of the most widely used methods to study solubilization of small molecules in micelles is the headspace GC method. The activity change resulting from the association between surfactants and these small molecules can be precisely determined if the vapor (headspace) phase solute concentration is measured with a GC without perturbing the equilibria. HSGC has been used extensively in the past to measure partition coefficients in micellar systems, study various solute-solvent interactions, and study solute- surfactant systems^{65,66}. It was also used to study the vapor phase of alcohols in equilibrium with the aqueous surfactant solution⁷⁷.

3.2. Apparatus

A custom-made computer-controlled head-space gas chromatograph was used to precisely sample the vapor phase which is in equilibrium with the solution phase. A block diagram of the HSGC is shown in **Figure 4**. It is similar to that described elsewhere with some modifications^{71, 78, 79, 80}. In the present apparatus, the heated valve box (HVB) is located on the top of the gas chromatograph injector. The three valves (Valco Instruments Co., Houston, TX) in the valve box are V₁, a six-port gas sampling valve , and V₂ and V₃, four-port sample selection valves. In **Figure 4** the valves are shown in a vapor loading position. The location of the valve box, the tubing

interconnections between valves, and the location of the gas sampling system are optimized to reduce the overall dead volume of the system. For example, the volumes of the ballast (B) and the sampling loop (L) are 130 and 57 μL , respectively. The total volume of equilibrium vapor drawn into sampling valves and tubing manifolds is about 200 μL for each measurement, and exactly 57 μL was injected onto a fused silica capillary column (HP, cross-linked methylsilicone, 25 m, 0.31 mm id., 0.52 μm film) of the GC (HP Model 5890). One end of the capillary column was inserted through the empty GC injector and directly connected to the gas sampling valve (V_1) situated above the injector. The vapor transfer line between the sample cell (C) and V_2 is a short piece of silico-steel tubing (12.0 μL in volume) to reduce vapor retention and adsorption.

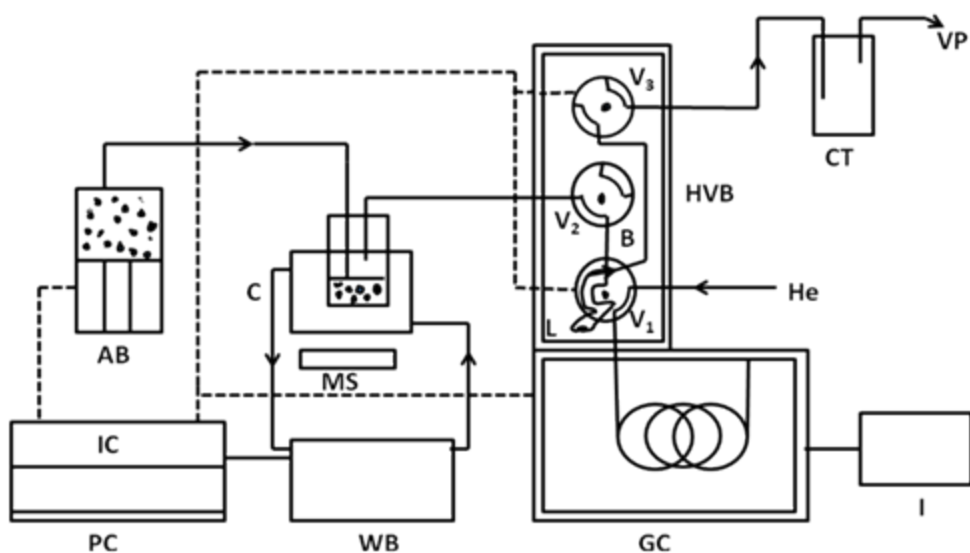


Figure 4. Block diagram of the headspace gas chromatograph. PC, personal computer; IC, interface controller; WB, water bath; GC, gas chromatograph; I, integrator; MS, magnetic stirrer; C, cell; AB, autoburet; HVB, heated valve box (thermostated to 165 0C); CT, cold trap; VP, vacuum pump; L, sampling loop; V₁, six-port gas sampling valve; V₂ and V₃ sample selection valves.

Similar fused silica tubing is also used to transfer liquids from the autosyringe (Razel Inc, NY). The entire system is controlled by a data-acquisition board (PMD 1208, Measurement Computing Inc., USA) and a custom-made control board interfaced to a PC). All programs are written in Delphi 6. The computerization allowed a precise control of valve actuation, temperature of the water bath (Haake Model A81), activation of the auto-syringe, the GC, and the integrator (HP 3392 A) at all times. The most important advantage of the HSGC apparatus is that one can measure all the volatile species in a single experiment from an extremely dilute vapor due to the very high sensitivity (1 ng/mL) of the flame ionization detector. Our lowest concentration was about 65 ng benzene sampled from the headspace, which is still higher than the detection limit of the

FID, 10- 100 pg. The instrument was thoroughly tested for sampling precision and accuracy as described elsewhere.^{71, 73, 78}

3.3. A general protocol for HSGC measurement

In the HSGC instrument as shown in **Figure 5**, the sample was in place and equilibrated for 30- 60 min before activating the valve for gas sampling. The computer program was started with the following parameters: delay time (5s) was the time before the sampling activation takes place, sampling time (10s) was the time for which the sample was allowed to fill the sampling loop and the ballast, residence time (10s) was the time allowed for the gas sample to equilibrate inside the tube, injection time (100s) was the time for which the sampling valve was activated for complete sample injection. These parameters and valve sequence are shown in **Figure 6 a** and **b**, respectively. A specific solute or a solvent can be added for a specific time by activating the autoburet. The general GC gas flow conditions are: Helium: 4- 5 mL/min, helium + auxiliary: 48-49 mL/min (total flow), hydrogen: 42-43 mL/min, and air: 180 mL/min. The GC temp program were 60⁰ for the first two minutes and then increased at 20⁰ C / minute rate until reaching 200⁰ C. The temperatures of the valve box and transfer line were 170⁰ and 165⁰ C, respectively. All precautions were taken to prevent solute carryover, leakage, interference and other issues.



Figure 5. Photograph shows the experimental setup of the HSGC. The valves are inside the valve box insulated with fiberglass and aluminum foil. The thermostated sample cell is placed on the magnetic stirrer and the autosyringe next to it.

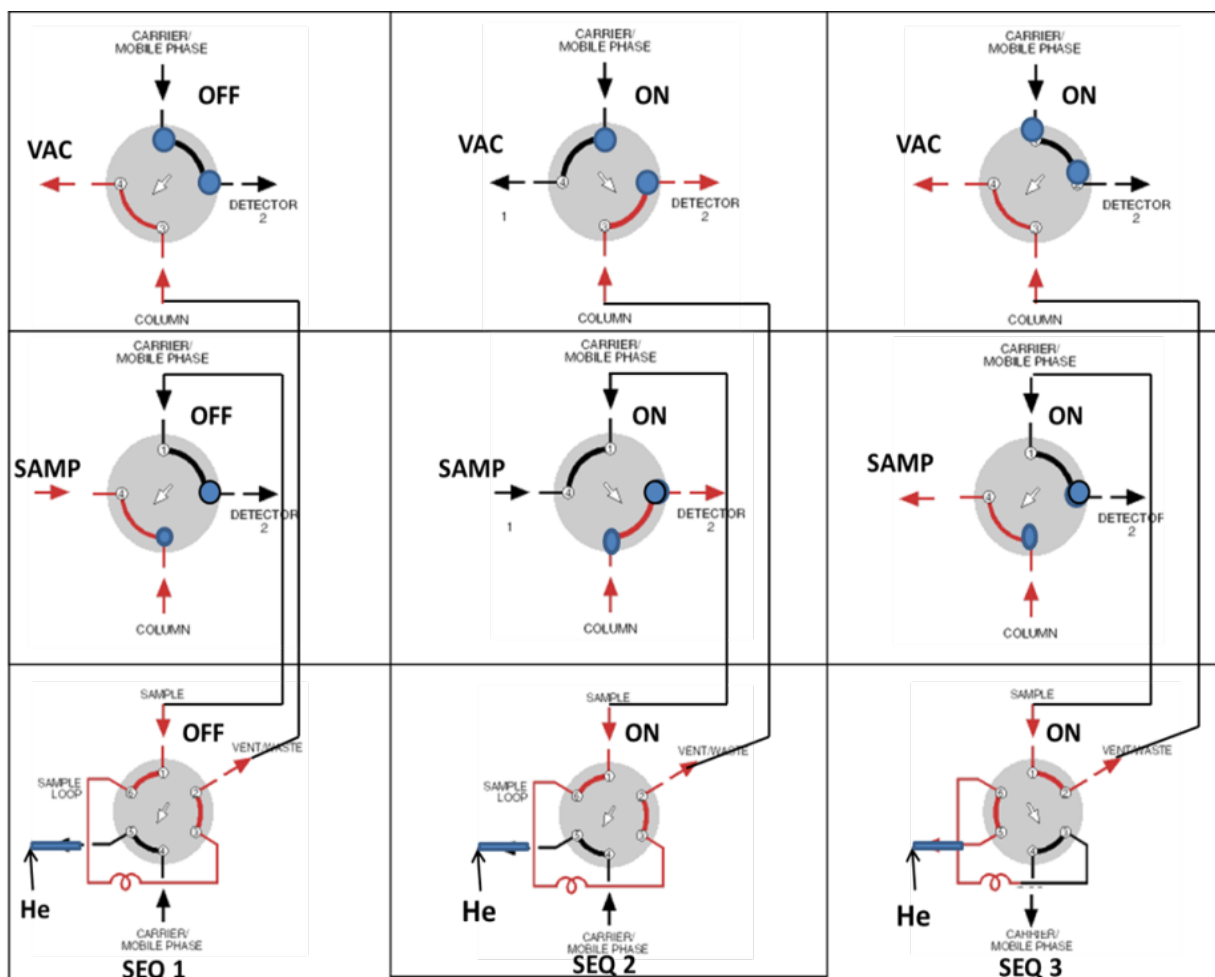
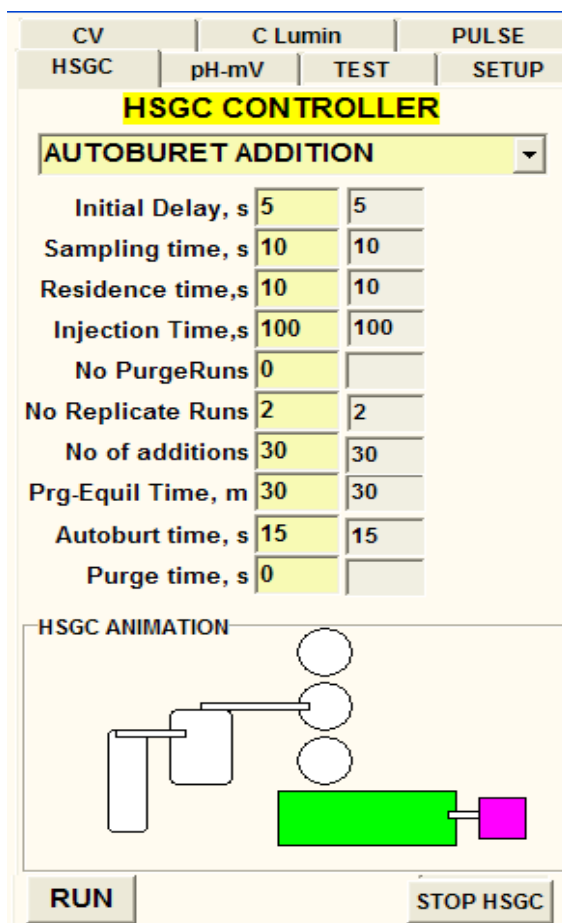


Figure 6 a. Diagram shows valve positioning, internal plumbing connections and the valve sequence: SEQ1: sample is isolated, the sample and the ballast are under vacuum, and the He is flowing through the sampling valve; SEQ2: the sample cell is opened; the headspace vapor fills the sampling loop and the ballast for 10s. Another 10s was allowed for the vapor to equilibrate inside the tubing and then injected into the GC in SEQ3: the sample cell is disconnected and the injection valve is turned on for 100s for flash transfer of samples into the GC. The two GC integrator are activated at the same time.



(b)

Figure 6 b. Snapshot of all the parameters used in the computer program.

3.4. Chemicals

A well characterized FA and HA extracted from the Bh horizon of a Spodosol was used in this study (a kind gift from Dr. Shahamat Khan of the Chemistry and Biochemistry Department of GMU). The material was thoroughly characterized in all its aspects over many years and reported elsewhere^{81, 82}. The compound is probably the

purest materials available. Detailed characteristics are listed in Table 1. The M_n (number-average) molecular weight of the FA is 951⁸¹. We used matrix-assisted laser desorption/ionization time-of-flight mass spectrometry (MALDI-TOF-MS) to measure the molecular weight of the humic acid used in this work. The HA sample was detected by MALD-TOF and show the presence of major species with a molecular weight of 656 Da. This molecular weight is close to the lower mass limit that MALDI is useful. There are other species as well as shown in the spectra in the appendix. All benzene homolog (benzene, toluene, ethyl benzene, n-propylbenzene, and n-butylbenzene) were either reagent grade or HPLC grade (Aldrich Chemical Co., Milwaukee, WI), therefore there was no need for further purification. Diesel fuel (Aviation kerosene from Prof. George Mushrush) was used as received. Sodium dodecylbenzenesulfonate, SDBS (99.0 %), n-dodecane (99.0%), HCl, and NaOH were received from Aldrich chemical company, Milwaukee (Technical grade). 1-octanol is HPLC grade (Fischer Scientific Company). Shell Regular 87 gasoline was obtained from Fairfax, VA Shell gas station. Crude oil was obtained from Fula field, Fula, Sudan.

3.5. B-BB stock solution

First a concentrated stock solution of n-alkylbenzenes mixture was prepared with a composition as shown in **Table 2**. The table also shows their molecular weights, mass, mole fractions, activity coefficients, gram fractions and density.

Table 2. Preparation of alkylbenzenes stock standard along with their densities. The activity coefficients are calculated from UNIFAC by using the mole fractions in the mixture.

Compound	molecular weight	stock, gram taken	moles	mole fraction	γ , UNIFAC	gram fraction	density, g/ml
Benzene	78.12	3.892	0.0498	0.2379	0.9713	0.1807	0.8740
Toluene	92	4.666	0.0507	0.2422	0.9895	0.2166	0.8650
Ethylbenzene	106	3.9782	0.0375	0.1792	0.9999	0.1847	0.8670
n-Propylbenzene	120.2	4.9012	0.0408	0.1947	0.9928	0.2275	0.8620
n-Butylbenzene	134.22	4.1039	0.0306	0.1460	0.9762	0.1905	0.8600

Aqueous stock solutions of n-alkylbenzenes were prepared by mixing 10.0 μL of the stock above in 1.000 L of water in a volumetric flask and the mixed by vigorous shaking. The flask was left upside down for at least 24 hours and then carefully inverted and drained from the top to remove any phase separation to maintain aqueous solubility, although such phase separation was never observed visually. The solution has an approximate mole fraction composition of 6.7×10^{-7} benzene, 6.8×10^{-7} toluene, 5.0×10^{-7} ethylbenzene, 5.5×10^{-7} n-propylbenzene, and 4.1×10^{-7} n-butylbenzene as shown in **table 3**.

Table 3. Preparation of dilute solution of alkylbenzenes in water. The table shows mole fractions of alkylbenzenes present in the water.

Solvent: water	1000	mL			
Solute mixture added	0.016	grams		Density, water	1, g/mL
Standard					
Compound	Molecular weight	gram fraction	grams in solution	moles	Mole fraction
Benzene	78.12	0.1807	0.0029	3.70E-05	6.66E-07
Toluene	92	0.2166	0.0035	3.77E-05	6.78E-07
Ethylbenzene	106	0.1847	0.0030	2.79E-05	5.02E-07
n-Propylbenzene	120.2	0.2275	0.0036	3.03E-05	5.45E-07
n-Butylbenzene	134.22	0.1905	0.0030	2.27E-05	4.09E-07
Water	18		1000	55.556	0.9999967

3.6. Surfactant and humic substances stock solution

Two natural surfactants namely FA and HA, and one synthetic surfactants, SDBS were used in this work and prepared as follows. Two fulvic acid (1.11 mM) stock solutions were prepared by dissolving 0.0053 g of fulvic acid in 50.0 mL deionized-water (18 MΩcm) in two different flasks. One has a natural pH of 2.4 and the other has a pH of 11.9 by adding 0.2 M NaOH (pH meter by Vernier Lab Quest). A humic acid stock solution was prepared by dissolving 0.0053 g of humic acid in 50.0 mL (106 mg/L) deionized-water and NaOH to give 10.77. Half of it was transferred to another flask and its pH brought down to 2.1 using 0.7 M HCl. A sodium dodecylbenzenesulfonate, SDBS (0.40 M) stock solution was prepared by dissolving 6.97 g of SDBS in 50.0 mL deionized-water. Pure n-dodecane and 1-octanol were used as received and without further purification.

3.7. HSGC sampling procedure

For (FA+ B-BB) study, the aqueous solution of n-alkylbenzene was allowed to equilibrate with continuous stirring for at least 40 minutes in a reaction cell held at 25.0 °C. Then, the gas phase above the solution was analyzed to obtain A^0 . An autosyringe was calibrated and programmed to add 7.5×10^{-3} g of FA in 15 s. This was done previously by calculating the average of three 15 -second additions of the FA stock solution from the autosyringe under computer control. After blank runs, 30 FA additions were made to vary the concentration of FA. The thermostated (25⁰ C) solution was allowed to equilibrate for 45 minutes before each of the 30 vapor sampling by HSGC. A typical gas sampling extracted less than 100 picomols (10 ng of toluene) of solute vapor (about 10 times the detection limit for FID). The loss of solute due to sampling is less than 0.02% of the total moles of solute after 20 sampling. A 1% loss of solute requires at least 300 sampling from the vapor phase. Therefore, solute concentration correction due to sampling is negligibly small. The FA concentration used here is similar to that of fresh water FA range 0.5 - 10 mg/L (= 10.5 μ M FA) ⁶¹. The pH of the final solution after adding 30 μ L of pH 2.4 stock was 5.5 ± 0.5 . Similarly, the pH of the final solution after adding 30 μ L of pH 11.9 stock was 7.6 ± 0.4 . These values correspond to the entire range of FA addition to a cell containing 18.0 mL of alkylbenzene-in-water stock solution. The pH showed no systematic trend and therefore no effect from the presence of alkylbenzenes in solution. We note the water used was not freed from dissolved atmospheric CO₂ (g). The same exact procedure was followed for, SDBS + B-BB system, n-dodecane + B-BB system, 1-octanol + B-BB system, and HA+ B-BB. The average pH

for HA stock solution was 7.5 ± 0.4 over the entire addition range without a systematic trend.

3.8. Gas chromatography–mass spectrometry procedure

To study the applicability of humic substance in enhanced oil recovery, GC/MS analysis was carried out on a contaminated sand (Play Sand, Home Depot, hardware store). This appears very similar to that of sand from New River, Virginia, USA with a diameter range of 200-500 μm . About 3.20 g of the sand was mixed with 1 mL (~0.85 gm) of neat diesel fuel in 10 different sealed glass bottles (labeled 1-9). The contents of the bottle were mixed in a sonicator (Model DA-3A) for three hours and then allowed to equilibrate at 22 °C for 3 days. A 10 mL of deionized-water was added to wash the sand in vial 1, 0.4 M SDBS was added to wash the sand in vial 2, 106 mg/L HA of pH 10.8 and 2.1 were added to wash the sand in vial 3 and 4, respectively. Then 10 mL of 1.11 mM FA of pH 2.35, 4.30, 10.70 and 11.92 were added to wash the sand in vial 5, 6, 7, and 8, respectively. Then vial 9 containing the contaminated sand was left intact. The mixtures inside the vials were left for 24 hours in the ambient condition. After decanting the washing solution, each sample was shaken vigorously using 5.0 mL each (1:1 - dichloromethane and hexane) of the extraction solvent and left to equilibrate for 24 hours. One mL of this solution was carefully removed from the top and placed in a 2 mL screw top vial with septa and analyzed with a Hewlett Packard GC-MS (GC-HP 5890 + MS-HP5971) using a DB-1, fused silica capillary column.

STUDY OF ASSOCIATION OF ALKYL BENZENES WITH SDBS, FULVIC ACID, AND HUMIC ACID

The following results and discussion sections are arranged in a sequence such that we could validate our experimental methodology and theoretical principles for the study of association of alkylbenzenes with a known synthetic surfactant SDBS. Though the HSGC method was previously validated to study similar solute-surfactant interactions⁷¹. The SDBS is chosen because it has a benzene ring which is a probe for polarizability interaction while the dodecyl aliphatic chain interacts with similar chain in the FA and HA studied here. Once we verified our procedure, we expanded this technique to the study natural surfactants FA and HA. This work was applied for the extraction of hydrocarbons from gasoline using FA. The theoretical basis of partitioning was also applied to the liquid/liquid extraction of n-alkylbenzenes with n-dodecane and 1-octanol as co-solvents.

4.1. Surfactant sodium dodecylbenzene sulphonate- n-alkylbenzenes system

Surfactant sodium dodecylbenzenesulphonate, SDBS is a series of organic compounds with the formula $C_{18}H_{29}SO_3Na$ as shown in **Figure 7**. It is a colorless salt with useful properties as a surfactant⁸³. It is an anionic surfactant with properties of

detergency, moistening, foaming, emulsivity and dispersity. It can be used directly to formulate detergents for household and industrial use. It is widely used in detergent industry, oil exploitation, forming agglomerated detergent production, chemical fertilizer, cement, industrial cleaning agent and others.

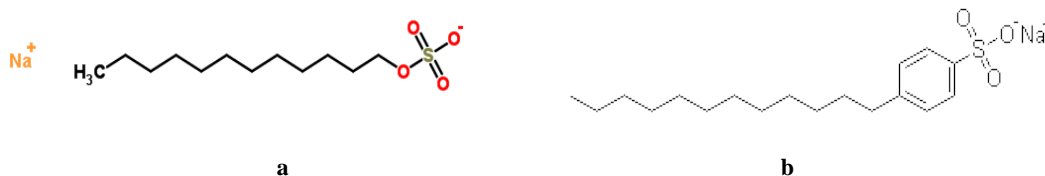


Figure 7. Structure of (a). Sodium dodecyl sulfate (SDS), and (b). Sodium dodecylbenzene sulfonates (SDBS).

SDBS is similar to SDS, except the presence of the benzene ring in the former as shown in **Figure 7**. This is one of the reasons for the choice of SDBS over SDS to validate our methods. SDS is the archetypal and most extensively studied surfactant known with published values for binding and partition coefficients^{84,85}. In general, all HSGC experiments start with a dilute n-alkylbenzene solution in a thermostated sample cell into which the surfactant was added in incremental fashion. The GC peak areas obtained from sampling of the headspace before and after the surfactant addition, as shown in **table 4**, are the bases of the following calculations. These have been detailed in the theory and experimental section.

Table 4. Table shows peak area ratio for the addition of SDBS in aqueous solution of n-alkylbenzenes at 25.0⁰ C. Given the A⁰ one can calculate A_i for each entry.

Run#	Moles of SDBS added	SDBS	Benzene	Toluene	Ethyl benzene	n-Propyl benzene	n-Butyl benzene
		Pure peak area, A ⁰ →	4555	24067	47878	98089	69511
		SDBS, mM	↓Peak area ratio, A ⁰ /A _i				
0.00	0.00E+00	0.00	1.00	1.00	1.00	1.00	1.00
1.00	9.59E-09	0.60	1.07	1.09	1.11	1.23	1.36
2.00	1.91E-08	1.20	1.17	1.19	1.27	1.64	1.60
3.00	2.87E-08	1.79	1.30	1.34	1.43	1.69	1.90
4.00	3.82E-08	2.39	1.46	1.58	1.64	2.04	2.24
5.00	4.76E-08	2.98	1.71	2.30	1.87	2.42	3.14
6.00	5.71E-08	3.57	1.91	2.75	2.40	3.18	4.61
7.00	6.65E-08	4.16	2.17	3.40	3.40	4.66	6.80
8.00	7.59E-08	4.74	2.40	4.11	5.03	6.57	8.81
9.00	8.52E-08	5.33	2.71	4.87	6.21	8.66	11.55
10.00	9.46E-08	5.91	3.07	5.65	7.72	10.94	13.89
11.00	1.04E-07	6.49	3.44	6.31	9.37	13.00	16.65
12.00	1.13E-07	7.07	3.78	7.20	10.71	14.93	18.98
13.00	1.22E-07	7.65	4.21	8.12	12.64	17.36	21.30
14.00	1.32E-07	8.23	4.61	9.07	14.20	19.17	23.11
15.00	1.41E-07	8.80	5.06	10.03	15.75	20.84	25.30
16.00	1.50E-07	9.38	5.35	10.88	15.46	21.83	25.69
17.00	1.59E-07	9.95	5.74	12.53	17.33	22.80	27.26
18.00	1.68E-07	10.52	6.58	14.08	19.11	24.11	28.96
19.00	1.77E-07	11.08	6.25	15.85	21.30	25.72	30.22
20.00	1.86E-07	11.65	6.41	17.81	23.54	32.35	30.30

4.1.1. Solute-SDBS association constant, K₁₁

The monomeric SDBS-solute complex with a binding constant K₁₁ is formed at adding SDBS to the aqueous alkylbenzene solutions. **Figure 9** shows the peak area ratios as a function of total SDBS, concentrations increases linearly due to the formation of the 1:1 complex. It clearly shows the pre- and post-aggregation regions by two lines with low

and high slopes intersecting at the critical micelles concentration. The post aggregation region is more linear than the pre-aggregation region. **Table 5** shows the results of the linear regression of the data in the pre-micellar region. The calculated K_{11} values showed increased magnitude as the number of methylene group increases in the benzene homologues. All members of the homologue show significant interactions between a monomer solute and a SDBS molecule and the strength of that interaction increases with increasing hydrophobicity in the members. The intercepts are all unity (within experimental error) as predicted by the theory. Our K_{11} values for the probes are not found in the literature. In absence of published literature on SDBS, we find the best surfactant to compare with is SDS, not only because it has the same 12 carbon alkyl chain, but also evaluates the effect of the presence of the benzene ring and the significance of the π - π interactions **Figure 7**. The K_{11} values for SDS by Hussam *et al*⁷¹ are also shown in **table 5** and they were much lower than those of the SDBS. This ring plays a role in the interactions between SDBS and benzene homologs. Apparently, it brings about additional attractive noncovalent interactions (polarity/ polarizability interaction) between the aromatic rings compared to that with an alkyl-alkyl chain in SDS resulting in large differences between $K_{11}(\text{SDS})$ and $K_{11}(\text{SDBS})$ for the same molecule. Therefore, the attractive force is stronger between solute-SDBS to form a solvation complex as depicted in **Figure 8**. It shows three types of possible noncovalent π - π interactions between the benzene ring of SDBS and that of alkylbenzenes- π stacking or sandwich, edge-to-face or T-shape, and parallel –displayed interactions.

Table 5. Values of K_{11} from linear least-squares regression of A^0/A_i vs. $[SDBS]_i$ in the pre-micellar region at 25.0°C.

Solute	K_{11} (M^{-1})	intercept	r^2	$K_{11}^{ref 71}$ (SDS-solute)
Benzene	234 ± 90	1.019 ± 0.009	0.9831	2.5 ± 2.6
Toluene	426 ± 109	0.9884 ± 0.005	0.9987	10 ± 2
Ethylbenzene	672 ± 151	0.9490 ± 0.014	0.9962	25 ± 3.1
n-propylbenzene	1184 ± 190	1.025 ± 0.022	0.9856	54.7 ^a
n-butylbenzene	1566 ± 221	1.057 ± 0.044	0.9935	124 ± 13.6

^a K_{11} is interpolated from a linear fit of $\ln K_{11}$ vs. # -CH₂- ($r^2 = 0.9846$)

4.1.2. Critical micelle concentration (cmc)

SDBS forms micelles starting at some critical concentration when the surface is saturated with SDBS monomers. Any excess SDBS added after this concentration goes into the formation of micelles as shown in **Figure 10**. These structured environments are vehicles for the solubilization of solutes. The *cmc* can be found from the point of intersection of two straight lines in the pre- and post-micelle regions, as shown in **Figure 9**. The average *cmc* was found to be 2.98 ± 0.76 mM compared to the literature value of 2.9 mM⁸⁶. The *cmc* value obtained for each solute showed no obvious systematic trend, thus eliminating the possibility of a solute induced *cmc* change. This is due to the very low concentration of n-alkylbenzenes in the aqueous media as described in the experimental section. The *cmc* of SDBS is lower than that of SDS (8 mM) due to the large size of the SDBS and significant steric effect during assembly on the surface and into micelles as shown in **Figure 10**.

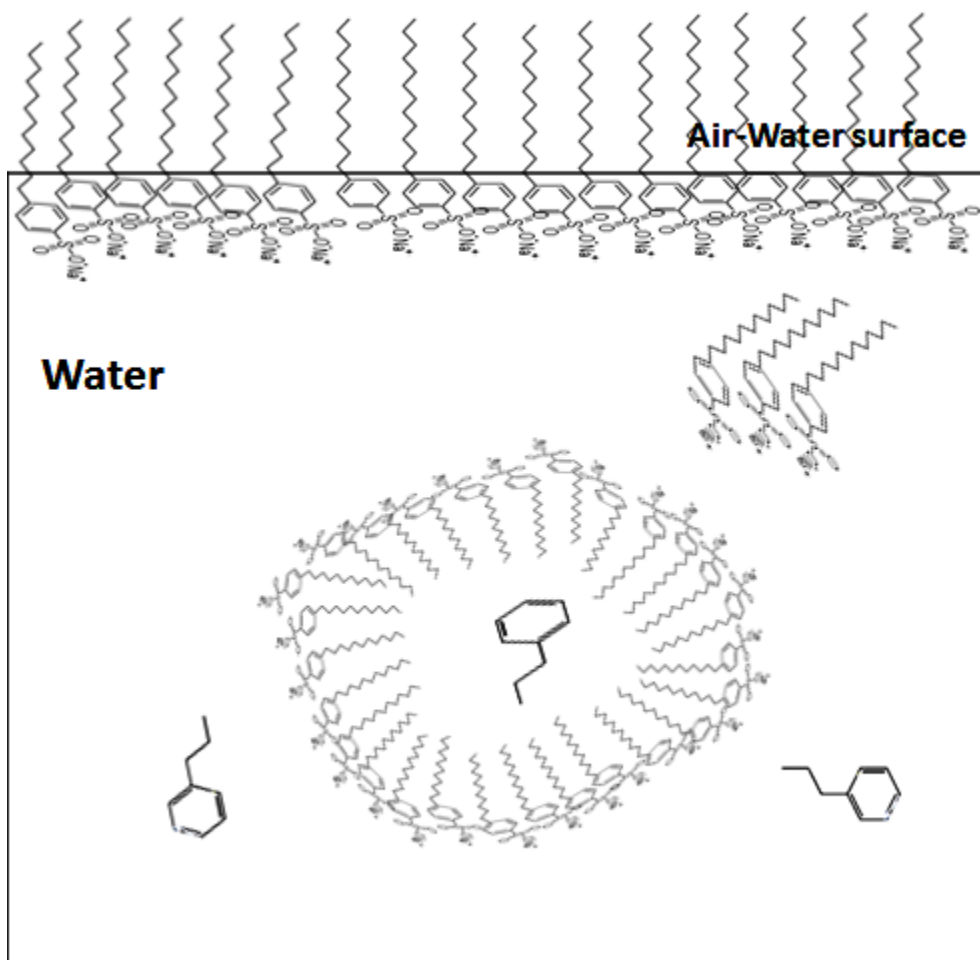


Figure 10. Sketch shows the water surface is covered by SDBS surfactants at low concentration of SDBS. As the concentration of SDBS starts to increase, the surfactant aggregates into micelles. The partitioning of n-butylbenzene in SDBS micelles (pseudophase) is shown.

4.1.3. Solute-micelle association constant, K_{n1}

If the solute-solute interaction in the water continuous bulk phase is neglected, then K_{11} and K_{n1} reported here can be regarded as their infinite dilution values. In the post-micelle region (**Figure 9**), the peak area ratio increases significantly as more solute solubilizes in the micelles, thus decreasing the concentration of free solute. **Table 6** lists values of K_{n1} as obtained from the regression of data in this region. According to **equation 17**, the slope is K_{n1}/n and hence K_{n1} is obtained by using SDBS's aggregation number, $n = 26$ obtained by light scattering studies⁸⁷. Our K_{n1} values for the probes are not found in the literature. But as a comparison to the values reported for SDS, we find that that SDBS-micelle K_{n1} values are at least one order of magnitude higher than that of SDS-n-alkylbenzene values. This is due to the presence of the 26 benzene ring in SDBS micelles and the strong attractive noncovalent interactions (polarity/polarizability interaction) with n-alkylbenzenes. By comparing K_{11} and K_{n1} (association constant per unit of SDBS in micelles), we find that the tendency of a single SDBS in the micelles to bind a benzene homologue is 6-8 higher than that of an isolated SDBS in the solution. These significant differences in the two binding constants show that the solute solubility from the bulk is very different than that in the micelles.

Table 6. Values of K_{n1} from linear least-squares regression of A^0/A_i vs. $[\text{SDBS}]_t$ in the post-micellar region at 25.0 °C.

Solute	K_{n1} (M^{-1})	r^2	Lit K_{n1}	K_{n1}, M^{-1} (SDS) ^{ref 71}
Benzene	15600 ± 251	0.9994	na	1474 ± 11
Toluene	33800 ± 261	0.9989	na	4171 ± 44
Ethylbenzene	49400 ± 192	0.9997	na	10197 ± 64
n-propylbenzene	78000 ± 83	0.9921	na	28302 ^a
n-butylbenzene	80600 ± 137	0.9877	na	76117 ± 100

^a K_{n1} is interpolated from a linear fit of $\ln K_{n1}$ vs. # -CH₂- ($r^2 = 0.9996$)

4.1.4. Solute- micelles partition coefficient, K_x

The partitioning of solute between two phases is of importance for many applications. According to **equation 22**, the mole fraction-based solute partition coefficient K_x can be calculated using the *cmc* value found above. The dependence of K_x vs. total [SDBS] concentration is shown in **Figure 11**. They show significant variation in K_x at $[\text{SDBS}]_t$, near *cmc* as $([\text{SDBS}]_t - \text{cmc})$ becomes very low. As $[\text{SDBS}]_t$, increases, the micelles concentration also increases, and K_x values appear to level off to a constant value accompanied with decreasing variation. K_x values shown in **Figure 11** become constant above *cmc*. 6 mM [SDBS]. These values are $3.81 \times 10^4 \pm 25$ for benzene, $8.67 \times 10^4 \pm 69$, for toluene, $1.26 \times 10^5 \pm 96$ for ethylbenzene, $1.94 \times 10^5 \pm 169$ for n-propylbenzene and $2.05 \times 10^5 \pm 212$ for n-butylbenzene. The results show that the partition coefficients increase with increasing the hydrophobicity of the solute and contribute to a large free energy of transfer of n-alkylbenzenes from bulk water to micellar phase. In comparison, K_x for SDS-benzene, for example, was found to be 1300,

⁷¹ which is one order of magnitude lower than that of SDBS-benzene and this is explained by the environment inside the micelle. It is benzene-like in case of SDBS.

The decrease in K_x from lower $[SDBS]_t$ to high $[SDBS]_t$ and subsequent leveling off may be the lack of inclusion of small aggregate complexes in our model in the transition region. It could also be due to the increase in packing density of the aggregate which could expel some hydrocarbon molecules dissolved in them. This could explain the decrease in K_x and increase in inter-aggregate activity coefficient, γ_m , to a nearly constant value, as $[SDBS]_t$ increases.

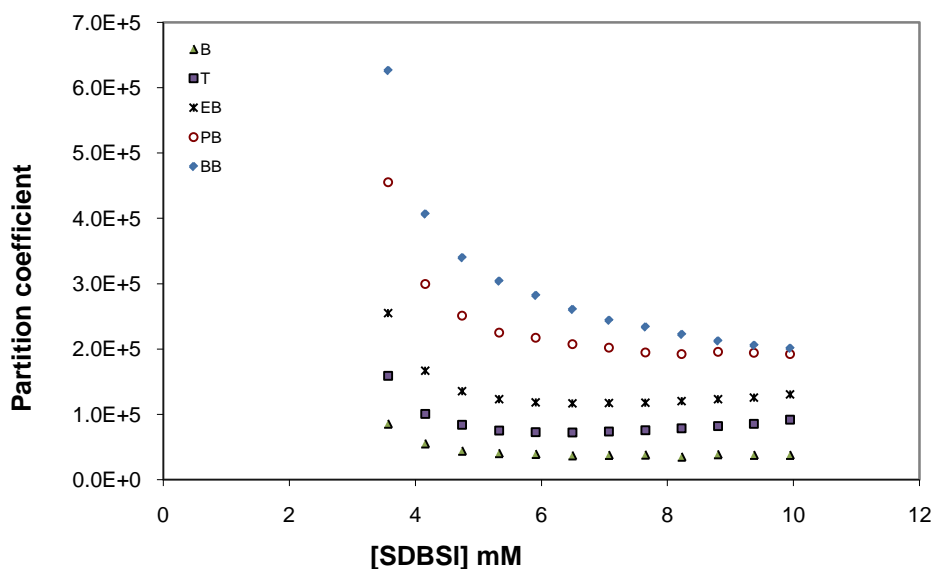


Figure 11. Effect of total SDBS concentration on water-micelles partition coefficient of n-alkylbenzenes at 25.0^o C.

4.1.5. Intra-micellar activity coefficient

One of the most important aspects of this work is the estimation of the activity coefficient of solutes inside the micelles by using **equation 25**. It required a reliable literature value of the activity coefficient of solute in water, γ_x , which was also found by HSGC technique⁸⁸. **Figure 12** shows plots of activity coefficients of solute as a function of total [SDBS]_t concentration. Like K_x , γ_m also approaches a limiting value at [SDBS] higher than 8 mM. γ_m is indicative of the interaction of solute and the interior solvophobic microenvironment of the micelles.

We also observed that the intra-micellar activity coefficients of n-alkylbenzenes are much lower than that in the water, which indicates that they preferred the microenvironment over the aqueous bulk. Moreover, it shows that the microenvironment of the solubilized species is not affected significantly on increasing the micelles concentration beyond a certain level. The average γ_m values after 8 mM SDBS for benzene, toluene, ethylbenzene, n-propylbenzene and n-butyl-benzene are 0.07 ± 0.04 , 0.11 ± 0.02 , 0.26 ± 0.04 , 0.71 ± 0.13 , and 2.74 ± 0.04 , respectively, as compared to that of 2480, 9190, 32700, 13600, and 566000 in water.

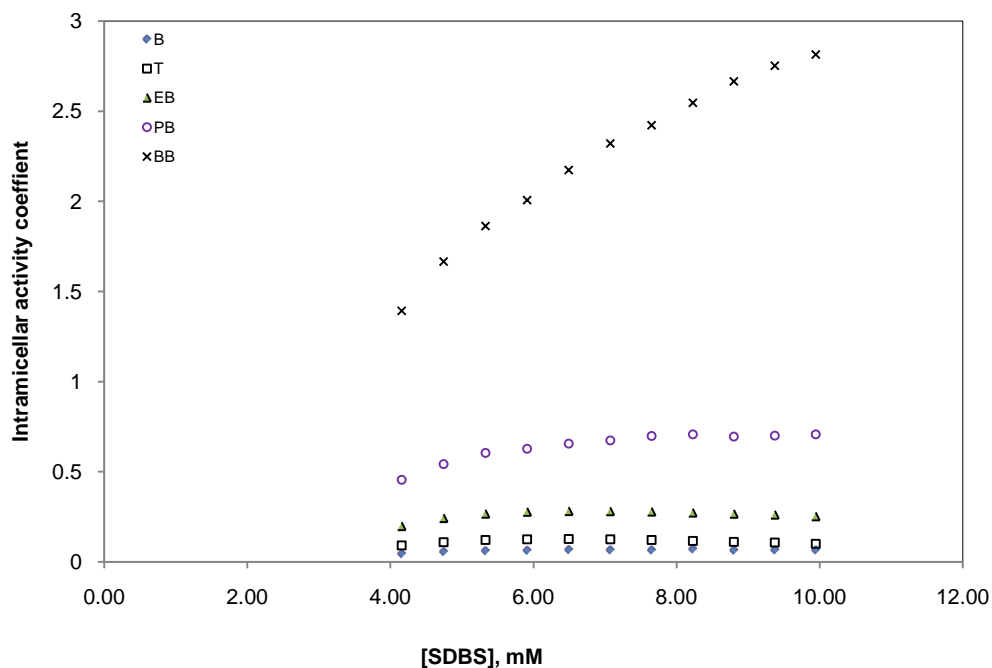


Figure 12. Effect of total SDBS concentration on intra-micellar activity coefficients of n-alkylbenzenes at 25.0⁰ C.

4.1.6. Transfer free energies of functional groups

It was possible to calculate the free energy of transfer of a methylene unit, $-\text{CH}_2-$, from aqueous to micelle phase as shown in **Figure 10**. Using the linear least squares fitting of $\ln(K_x)$ vs. $n-\text{CH}_2-$ in n-alkylbenzene at three different $[\text{SDBS}]_t$ concentrations at 4.7, 7.07, and 9.95 mM SDBS yield average slope = 0.3986 ± 0.047 , average intercept = 10.85 ± 0.07 , and average $r^2 = 0.9593$. The transfer free energy, $\Delta G_{\text{transfer}} = -RT \text{ slope}_{\text{average}}$, calculated from the average slope was -236 ± 12 cal/mol per $-\text{CH}_2-$. This value is much higher than those of transfer of $-\text{CH}_2$ groups of several solute homolog series from aqueous to various nonpolar and SDS micellar phases between -550 and -884

cal/mol⁸⁸. This is indicative of lower affinity (higher free energy) for partitioning of an alkyl group in the SDBS micelle compared to those of surfactants containing long alkyl chain and no aromatic rings. In contrast, a much lower free energy of transfer of benzene -6426 ± 20 cal/mol ($\Delta G_{transfer,benzene} = -RT \text{ intercept}_{average}$) indicates a substantially higher affinity of benzene for SDBS aggregate than SDS. These observations indicate that the SDBS micelle is more benzene-like (highly polarizable) with specific affinity for such molecules and less alkyl-hydrocarbon like.

4.2. Fulvic acid- n-alkylbenzene system

In this section we describe the association and partitioning of n-alkylbenzenes with fulvic acid. We studied the aggregation process using HSGC the same way we followed in the case of SDBS. **Figure 13** shows typical HSGC of n-alkylbenzenes after 0th and 20st addition of FA. It shows peaks for all n-alkylbenzenes (B-BB) in absence (a) and in presence of 30.7 μ M FA (b).

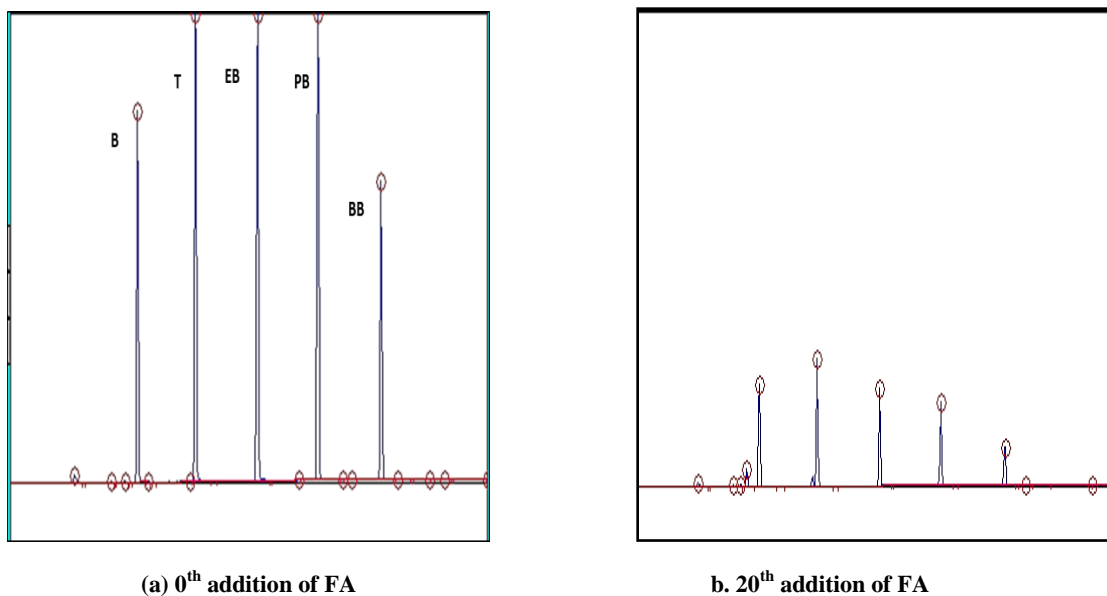


Figure 13. Changes in peak areas as the concentration of FA increases at 25.0⁰ C.

Also **Figure 13** shows the apparent solubility property of fulvic acid for the benzene homolog. It shows the decrease in the peak areas due to the reduction of solute concentration in the vapor phase as more solute is solubilized in the FA-aggregate pseudo-phase. The data obtained from this experiment is shown in **table 7**.

Table 7. Table shows peak area ratio for the addition of FA in aqueous solution of n-alkylbenzenes at pH 5.5 and 25.0⁰ C. Given the A⁰ one can calculate A_i for each entry.

Run #	Moles of FA added	Fulvic	Benzene	Toluene	Ethyl benzene	n-Propyl benzene	n-Butyl benzene
		Pure peak area, A ⁰ →	4180	20644	41223	86461	71759
		FA, μM	↓Peak area ratio, A ⁰ /A _i				
0.00	0.00E+00	0.00	1.00	1.00	1.00	1.00	1.00
1.00	2.66E-08	1.66	1.04	1.03	1.05	1.06	1.08
2.00	5.30E-08	3.31	1.16	1.22	1.24	1.31	1.30
3.00	7.94E-08	4.97	1.24	1.36	1.50	1.75	1.86
4.00	1.06E-07	6.61	1.36	1.60	1.83	2.23	2.52
5.00	1.32E-07	8.25	1.49	1.85	2.20	2.85	3.45
6.00	1.58E-07	9.89	1.70	2.15	2.67	3.69	4.59
7.00	1.84E-07	11.52	1.89	2.45	3.18	4.58	6.02
8.00	2.10E-07	13.14	2.10	2.78	3.61	5.42	7.25
9.00	2.36E-07	14.76	2.41	3.28	4.15	6.27	8.63
10.00	2.62E-07	16.38	2.69	3.69	4.82	7.23	9.65
11.00	2.88E-07	17.99	2.99	4.34	5.41	8.18	11.01
12.00	3.14E-07	19.60	3.43	5.03	6.21	8.93	12.14
13.00	3.39E-07	21.20	3.79	5.68	7.09	9.85	13.14
14.00	3.65E-07	22.80	4.25	6.23	7.94	10.85	14.21
15.00	3.90E-07	24.39	4.69	6.95	8.73	11.95	15.37
16.00	4.16E-07	25.98	5.14	7.63	9.68	12.88	16.03
17.00	4.41E-07	27.56	5.65	8.28	10.68	13.85	17.29
18.00	4.66E-07	29.14	6.01	9.09	11.88	14.97	18.40
19.00	4.91E-07	30.71	6.60	9.82	12.93	15.95	19.19
20.00	5.16E-07	32.28	7.08	10.67	13.93	17.40	19.92

4.2.1. Solute-fulvic acid association constant, K₁₁

The addition of FA to a solution containing n-alkylbenzenes as solute reduces the free concentration of monomer solute in the aqueous and vapor phase due to binding and partitioning of solute in solution. This is observed as a decrease in peak area of the solute sampled from the headspace of the sample cell. The peak area ratio (A⁰/ A_i) vs. total fulvic acid concentration ([FA]_t) is shown in **Figure 14**. It clearly shows the pre- and

post-aggregation regions. The post aggregation region is more linear than the pre-aggregation region. The result of the linear regression of the limited data in the pre-aggregation region is shown in **table 8**. The calculated K_{11} value increases as the number of methylene group increases in the n-alkylbenzenes. This association is driven partly by the hydrophobicity of alkyl chain of n-alkylbenzenes. Since there is no such study to compare with these results, we took the literature values with that of sodium dodecylsulfate (SDS) monomer. Although FA is not similar to SDS, but it was the most thoroughly studied synthetic surfactant known and can be used as a reference for hydrocarbon like pseudo-microenvironment. The K_{11} values for SDBS- and SDS-n-alkylbenzenes are also listed in **table 8**. Clearly, the K_{11} for FA is at least 2 and 4 orders of magnitude higher than that for SDBS and SDS respectively. This is due to the small size of SDS and SDBS monomer compared to a single FA monomer which has sizeable nonpolar hydrophobic aromatic and aliphatic groups. In both SDBS and SDS, the pre-micellar region of the plot (K_{11} vs. [SDBS or SDS]) is linear with a sharp break at *cmc*. In FA, however, the pre-aggregation portion shows a gradual increase from the initial linearity. This could be an indication of a step-wise aggregation of FA molecules to a limiting aggregate structure compared to that for SDS. This transition region could be modeled by assuming the presence of higher complexes such as $(FA)_2^- X$ ($X = n$ -alkylbenzene).

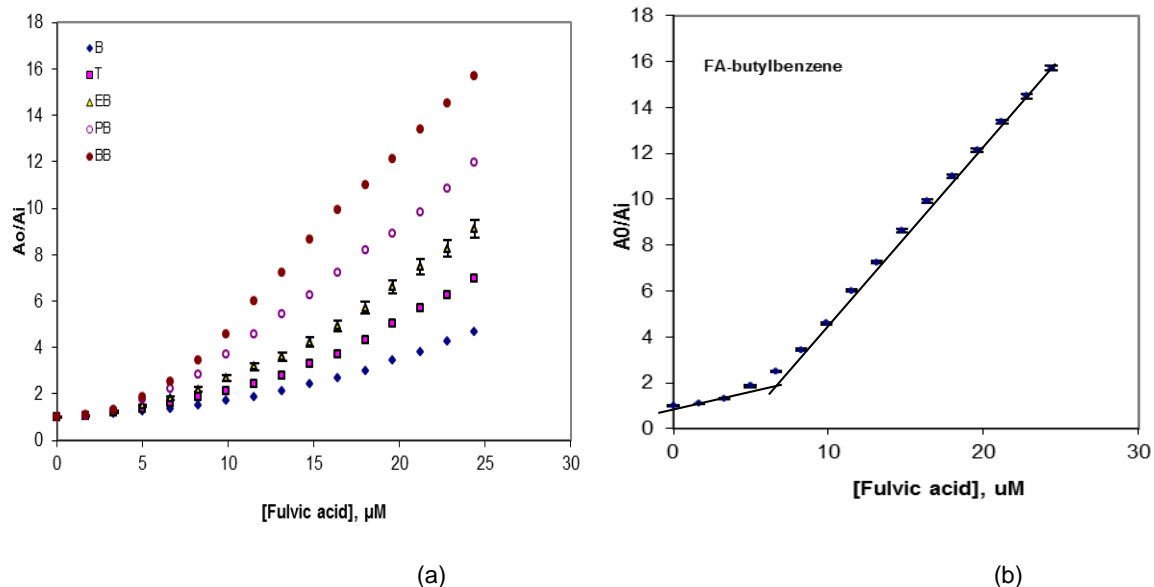


Figure 14. (a) Peak area ratio A^0/A_i vs. $[FA]_t$ for n-alkylbenzenes 25.0°C . (b) Figure shows the intersection of two lines outlined in the theory section. Typical experimental errors are shown for ethylbenzene and the straight line. The error bars indicate larger error at lower vapor phase concentration.

Table 8. Values of K_{11} from linear least-squares regression of A^0/A_i vs. $[FA]_t$ in the pre-aggregation region at 25.0°C . Literature K_{11} for SDS-solutes are listed in the last column.

Solute	$K_{11}, (\times 10^3) \text{ M}^{-1}$	Intercept	r^2	K_{11}, M^{-1} (SDBS-solute)	K_{11}, M^{-1} (SDS-solute) ref 71
Benzene	69.5 ± 1.0	0.9631 ± 0.032	0.9793	234 ± 90	2.5 ± 2.6
Toluene	118.6 ± 1.3	0.9461 ± 0.053	0.9585	426 ± 109	10 ± 2
Ethylbenzene	171.0 ± 3.1	0.9550 ± 0.088	0.9471	672 ± 151	25 ± 3.1
n-Propylbenzene	272.1 ± 6.1	0.8512 ± 0.160	0.9345	1184 ± 190	54.7^a
n-Butylbenzene	362.5 ± 14.3	0.8432 ± 0.138	0.9913	1566 ± 221	124 ± 13.6

^a K_{11} is interpolated from a linear fit of $\ln K_{11}$ vs. $\# -\text{CH}_2-$ ($r^2 = 0.9846$)

4.2.2. Critical fulvic acid aggregation concentration (*cfc*)

Like most large molecules and surfactants containing hydrophobic moieties, FA forms aggregate starting at some critical concentration, *cfc*. Any excess FA added after this concentration results in the formation of more aggregates. The formation of *cfc* is necessary for a significant solubilization, transport, and removal of insoluble organic species and binding of metal ions. The *cfc* was found from the point of intersection of two straight lines in the pre- and post-aggregate regions, as shown in **Figure 14b**. The average *cfc* was found to be $8.87 \pm 0.06 \mu\text{M}$ FA, from the regression slope and intercept for all five n-alkylbenzenes. The *cfc* values of these solute showed no systematic trend with respect to alkyl chain length. This eliminates the possibility of a solute induced *cfc* change with increase in alkyl chain length. Apparently, the very low concentration of n-alkylbenzenes (10^{-7} mole fraction) used in this study has no influence on the aggregate structure. The value obtained in our study is slightly higher than those reported in the literature *cfc* $3.6 \mu\text{M}$ ⁹⁰ and $2 - 4 \mu\text{M}$ ⁹¹ using completely different techniques. The later study also showed *cfc* were almost independent of pH 2-11. Although *cfc* could vary depending on the origin and molecular weight of FA, it appears to have the same order of magnitude. Similarly, low molecular weight humic acid fractions showed aggregation concentration in the range 50-100 mg/L, which is even lower than FA⁹². In contrast, critical micelles concentrations (*cmc*) for most synthetic surfactants are 2-3 orders of magnitude higher. Therefore, FA is a much better solubilizing agent than synthetic surfactants. This is also proven by the following measurements.

4.2.3. Solute-aggregation association constant, K_{n1}

Figure 14 shows the peak area ratio increases monotonically as the concentration of FA increases post aggregation as more solute binds with the aggregate. This further decreases the concentration of free monomer solute in aqueous phase and in the vapor phase. According to equation 17, the slope (K_{n1}/n) was used to calculate the value of the aggregation-solute association constant by using the FA's aggregation number, $n = 20$ obtained from literature static light scattering measurements¹⁰. The K_{n1} values, obtained from the regression of the data in this region, are shown in **table 9**. It shows that FA-aggregate K_{n1} values are at least 2 and 3 orders of magnitude higher than that of SDBS- and SDS-n-alkylbenzene values, respectively. This is also consistent with K_{11} measurements. Furthermore, this is also consistent with the observation that small surfactant molecules (SDS or Triton-X) cannot break FA aggregates¹⁰. By comparing K_{11} and K_{n1}/n (association constant per unit of FA in aggregations), we find that the tendency of a single FA in the aggregate pseudo-phase to bind an n-alkylbenzene is 3-5 times higher than that of an isolated FA in the solution. These significant differences in the two binding constants show that the solute solubility from the bulk is very different in the aggregate pseudo-phase due to their structure and the hydrophobicity. Although, there is no literature exists to compare with our results, we find that fluorescence polarization measurement of K_{n1} of perylene with FA at similar concentrations is $1.8 \times 10^6 \text{ M}^{-1}$ (independent of pH 2-11)⁹¹. This value is one order of magnitude lower than that for n-butylbenzene, $13.8 \times 10^6 \text{ M}^{-1}$. The large binding constants confirm the presence of a strongly hydrophobic region in the aggregate for n-alkylbenzene like molecules. We note

that literature studies on the solubility of PAH and other nonvolatile organics in FA solution used organic solvent (glycerol, methanol etc) to make the standards¹⁹, where even at low concentrations of the organic solvent can help retain more solutes in the aqueous phase and lower K_{n1} values⁹³. This is also true for literature partition coefficient values as discussed later.

It is estimated that there are 1-9 aggregates per n-alkylbenzene solute molecule; therefore, the solute-solute interaction in the aqueous bulk phase and that inside the aggregate pseudo-phase can be neglected. Thus, K_{11} , K_{n1} , and other distribution properties reported here can be regarded as their infinite dilution values.

Table 9. Values of K_{n1} from linear least-squares regression of A^0/A_i vs. $[FA]_t$ in the post-aggregation region at 25.0 °C.

Solute	$K_{n1}, (x 10^3) M^{-1}$	r^2	K_{n1}, M^{-1} (SDBS)	K_{n1}, M^{-1} (SDS) ^{ref 71}
Benzene	1390 ± 1.2	0.9842	15600 ± 251	1474 ± 11
Toluene	2372 ± 4.3	0.9887	33800 ± 261	4171 ± 44
Ethylbenzene	8910 ± 5.5	0.9820	49400 ± 192	10197 ± 64
n-Propylbenzene	11408 ± 7.1	0.9982	78000 ± 83	28302 ^a
n-Butylbenzene	13812 ± 3.9	0.9972	80600 ± 137	76117 ± 100

^a K_{n1} is interpolated from a linear fit of $\ln K_{n1}$ vs. # -CH₂- ($r^2 = 0.9996$)

4.2.4. Solute-aggregate partition coefficient, K_x

The mole fraction partition coefficient, K_x , is a practical parameter and its value indicates the partitioning of solute between two immiscible but mutually saturated phases. K_x can be calculated by applying equation 22 and easily converted to molar concentration based

K_c by equation 23. While K_{11} and K_{n1} are model dependent, K_x and K_c are not. Measurements of these parameters by HSGC do not require solute concentrations for a dilute solution. **Figure 15** shows the dependency of K_x on the total [FA] concentration. It shows, as $[FA]_t$ increases the aggregates concentration also increases and K_x values appear to level off. From **Figure 15**, it is seen that K_x values become constant above ca. 15 μM $[FA]_t$. The average K_x value after 15 μM FA remains relatively constant within 6% *rsd*. The K_x values show that the enhanced solubilization of hydrophobic *n*-alkylbenzenes is due to the partitioning of the solutes into the FA aggregate phase by the virtue of hydrophobic interaction. Therefore, for homologous series, the more hydrophobic the molecule is the higher its partitioning becomes as seen from the trend in K_x values moving from the least hydrophobic benzene to the most hydrophobic *n*-butylbenzene. This is also consistent with the findings that large humic molecules associate with small ones by forming micelle-like aggregates^{94,95}. The partitioning of *n*-alkylbenzenes in FA is more favored than that in SDBS and SDS as seen in **table 10**.

The decrease in K_x from lower $[FA]_t$ to high $[FA]_t$ and subsequent leveling off may be the lack of inclusion of small aggregate complexes in our model in the transition region. It could also be due to the increase in packing density of the aggregate which could expel some hydrocarbon molecules dissolved in them. There exists some evidence that a transition of FA molecule from small flexible entity to a globular (even rigid) shape is possible as the concentration of FA increases⁹¹. A rigid shape, after losing its rotational degrees of freedom due to self-association, can exclude hydrophobic solutes and eventually reaches a constant volume. This could explain the decrease in K_x and

increase in inter-aggregate activity coefficient, γ_m , to a nearly constant value, as $[FA]_t$ increases. Unfortunately, no similar data for the partitioning of n-alkylbenzenes in the literature are available for comparison.

Table 10. Partition coefficients of n-alkylbenzenes in FA compared to other surfactants at 25.0⁰ C.

Surfactant	FA	SDBS	SDS ^{ref 71}
Solute	K_x ($\times 10^4$)	K_x ($\times 10^4$)	K_x ($\times 10^4$)
Benzene	134.0	3.81	0.13
Toluene	2130.0	8.67	0.40
Ethylbenzene	2830.0	12.6	0.96
n-Propylbenzene	3730.0	19.4	na
n-Butylbenzene	4640.0	20.5	na

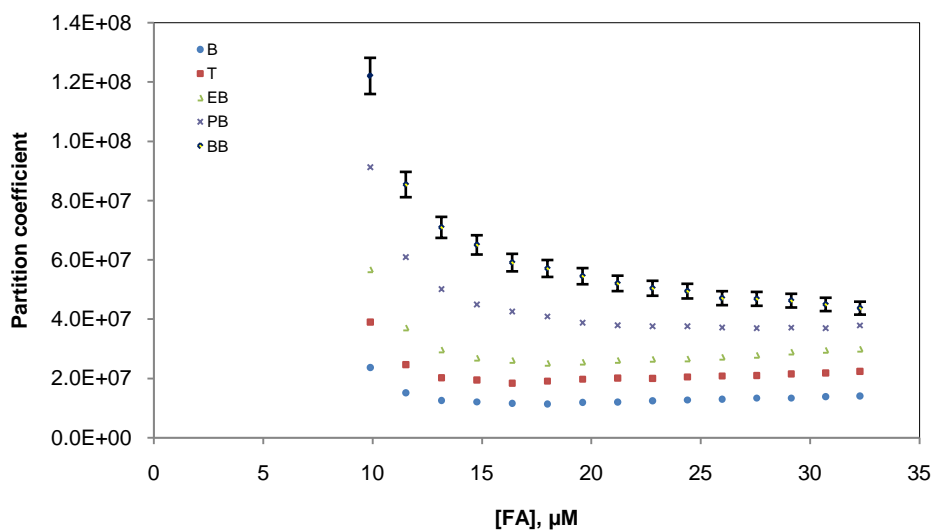


Figure 15. Effect of total FA concentration on water-aggregate pseudophase partition coefficient of n-alkylbenzene at 25.0⁰ C.

4.2.5. Intra-aggregate activity coefficient

As shown earlier that estimation of activity coefficient of n-alkylbenzene solute partitioned inside the aggregate is possible by using equation 25 and the literature values of the infinite dilution activity coefficient of solute in water ⁷¹. **Figure 16** shows the intra-aggregate activity coefficients (γ_m) of n-alkylbenzenes with increasing FA concentrations. The data shown here are only for FA concentrations after the *cfc*. These γ_m values are 2-3 orders of magnitude lower than that of SDS and SDBS micelles. This indicates that there may be strong solvophobic and specific interactions between FA-aggregate and n-alkylbenzenes. These interactions are stronger for benzene and decrease with the length of the side chain. The average γ_m values after 20.0 μM FA for benzene, toluene, and ethylbenzene, n-propylbenzene, and n-butylbenzene are shown in **table 11**. These very low γ_m values compared to those in aqueous phase means that the aggregate interior is extremely favorable (by 8-10 orders of magnitude) compared to water for retaining these solutes and a thermodynamically, non-ideal pseudo-phase microenvironment. Also, the γ_m values obtained here are less than unity and are 2-4 orders of magnitude lower than pure n-alkylbenzene (unity as the standard state). This indicates the added attractions between the inner-core of the aggregate are greater than those between identical n-alkylbenzenes in their pure state. The leveling off of γ_m values at higher [FA] concentrations indicates that the microenvironment of the solubilized species is not altered significantly on increasing the aggregate concentration beyond a certain level. The variation of γ_m as a function of [FA] simply indicates the changing nature of the interior microenvironment of the aggregate. The data also shows benzene

has the lowest γ_m and n-butylbenzene has the highest γ_m , which indicates the aggregate microenvironment is more polarizable benzene-like and less aliphatic-like.

We estimated that the intra-aggregate volume fraction is 44 times (ratio of molar volume of FA/ benzene) lower than the intra-aggregate mole fraction (the molar volume of FA was estimated at 3950 ml/mol in water at pH 6.5 ⁸¹ and the molar volume of micellar SDS is 250 mL/mol) ⁸². Consequently, the volume fraction activity coefficients are 44 times larger. At these intra-aggregate mole fraction (10^{-7}) and volume fraction (10^{-9}) there is no significant solute-solute interaction inside the aggregate pseudo-phase. Therefore, γ_m can be regarded as the infinite dilution value for the solute inside the aggregate.

Table 11. Activity coefficients of n-alkylbenzenes in FA compared to synthetic surfactants at 25.0⁰ C. The molar volumes, mL/mol, are shown in parenthesis.

Surfactant (MV)	FA (3950)	SDBS (348)	SDS(250) ^{ref 71}
Solute	$\gamma(x10^{-4})$	$\gamma(x10^{-4})$	$\gamma(x10^{-4})$
Benzene	1.83	700	18000
Toluene	4.29	1100	23100
Ethylbenzene	11.40	2600	34800
n-Propylbenzene	36.70	7100	na
n-Butylbenzene	123.00	27400	74300

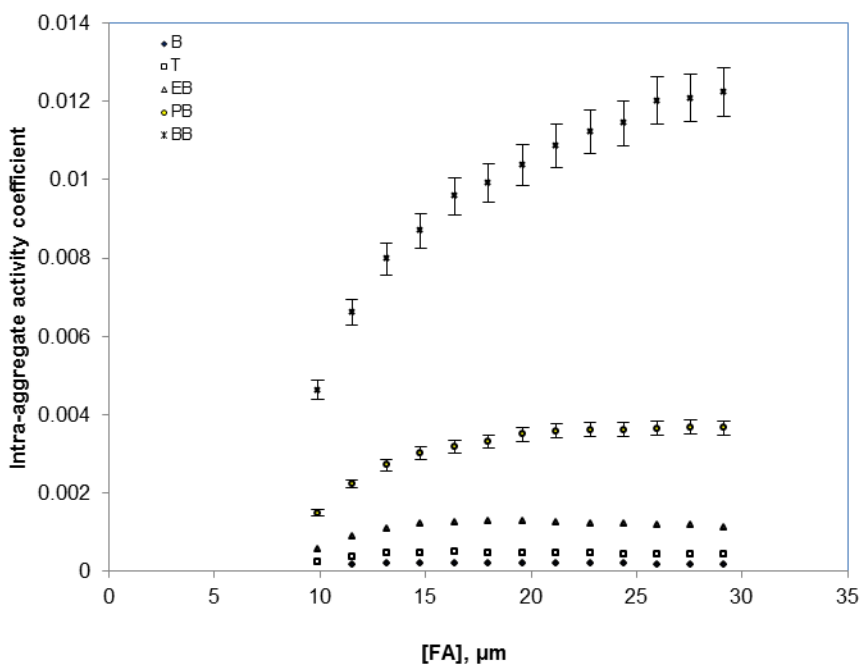


Figure 16. Effect of total FA concentration on intra-aggregate activity coefficients of n-alkylbenzene at 25.0^o C.

4.2.6. Transfer free energies of functional groups

To get further insight for the transfer of n-alkylbenzene from water to aggregate pseudo-phase, we calculated the transfer free energy of a methylene unit for such a process. Using the linear least squares fitting of $\ln(K_x)$ vs. $n\text{-CH}_2\text{-}$ in n-alkylbenzene at four different $[\text{FA}]_t$ concentrations at 14.7, 22.8, 26.5, and 30.0 μM FA yield average slope = 0.2604 ± 0.011 , average intercept = 16.63 ± 0.03 , and average $r^2 = 0.9965$. The transfer free energy, $\Delta G_{\text{transfer}} = -RT \text{ slope}_{\text{average}}$, calculated from the average slope was -155 ± 6 cal/mol per $\text{-CH}_2\text{-}$. This value is much higher than those of transfer of $\text{-CH}_2\text{-}$ groups of several solute homolog series from aqueous to various nonpolar and SDS micellar phases between -550 and -884 cal/mol⁸⁸ and SDBS (**table 12**). This is indicative

of a much lower affinity (higher free energy) for partitioning of an alkyl group in the FA aggregate pseudo-phase compared to those of surfactants containing long alkyl chain. In contrast, a much lower free energy of transfer of benzene -9722 ± 17 cal/mol ($\Delta G_{\text{transfer, benzene}} = -RT \text{ intercept}_{\text{average}}$) indicates a substantially higher affinity of benzene for FA aggregate. This is also supported by large binding constants and low intra-aggregate activity coefficient. These observations indicate that the aggregate environment is more benzene-like (highly polarizable) with specific affinity for such molecules and less alkyl-hydrocarbon like. This is also consistent with various molecular models of FA and favorable aromatic ring π - π interactions^{96,97}.

Table 12. Thermodynamic transfer free energy of n-alkylbenzenes in various surfactants at 25.0⁰ C.

Surfactant	FA	SDBS	SDS ^{ref71}
Transfer free energy of	Cal/mol	Cal/mol	Cal/mol
-CH ₂ -	-155	-236	-580
	-9722	-6426	-4150 ^a

a. from reference (98)

4.3. Humic acid-n- alkylbenzene system

In this section, we studied the aggregation process of HA the same way we followed in the case of SDBS and FA. Since humic substances (FA and HA) strongly affect the bioavailability and transport of organic substances in sediments, aquifers, and soils, we extended this work to cover HA to compare its data to those of FA. Like fulvic

acid, the present work shows HA forms aggregates starting at some critical concentration called critical humic acid aggregation constant, chc . Since the molecular weight of HA acid is not known, the concentration used for the following work is reported in mg/L and therefore, the moles cannot be calculated and the data from this experiment are shown in

Table 13.

Table 13. Table shows peak area ratio for the addition of HA in aqueous solution of n-alkylbenzenes at pH 7.5 and 25.0⁰ C. Given the A^0 one can calculate A_i for each entry.

Run#	Humic acid	Benzene	Toluene	Ethylbenzene	n-Propylbenzene	n-Butylbenzene
	Pure peak area, $A^0 \rightarrow$	22725	54885	48514	48583	25791
	HA, mg/L	↓Peak area ratio, A^0/A_i				
0.00	0.00	1.00	1.00	1.00	1.00	1.00
1.00	1.61	1.01	1.03	1.04	1.04	1.04
2.00	3.21	1.02	1.04	1.07	1.08	1.09
3.00	4.81	1.04	1.10	1.14	1.16	1.15
4.00	6.41	1.04	1.19	1.30	1.37	1.36
5.00	8.00	1.05	1.26	1.42	1.57	1.59
6.00	9.58	1.06	1.34	1.52	1.74	1.81
7.00	11.16	1.06	1.42	1.63	1.88	2.03
8.00	12.74	1.06	1.49	1.77	2.05	2.32
9.00	14.31	1.06	1.57	1.87	2.21	2.58
10.00	15.87	1.07	1.66	1.98	2.38	2.84
11.00	17.43	1.07	1.73	2.10	2.57	3.03
12.00	18.99	1.07	1.82	2.21	2.70	3.22
13.00	20.54	1.07	1.91	2.34	2.89	3.47
14.00	22.09	1.08	2.00	2.45	3.10	3.68
15.00	23.63	1.08	2.09	2.58	3.25	3.85
16.00	25.17	1.08	2.18	2.69	3.40	4.01
17.00	26.71	1.08	2.28	2.81	3.54	4.18
18.00	28.24	1.08	2.38	2.95	3.70	4.33
19.00	29.76	1.09	2.48	3.10	3.82	4.45

4.3.1. Solute-humic acid association constant, K_{11}

Like the case with FA, the addition of HA to a solution containing n-alkylbenzenes as solute reduces the free concentration of monomer solute in the aqueous and the vapor phase due to binding and partitioning of solute in solution. The peak area ratio (A^0/A_i) vs. total humic acid concentration is shown in **Figure 17**. It clearly shows the pre- and post-aggregation regions. The post aggregation region is more linear than the pre-aggregation region. The results of the linear regression of the limited data in the pre-aggregation region are shown in **table 14**. The calculated K_{11} value increases as the number of methylene group increases in the benzene homologues with comparable values for n-propylbenzene and n-butylbenzene. This association is also driven by hydrophobic forces, because the strength of that interaction increases with increasing hydrophobicity of the n-alkylbenzenes (length of the side chain). The large K_{11} values indicate there is strong association of n-alkylbenzenes with humic acid. Our results are similar to that of pyrene- humic binding constant found to be in the range of $(3.1 - 55.1) \times 10^3 \text{ L/mg}^{99}$ which are in the same order of magnitude. The K_{11} values for FA-, SDBS- and SDS-n-alkylbenzenes are listed in **table 14**. Clearly, the K_{11} for HA is at least 2, 3 and 4 orders of magnitude higher than those for FA, SDBS, and SDS, respectively. This is due to the small size of FA, SDBS and SDS monomer compared to a single HA; the latter has sizeable nonpolar hydrophobic aromatic and aliphatic groups, greater phenolic content, greater carbon content, and greater molar volume (molecular weight), than the corresponding SDBS, SDS or the fulvic acids^{100,101}.

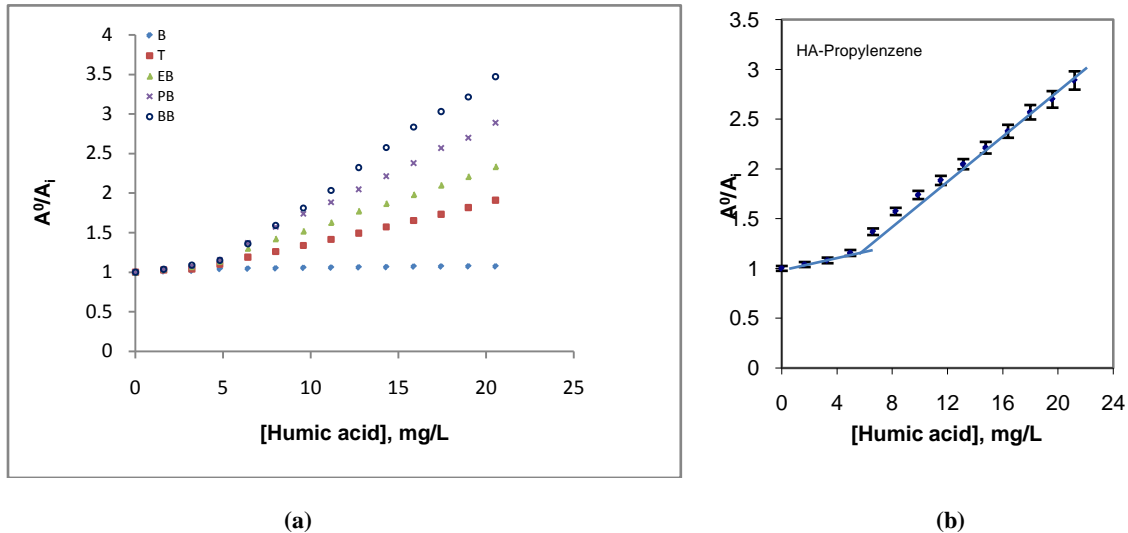


Figure 17. (a) Peak area ratio A^0/A_i vs. $[HA]_t$ for n-alkylbenzenes at 25.0°C . (b) Figure shows the intersection of two lines outlined in the theory section. Typical experimental errors are shown for benzene and the straight line. The error bars indicate larger error at lower vapor phase concentration.

Table 14. Values of K_{11} from linear least-squares regression of A^0/A_i vs. $[HA]_t$ in the pre-aggregation region at pH 7.5 and 25.0°C . Literature K_{11} for SDS-solute, our FA-, and SDBS-solute values are listed in the table. The values for FA, SDBS, and SDS are converted to L/g from L/mol described earlier.

Solute	K_{11} (L/g)	Intercept	r^2	K_{11} , L/g (FA-solute)	K_{11} , L/g (SDBS-solute)	K_{11} , L/g (SDS-solute) ^{ref 71}
Benzene	8701 ± 3.0	1.0034 ± 0.032	0.9330	73	0.67	0.0009
Toluene	24899 ± 13	0.9933 ± 0.053	0.9592	125	1.22	0.0347
Ethylbenzene	39963 ± 3.1	0.9863 ± 0.088	0.9584	180	1.93	0.0867
n-Propylbenzene	70655 ± 6.1	0.9590 ± 0.160	0.8862	286	3.40	0.1897
n-Butylbenzene	67657 ± 14.3	0.9628 ± 0.138	0.9085	381	4.50	0.4300

^a K_{11} is interpolated from a linear fit of $\ln K_{11}$ vs. # $-\text{CH}_2-$ ($r^2 = 0.9846$)

4.3.2. Critical humic acid aggregation concentration (*chc*)

Like most surfactants and FA, HA forms aggregate starting at some critical concentration. We call it critical humic acid aggregate concentration, *chc*. Any excess HA added after this concentration goes into the formation of more aggregates. The *chc* was found from the point of intersection of two straight lines in the pre- and post-aggregate regions, as shown in **Figure 17b** and was found to be 4.81 ± 0.02 mg/L HA. The *chc* values of these solutes showed no systematic trend with respect to alkyl chain length. This eliminated the possibility of a solute induced *chc* change with increase in alkyl chain length. Apparently, the very low concentration of n-alkylbenzenes (10^{-7} mole fraction) used in this study has no influence on the aggregate structure. It is reported that some critical aggregation concentration of HA occurs at 1.0 mg/L or lower with uncertainty in the exact concentration¹⁰². There is a wide range from the literature for *chc* values ranging from 100-1010 mg/L using completely different techniques and different solution preparations¹⁰³. The diversity in *chc* values in the literature are also attributed to HAs origin or biomass manipulations^{104,105}. And since *chc* values are highly affected by the origin and other structure related parameters, the adjustment and modification for highest potency is possible^{104,105}. Qudari *et al* reported that mixing food wastes with lignocelluloses wastes decreased the *cmc* value by a factor of up to 8.63¹⁰⁵. It is important to note that the *chc* obtained by our method is clearly discernible as a breakpoint in change of concentration solute in the vapor phase. The literature values of *chc* are much higher because the techniques used by others are not sensitive to detect small changes in concentrations of solute in liquid or in vapor. It is entirely possible that

there may exist more than one *chc* for HA. The first one is at low concentration with low aggregation number and the second one is at much higher concentration with a large aggregation number. Such as the *chc* with a range 100 – 1010 mg/L was reported by others¹⁰³. Clearly, the huge uncertainties in literature values of *chc* stem from nature, origin, and the chemical composition of humic acid. Apparently, HA is not available as pure as FA.

4.3.3. Solute-aggregation association constant, K_{n1}

The exact nature of humic acid aggregate is not known with a fixed aggregation number. However, we have shown that there is a critical concentration of HA where a pseudo-phase aggregation can be inferred. **Figure 17** shows the peak area ratio increases significantly as the concentration of HA increases and more solute associates with the aggregate. This decreases the concentration of free monomer solute in aqueous phase and in the vapor phase. The HS's aggregation number, n , is assumed to be 20 same as that of FA¹⁰. If we assume that aggregation number, n , is inversely proportional to the molecular weight (~1000 for FA and 3000 for HA), the n for HA would be 6. In absence of any information on the aggregation number for HA, this assumption is made for the sake of comparison. The K_{n1} values, obtained from the regression of the data in this region, are shown in **table 15** assuming this aggregation number. It shows that HA-aggregate K_{n1} values are at least 3 orders of magnitude higher than that of SDS- n -alkylbenzene values. This is also consistent with K_{11} measurements. By comparing K_{11} and K_{n1}/n (association constant per unit of HA in aggregations), we find that the tendency

of a single HA in the aggregate pseudo-phase to bind an n-alkylbenzene is 5-30 times higher than that of an isolated HA in the solution. These significant differences in the two binding constants show that the solute solubility from the bulk is very different in the aggregate pseudo-phase due to their structure and the hydrophobicity. The large binding constants confirm the presence of a strongly hydrophobic region in the aggregate for n-alkylbenzene like molecules and even more hydrophobic than FA. For HA the number of aggregates per n-alkylbenzene could even be less due to its smaller aggregation number. Therefore, K_{11} , K_{n1} , and other distribution properties for HA reported here can be regarded as their infinite dilution values.

Table 15. Values of K_{n1} from linear least-squares regression of A^0/A_i vs. $[HA]_t$ in the post-aggregation region at pH 7.5 and 25.0⁰C. The aggregation number n is also shown for the surfactants. The values for FA, SDBS, and SDS are converted to L/g from L/mol.

Solute	K_{n1} , (L/g) n= 6	r^2	K_{n1} , (L/g) (FA) _n n= 20	K_{n1} , (L/g) (SDBS) _n n= 26	K_{n1} , (L/g) (SDS) _n ^{ref 71} n= 60
Benzene	15190 ± 1200	0.9842	4781	44.8	5.1
Toluene	296844 ± 4300	0.9887	7718	97.0	14.5
Ethylbenzene	433740 ± 5500	0.9820	9585	141.8	35.4
n-Propylbenzene	593088 ± 7100	0.9982	12044	231.8	98.1
n-Butylbenzene	659880 ± 3900	0.9972	15870	231.3	264.0

^a K_{n1} is interpolated from a linear fit of $\ln K_{n1}$ vs. # -CH₂- ($r^2 = 0.9996$)

4.3.4. Solute-aggregate partition coefficient, K_x

The solute–aggregate partition coefficient is a quantitative measure of solubilization of hydrocarbons in presence of HA and indicates the partitioning of solute between two immiscible but mutually saturated phases. **Figure 18** shows the dependency of K_x on the total [HA] concentration. It shows as $[HA]_t$ increases, the aggregates concentration also increases and K_x values appear to level off at the end. From **Figure 18**, it is seen that K_x values become constant above ca. 12 mg/L [HA]. The average K_x after 12 mg/L HA is relatively constant within 5% rsd. The values are 2.25×10^5 , 29.5×10^5 , 43.0×10^5 , 56.4×10^5 , and 65.8×10^5 for benzene, toluene, ethylbenzene, n-propylbenzene, and n-butylbenzene, respectively and these values are two orders of magnitude lower than that of FA as shown in **table 16**. From these results, we conclude that pseudo-phase microenvironment of FA is more aromatic from inside and covered with $-\text{COOH}$ from the outside than that of HA. However, the binding of single n-alkylbenzene is much higher with HA compared to that of FA due to the larger size of HA and the nonpolar-polarizable environment.

Similar to FA, the K_x values show that the enhanced solubilization of hydrophobic n-alkylbenzenes is due to the partitioning of the solutes into the HA aggregate phase. Therefore the more hydrophobic the solute molecule is the higher its partitioning becomes as seen with the trend in K_x values moving from the least hydrophobic benzene to the most hydrophobic n-butylbenzene. This is true for HA, FA, SDBS, and SDS. The drop in K_x from lower [HA] to high [HA] and subsequent leveling

off may be due to the same reasons explained earlier. There is no similar data for the partitioning of n-alkylbenzenes in the literature to compare with.

Table 16. Partition coefficients of n-alkylbenzenes in HA compared to other surfactants at 25.0⁰ C.

Surfactant	HA	FA	SDBS	SDS ^{ref71}
Solute	$K_x (x10^4)$	$K_x (x10^4)$	$K_x (x10^4)$	$K_x (x10^4)$
Benzene	22.5	1342.0	3.81	0.13
Toluene	295.0	2130.0	8.67	0.40
Ethylbenzene	430.0	2830.0	12.6	0.96
n-Propylbenzene	564.0	3730.0	19.4	na
n-Butylbenzene	658.0	4640.0	20.5	na

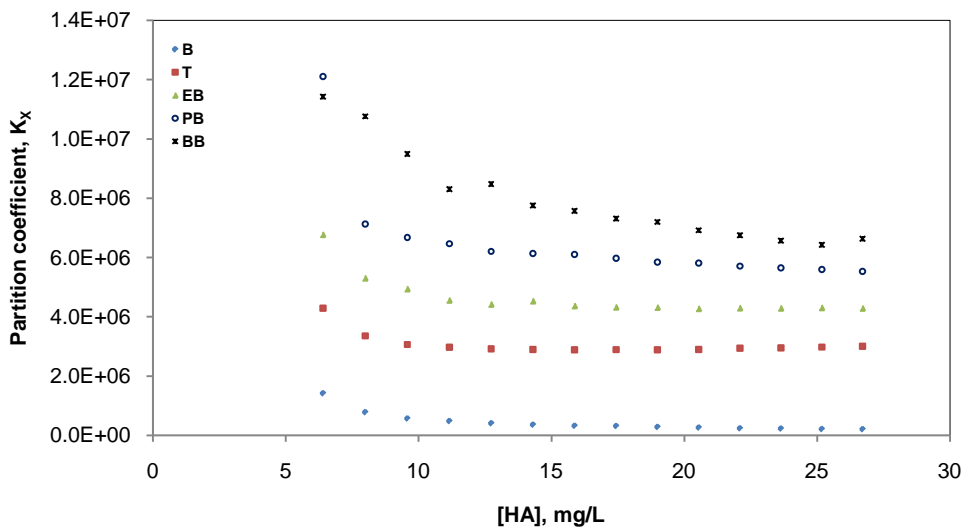


Figure 18. Effect of total HA concentration on water-aggregate pseudo-phase partition coefficient of n-alkylbenzene at pH 7.5 and 25.0⁰ C.

4.3.5. Intra-aggregate activity coefficient of n-alkylbenzene in HA

The activity coefficient is a measure of non-ideality or hydrophobicity of a solute in a solvent compared to a standard state of pure solute. Therefore, it is a direct measure of solute-solvent interactions at infinite dilution. As shown earlier that estimation of activity coefficient of n-alkylbenzene solute partitioned inside the aggregates is possible by using **equation 25** and the literature values of the infinite dilution activity coefficient of solute in water. **Figure 18** shows the intra-aggregate activity coefficients (γ_m) of n-alkylbenzenes with increasing HA concentrations. The data shown here are only for HA concentrations after the cac. As shown in **table 17**, γ_m values are 1-2 orders of magnitude higher than those of FA and 1-2 orders of magnitude lower than those of SDS micelles⁷¹. This could mean there are strong solvophobic (repulsive) and specific interactions between HA-aggregate and n-alkylbenzenes. These interactions are stronger for benzene and decreases with the length of the side chain as the γ_m increases. The average γ_m values after 12.5 mg/L HA for benzene, toluene, and ethylbenzene, n-propylbenzene, and n-butylbenzene are 0.0110, 0.0031, 0.0076, 0.0241, and 0.0861 compared to that of 2480, 9190, 32700, 136000, and 566000, respectively, in water continuous phase.

This means the aggregate interior is extremely favorable (by 5-7 orders of magnitude) compared to water for housing these solutes. Also, all of the γ_m values obtained here are less than unity and 1-2 orders of magnitude lower than pure alkyl benzene (unity as the standard state). This indicates the added attractions between the hydrophobic inner core of the aggregate are greater than those between identical n-alkylbenzenes in their pure state.

Similar to FA, the γ_m values at higher [HA] stabilized and did not change much. The variation of γ_m as a function of [HA] simply indicates the changing nature of the interior solvophobic microenvironment of the aggregate. **Figure 18** shows benzene has the lowest γ_m and n-butylbenzene has the highest, which indicates the aggregate microenvironment is more polarizable benzene like and less aliphatic like.

Table 17. Activity coefficient of humic acid compared to other surfactants at pH 7.5 and 25.0^o C.

Surfactant	HA	FA	SDBS	SDS^{ref 71}
Solute	$\gamma(x10^{-4})$	$\gamma(x10^{-4})$	$\gamma(x10^{-4})$	$\gamma(x10^{-4})$
Benzene	110	1.83	700	18000
Toluene	31	4.29	1100	23100
Ethylbenzene	76	11.40	2600	34800
n-Propylbenzene	241	36.70	7100	na
n-Butylbenzene	861	123.00	27400	74300

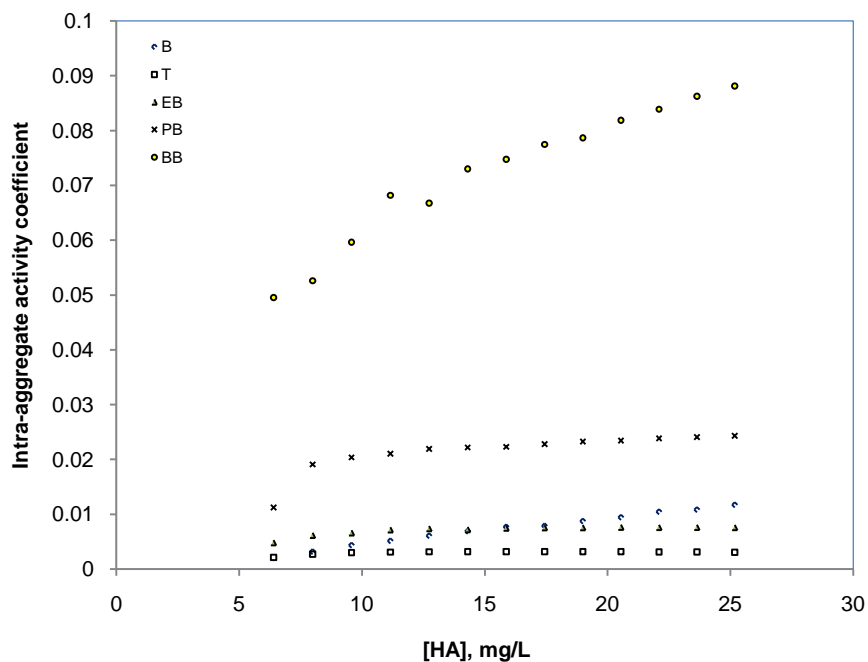


Figure 19. Effect of total HA concentration on intra-aggregate activity coefficients of n-alkylbenzene at pH 7.5 and 25.0⁰ C.

4.3.6. Transfer free energies of functional groups

The transfer free energy of a methylene and aryl units from aqueous medium to HA aggregate were calculated using the linear least squares fitting of $\ln(K_x)$ vs. $n\text{-CH}_2\text{-}$ in n-alkylbenzene at three different $[\text{HA}]_t$ concentrations at 15.9, 20.5, and 25.2 mg/L HA. The results are shown in **table 18**. The value of $-\text{CH}_2\text{-}$ is much higher than those of transfer of $-\text{CH}_2\text{-}$ groups of SDS and SDBS, and slightly lower than that of FA. This is indicative of a much lower affinity (higher free energy) for partitioning of an alkyl group in the HA aggregate pseudo-phase compared to those of the aforementioned synthetic surfactants. Also, the value of free energy of transfer of benzene was higher than that of FA and lower than those of SDS and SDBS. And that tells the affinity of aryl group for

HA aggregate. These values indicate that the aggregate environment is more benzene-like (highly polarizable), with specific affinity for such molecules and less alkyl-hydrocarbon like. Humic aggregate environment is less aromatic compared to that of FA. It could be due to the larger number of aggregate FA.

Table 18. Thermodynamic transfer free energy of n-alkylbenzenes in various surfactants at pH 7.50 and 25.0 °C.

Surfactant	HA	FA	SDBS	SDS ^{ref 71}
Transfer free energy of	cal/mol	cal/mol	cal/mol	cal/mol
-CH ₂ -	-194	-155	-236	-580
	-8013	-9722	-6426	-4150 ^a

4.4. Effect of pH on the association of n-alkylbenzenes with FA

Both FA and HA are molecules containing large numbers of -COOH and phenolic-OH groups as shown in **Table 1**. It is reported by Chen and Schnitzer⁶² humic substances are neutral at low pH and charged at higher pH. Therefore, one would expect to observe significant change in their structure and conformation when pH is changed, particularly when the solution is acidic. In this section, we tested the effect of the pH on the association and partitioning of n-alkylbenzenes with fulvic acid. This study compares the data for pH 5.5 and pH 7.6. The solutions were freshly prepared to make sure there was no change in the pH since no buffer was use. The conditions used for this experiment

were similar to that described for FA and the only change was raising the pH to 7.6; the data from this experiment are shown in **table 19**.

Table 19. Table shows peak area ratio for the addition of FA in aqueous solution of n-alkylbenzenes at 25.0⁰ C and pH 7.6. Given the A⁰ one can calculate A_i for each entry.

Run#	moles of FA added	Fulvic	Benzene	Toluene	Ethyl benzene	n-Propyl benzene	n-Butyl benzene
		Pure peak area, A ⁰ →	3347	16405	31277	62555	48492
		FA, uM	↓Peak area ratio, A ⁰ /A _i				
0.00	0.00E+00	0.00	1.00	1.00	1.00	1.00	1.00
1.00	2.66E-08	1.66	1.21	1.38	1.43	1.58	1.65
2.00	5.30E-08	3.31	1.55	1.90	2.06	2.55	2.93
3.00	7.94E-08	4.97	1.73	2.51	3.00	4.00	5.02
4.00	1.06E-07	6.61	2.15	2.94	4.02	6.02	8.22
5.00	1.32E-07	8.25	2.56	3.83	5.43	8.99	13.25
6.00	1.58E-07	9.89	3.07	4.83	6.90	12.23	19.03
7.00	1.84E-07	11.52	3.58	6.14	8.81	15.68	25.26
8.00	2.10E-07	13.14	4.06	6.67	10.33	18.79	31.31
9.00	2.36E-07	14.76	4.89	7.90	11.91	21.74	33.96
10.00	2.62E-07	16.38	5.60	9.40	13.96	24.08	37.22
11.00	2.88E-07	17.99	5.81	10.03	15.18	27.63	41.09
12.00	3.14E-07	19.60	6.86	11.95	17.94	29.60	43.49
13.00	3.39E-07	21.20	7.50	13.74	19.54	31.18	46.23
14.00	3.65E-07	22.80	8.28	14.86	21.08	33.26	48.01
15.00	3.90E-07	24.39	9.22	16.84	23.10	35.26	50.72
16.00	4.16E-07	25.98	9.99	18.05	24.25	38.28	53.64
17.00	4.41E-07	27.56	10.80	20.71	26.00	39.49	55.48
18.00	4.66E-07	29.14	11.70	22.41	29.18	42.35	58.28
19.00	4.91E-07	30.71	12.49	26.63	30.22	44.81	60.84
20.00	5.16E-07	32.28	19.13	26.50	33.45	46.30	60.62

4.4.1. Solute-fulvic acid association constant, K_{11} : Effect of pH

The peak area ratio (A^0/A_i) vs. total fulvic acid concentration at the two different pH values are shown in **Figure 20**. Obviously, the pH adjustment has an insignificant effect on *cfc* value. The results of the linear regression of the limited data in the pre-aggregation region for the two pH values are shown side by side in **table 20**. The calculated K_{11} value increases as the number of methylene group increases in the benzene homologues and with increasing pH in water. At pH 5.5 (low), most of the functional groups namely, -OH and -COOH are neutral⁶², and they become ionized at pH 7.6 (higher pH). When these groups are fully or partly ionized, the electrostatic interaction (intramolecular repulsion) among these charged functional groups as well as their interactions with the bulk solution affects their conformation and consequently their hydrophobic interactions with the solute. It has been reported that increasing pH of FA results in more expanded structure of FA molecules, opening more exposed sites for interactions^{24,81, 106, 107}.

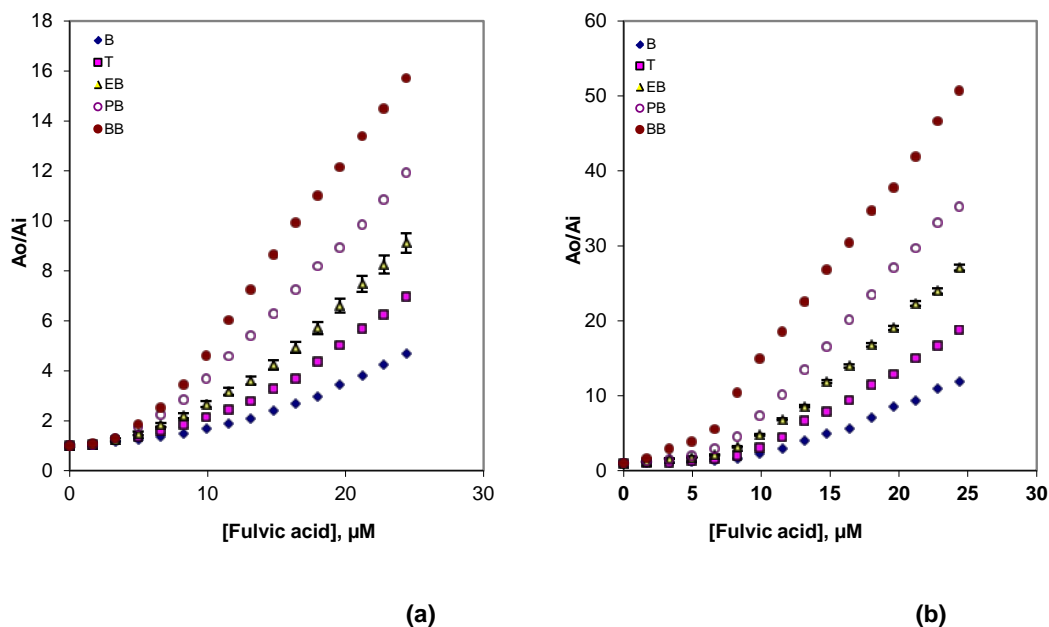


Figure 20. Peak area ratio A^0/A_i vs. $[FA]_t$ for n-alkylbenzenes at 25.0⁰ C and pH (a) 5.5 (b) 7.6.

Table 20. Values of K_{11} from linear least-squares regression of A^0/A_i vs. $[FA]_t$ in the pre-aggregation region at 25.0⁰ C and three different pH values.

pH	5.5	7.6
Solute	$K_{11} (10^3 \times M^{-1})$	$K_{11} (10^3 \times M^{-1})$
Benzene	69.5 ± 1.0	186.9 ± 2.5
Toluene	118.6 ± 1.3	335.9 ± 7.0
Ethylbenzene	171.0 ± 3.1	317.0 ± 6.5
n-Propylbenzene	272.1 ± 6.1	947.1 ± 16.3
n-Butylbenzene	362.5 ± 14.3	1437.1 ± 19.7

4.4.2. Critical fulvic acid aggregation concentration (cfc): Effect of pH

As shown in **Figure 20**, the *cfc* decreases slightly with increasing pH of FA. The average *cfc* was found to be 8.87 ± 0.06 and 8.21 ± 0.05 μM FA at pH 5.5, and 7.6, respectively. This decrease in *cfc* may be due to the fact that the development of charged

acidic functional groups on FA begins at pH 7.6. Therefore, the resulting electrostatic repulsion produces stability for any premature aggregate.

4.4.3. Solute-aggregation association constant, K_{n1} , at different pH

Figure 20 shows the peak area ratio increases significantly as the concentration of FA increases and more solute associates with the aggregate. The K_{n1} values for the two pH values are summarized in **table 21**. Similar to K_{11} , K_{n1} values increase with increasing pH and increase up to one order of magnitude from neutral form to partially charged forms of FA. The large binding constants show that the hydrophobic domain in FA increase in size with increasing pH. The electrostatic forces between the functional groups cause an increase in the size of the aggregate to impart the maximum stability. Therefore, the pseudo-phase will be composed of more extended FA monomers and more sites for interaction become available.

Table 21. Values of K_{n1} from linear least-squares regression of A^0/A_i vs. $[FA]_t$ in the post-aggregation region at 25.0 °C and different pH values.

pH	5.5	7.6
Solute	$K_{n1} (10^3 \times M^{-1})$	$K_{n1} (10^3 \times M^{-1})$
Benzene	1390 ± 1.2	8088 ± 8.3
Toluene	2372 ± 4.3	15614 ± 12.4
Ethylbenzene	8910 ± 5.5	22184 ± 13.8
n-Propylbenzene	11408 ± 7.1	32678 ± 16.0
n-Butylbenzene	13812 ± 3.9	43472 ± 18.2

4.4.4. Effect of pH on solute-aggregate partition coefficient, K_x

Figure 22a and **b** show a plot of K_x on the total [FA] concentration. They show, as $[FA]_t$ increases the aggregates concentration also increase and K_x values appear to level off to a constant value at the end. From these **Figures**, it is seen that K_x values become constant above cfc. 15 and 18 μM [FA] at pH 5.5 and 7.6, respectively. The average K_x values are summarized in **table 22**. And as shown, the partition coefficients increase considerably with increasing pH. This trend is attributed to the increased size and stability of the aggregate as pH increases. From these results we conclude that the microenvironment formed by FA consists of a hydrophobic core of aromatic nature and hydrophilic outer layer of acidic groups as shown in **figure 21**.

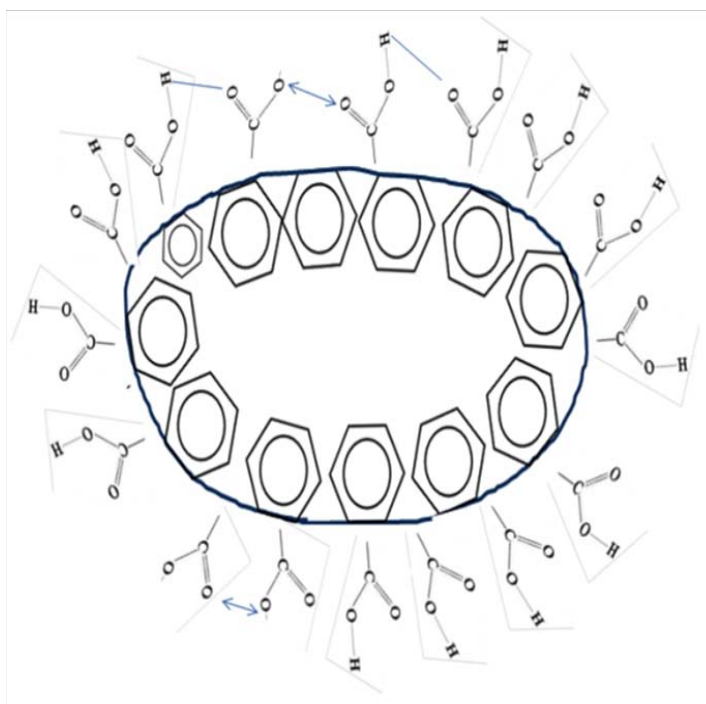


Figure 21. Proposed microenvironment of n-alkylbenzenes in the pseudo-phase of FA aggregate. It shows the inner core is of aromatic nature and the outer layer H-bonded carboxylic groups.

Table 22. Partition coefficients of n-alkylbenzenes in FA at 25.0⁰ C and different pH values.

pH	5.5	7.6
Solute	$K_x (x10^1)$	$K_x (x10^1)$
Benzene	1.34	2.83
Toluene	2.13	5.90
Ethylbenzene	2.83	7.30
n-Propylbenzene	3.73	10.97
n-Butylbenzene	4.64	15.24

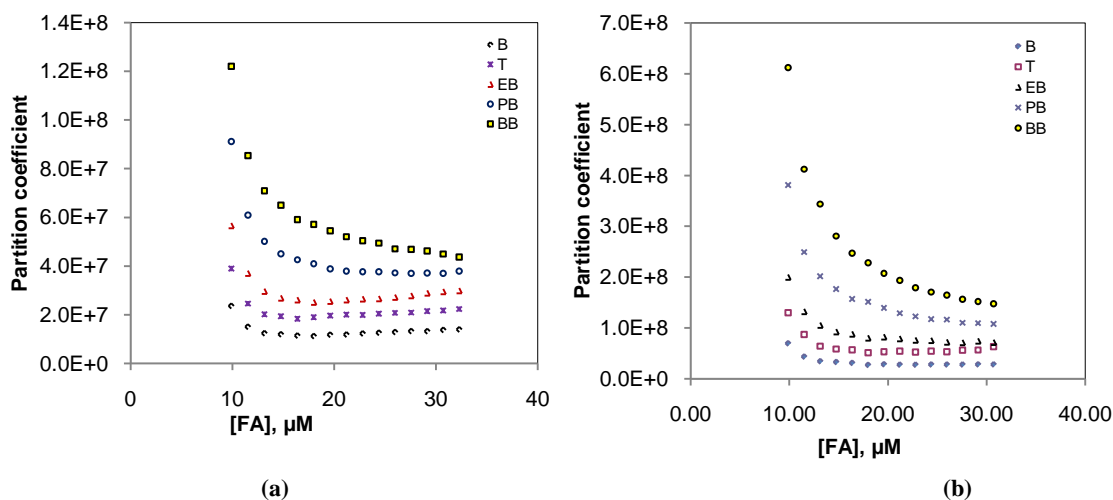


Figure 22. Effect of total FA concentration on water-aggregate pseudo-phase partition coefficient of n-alkylbenzene at 25.0⁰ C and pH (a) 5.5 and (b) 7.6.

4.4.5. Effect of pH on intra-aggregate activity coefficient

Although n-alkylbenzenes are neutral species, there is no direct effect of pH on them. However, pH could change the hydrophobicity of the humic materials and change their conformation and even cause precipitation at lower pH. Consequently, the binding and partitioning of the solute can change. **Figure 23** shows the intra-aggregate activity coefficients (γ_m) of n-alkylbenzenes with increasing FA concentrations at both pH values. The average γ_m values are shown in **table 23**. The γ_m values decrease with increasing pH and this could mean there are stronger solvophobic and specific interactions between FA-aggregate and n-alkylbenzenes in the basic medium where some functional groups are ionized. The variation of γ_m as a function of pH simply indicates the changing nature of the interior solvophobic microenvironment of the aggregate. In both mediums, these interactions are stronger for benzene and decrease with the length of the side chain.

Table 23. Intra-aggregate activity coefficients of n-alkylbenzene in FA at 25.0⁰ C and different pH values.

pH	5.5	7.6
Solute	$\gamma(\times 10^{-4})$	$\gamma(\times 10^{-4})$
Benzene	1.83	0.86
Toluene	4.29	1.56
Ethylbenzene	11.40	4.48
n-Propylbenzene	36.70	12.40
n-Butylbenzene	123.00	37.21

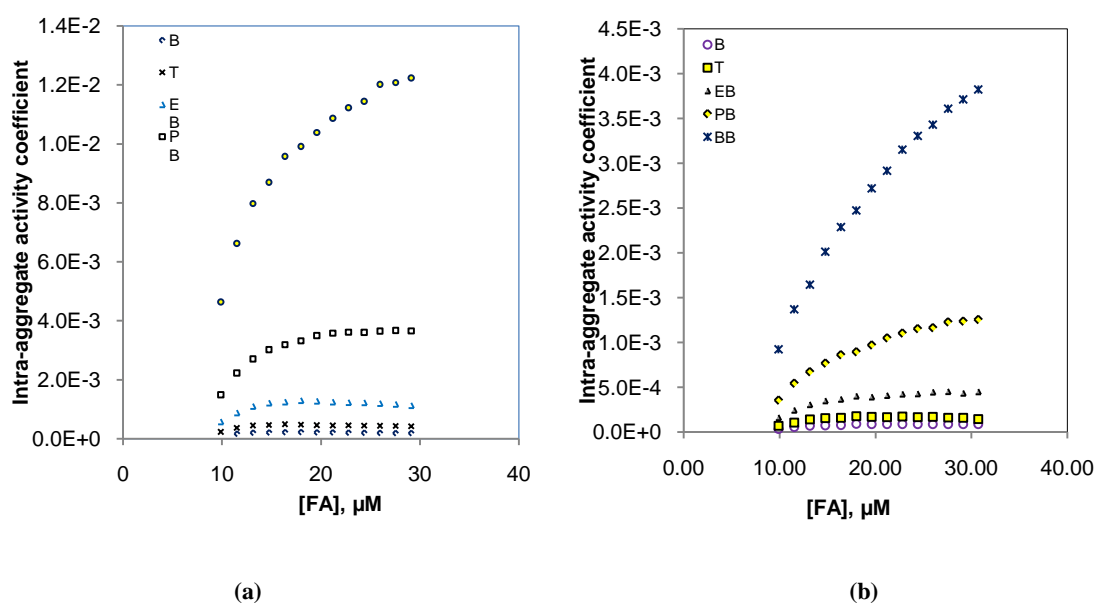


Figure 23. Effect of total FA concentration on intra-aggregate activity coefficients of n-alkylbenzene at 25.0⁰ C and pH (a) 5.5 and (b) 7.6.

4.4.6. Effect of pH on the transfer free energies of functional groups

Transfer free energy of a methylene and aryl units from aqueous to FA aggregate at each FA medium is shown in **table 24**. The results of the transfer free energy of $-\text{CH}_2-$

decreases with increasing pH indicating more favorable environment for $-\text{CH}_2-$ partitioning at higher pH. Also, the much lower free energy of transfer of benzene decrease with increasing pH. This again, shows the ordering of aromatic moieties of FA aggregates is better at higher pH. It is known that at lower pH (5.5), there are homo and hetero inter- or intra-molecular hydrogen bonding between the carboxylic $-\text{COOH}$ groups and the phenolic $-\text{OH}$. This decreases the size of FA by folding around itself. Therefore, the exposed aromatic moieties available for interaction are limited. On the other hand, at elevated pH these acidic groups become deprotonated. As a result, the size increases due to two reasons; first, these charged groups repel each other, and secondly, the hydrogen bonding decreases.

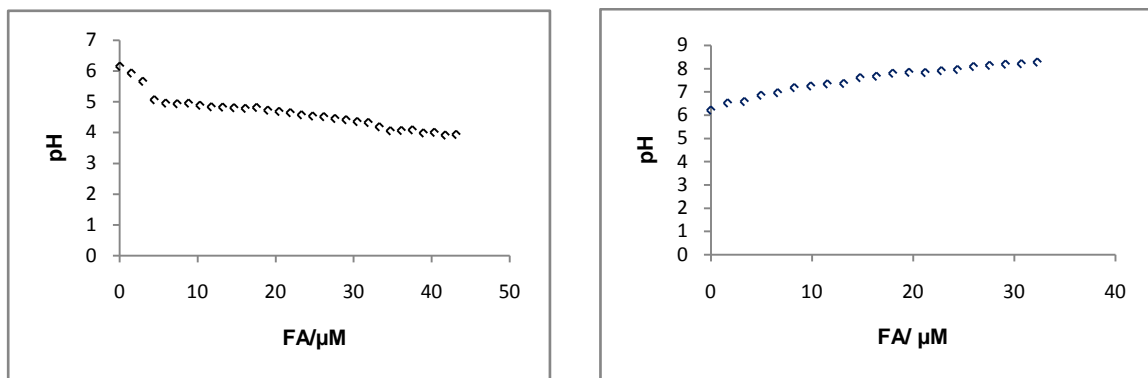
Table 24. Thermodynamic transfer energy of alkylbenzenes 25.0 °C and different pH values.

pH	5.5	7.6
Transfer free energy of	cal/mol	cal/mol
$-\text{CH}_2-$	-155 ± 6	-245 ± 35
	-9722 ± 17	-10300 ± 50

4.4.7. pH profile during addition of FA

In order to understand the change in pH during addition of FA in the HSGC experiments; we measured the pH of the solution in separate similar experiments. The results show pH change has a significant effect on acidic functional groups- carboxylic

and phenolic groups- and hence, affects the aqueous behavior of fulvic acid. Since the pH adjustment was not carried out using buffer, this experiment was essential because the pH of the aqueous solution containing n-alkylbenzenes may not remain the same during the addition of FA. The experiment started with addition of FA stock solution at both pH values covered in this work (2.4 and 11.9). The initial pH of the B-BB stock solution was 6. It is slightly acidic due to the dissolved atmospheric CO₂ (g). **Figure 24** shows the pH change during the addition of FA to the aqueous B-BB solution. The pH of the mixture drops from 6 until it reaches concentration near the *cfc*, then remains constant with an average of 5.5 and standard deviation of 0.41 in the case of pH 2.4 as shown in figure **24 a**. And it rises from pH 6 until it reaches concentration near the *cfc*, then remains steadily with an average of 7.6 and standard deviation of 0.32 in the case of pH 11.9 as shown in figure **24 b**. We note that the use of buffer is not common in such studies except for metal ion complexation studies¹⁰⁸.



(a)

(b)

Figure 24. Figures show pH change during addition of FA stock solution at 25.0⁰ C and initial pH of (a) 2.35 and (b) 11.92.

4.5. Effect of temperature on the association of n-alkylbenzenes with FA

In order to get a clear understanding of thermodynamic parameters for the binding and partitioning of n-alkylbenzenes with fulvic acid we studied the temperature dependence of the parameters discussed earlier. Binding and association parameters were obtained at 25⁰, 30⁰, and 40⁰C and the data for the experiment done at 30 and 40⁰ C are shown in **table 25** and **26**, respectively.

Table 25. Table shows peak area ratio for the addition of FA in aqueous solution of n-alkylbenzenes at pH 5.5 and 30.0⁰ C. Given the A⁰ one can calculate A_i for each entry.

Run#	moles of FA added	Fulvic	Benzene	Toluene	Ethyl benzene	n-Propyl benzene	n-Butyl benzene
		Pure peak area, A ⁰ →	4180	20644	41223	86461	71759
		FA, uM	Peak area ratio, A ⁰ /A _i				
0.00	0.00E+00	0.00	1.00	1.00	1.00	1.00	1.00
1.00	2.66E-08	1.66	1.05	1.14	1.09	1.10	1.06
2.00	5.30E-08	3.31	1.17	1.22	1.27	1.29	1.23
3.00	7.94E-08	4.97	1.29	1.39	1.52	1.55	1.48
4.00	1.06E-07	6.61	1.42	1.68	1.71	2.29	2.21
5.00	1.32E-07	8.25	1.52	1.95	2.02	3.48	4.62
6.00	1.58E-07	9.89	1.74	2.20	2.88	4.68	7.13
7.00	1.84E-07	11.52	2.09	2.68	3.61	6.61	9.30
8.00	2.10E-07	13.14	2.29	3.20	4.86	7.90	11.78
9.00	2.36E-07	14.76	2.49	3.85	6.28	9.88	14.18
10.00	2.62E-07	16.38	2.81	4.55	7.21	12.02	16.24
11.00	2.88E-07	17.99	3.21	5.40	8.38	13.60	18.45
12.00	3.14E-07	19.60	3.82	6.20	9.32	15.52	20.38
13.00	3.39E-07	21.20	4.29	7.14	10.55	17.44	22.22
14.00	3.65E-07	22.80	4.77	7.89	12.02	18.84	23.80
15.00	3.90E-07	24.39	5.44	9.06	13.58	21.10	25.49
16.00	4.16E-07	25.98	6.20	10.67	15.29	22.27	27.18
17.00	4.41E-07	27.56	6.92	12.14	17.25	24.15	29.05
18.00	4.66E-07	29.14	7.61	13.24	18.79	26.50	30.57
19.00	4.91E-07	30.71	8.42	15.94	21.53	28.14	32.09
20.00	5.16E-07	32.28	9.73	17.13	23.32	30.61	34.76

Table 26. Table shows peak area ratio for the addition of FA in aqueous solution of n-alkylbenzenes at pH 5.5 and 40.0⁰ C. Given the A⁰ one can calculate A_i for each entry.

Run#	moles of FA added	Fulvic	Benzene	Toluene	Ethyl benzene	n-Propyl benzene	n-Butyl benzene
		Pure peak area, A ⁰ →	6297	29971	58244	108294	77654
		FA, uM	↓Peak area ratio, A ⁰ /A _i				
0.00	0.00E+00	0.00	1.00	1.00	1.00	1.00	1.00
1.00	2.66E-08	1.66	1.09	1.17	1.36	1.27	1.24
2.00	5.30E-08	3.31	1.19	1.23	1.43	1.40	1.51
3.00	7.94E-08	4.97	1.26	1.39	1.78	1.74	2.25
4.00	1.06E-07	6.61	1.31	1.43	1.93	2.15	3.72
5.00	1.32E-07	8.25	1.42	1.75	2.59	3.50	5.05
6.00	1.58E-07	9.89	1.63	2.18	3.12	4.86	7.09
7.00	1.84E-07	11.52	1.94	2.80	4.16	6.35	9.16
8.00	2.10E-07	13.14	2.43	3.69	5.48	8.07	11.32
9.00	2.36E-07	14.76	2.70	4.35	6.63	9.35	12.82
10.00	2.62E-07	16.38	3.15	5.05	7.81	11.29	14.61
11.00	2.88E-07	17.99	3.73	6.28	9.08	12.80	16.93
12.00	3.14E-07	19.60	4.10	7.02	10.14	14.28	19.08
13.00	3.39E-07	21.20	4.55	8.18	11.24	16.24	20.67
14.00	3.65E-07	22.80	5.03	9.02	12.37	17.57	23.16
15.00	3.90E-07	24.39	5.56	10.05	13.71	19.14	25.94
16.00	4.16E-07	25.98	6.02	11.93	14.30	18.06	26.02
17.00	4.41E-07	27.56	6.52	12.24	15.49	17.50	26.33
18.00	4.66E-07	29.14	7.06	13.13	17.06	16.95	27.22
19.00	4.91E-07	30.71	7.51	13.76	17.69	14.69	28.21
20.00	5.16E-07	32.28	8.29	14.10	19.12	14.11	28.60

4.5.1. Solute-fulvic acid association constant and thermodynamic parameters: Effect of temperature on K₁₁

The values of the solute-fulvic acid association constant, K₁₁ at various temperatures are summarized in **Table 27**. These values increase with increasing temperature which is a sign of an endothermic association process driven by entropy. This is a common observation in surfactant interactions. SDS- lysozyme binding process was reported as an

endothermic process and entropy driven ¹⁰⁹ and also similar observations have been reported by others ¹¹⁰. The fact that enthalpy value is positive and relatively large indicates that this association is strong and complicated. Going from toluene to n-butylbenzene the translational entropy decreases due the increased size of the solute. For the binding process of FA, the entropy decreases due to the increased size of the solute. The total entropy change, ΔS is equal to $(S_{FA-B} - (S_{FA} + S_B))$. The entropy of n-butylbenzene, S_B is higher than that of toluene, S_T .

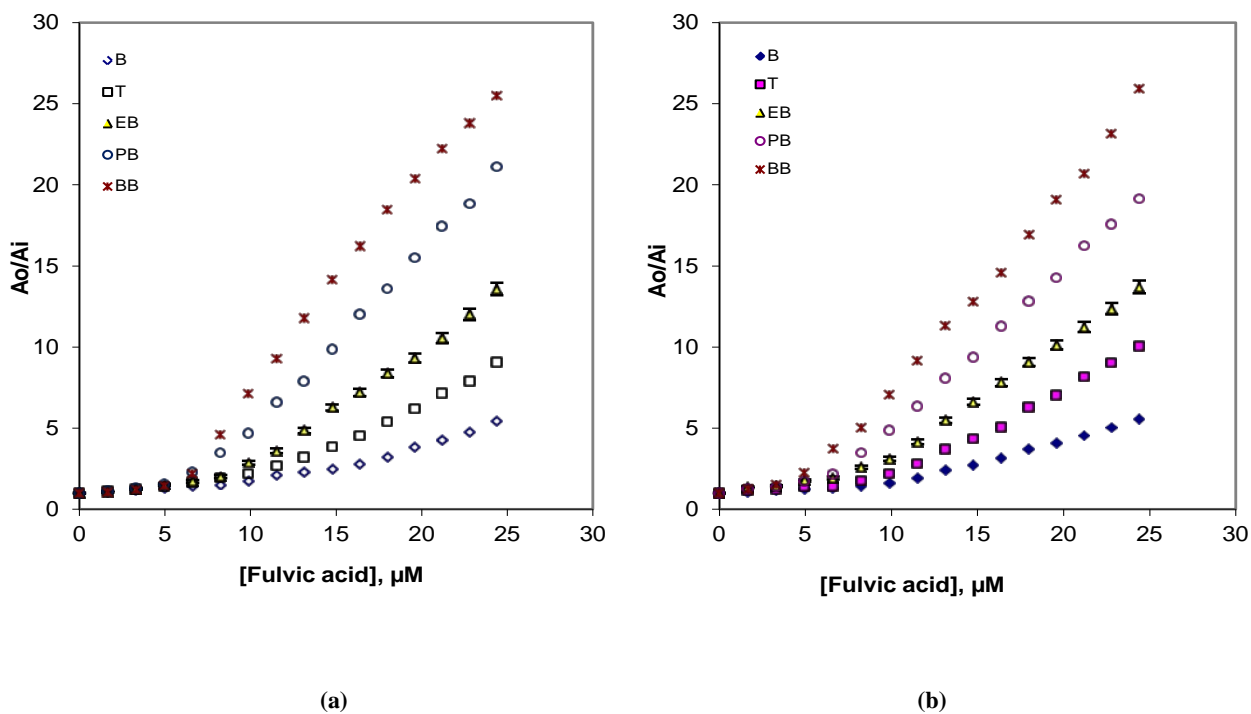


Figure 25. Peak area ratio A_o/A_i vs. $[FA]_t$ for n-alkylbenzenes at pH 5.5 and (a) 30.0 C and (b) 40.0 C.

Table 27. The solute-FA association constant, K_{11} and the thermodynamic parameters for n-alkylbenzenes-FA system at pH 5.5 and different temperatures. ^a

Solute	Benzene	Toluene	Ethylbenzene	n-Propylbenzene	n-Butylbenzene
Temperature	K_{11} ($10^3 \times M^{-1}$), ΔG^0 , ΔH^0 (k cal mol ⁻¹), ΔS^0 (cal K ⁻¹ mol ⁻¹)				
25	69.5 ± 1.0	118.6 ± 1.3	171.0 ± 3.1	272.1 ± 6.1	362.5 ± 14.3
30	87.0 ± 2.1	151.4 ± 3.1	247.6 ± 4.2	427.3 ± 11.0	498.2 ± 10.6
40	110.1 ± 2.9	186.7 ± 5.0	317.0 ± 8.2	479.3 ± 10.2	598.6 ± 13.1
ΔG^0	-22.1 ± 2.1 -22.6 ± 3.1 -23.1 ± 2.8	-23.2 ± 1.1 -23.7 ± 2.0 -24.1 ± 1.9	-23.9 ± 1.0 -24.7 ± 1.9 -25.2 ± 3.0	-24.8 ± 1.2 -25.8 ± 1.7 -26.0 ± 2.4	-25.4 ± 1.6 -26.1 ± 1.7 -26.4 ± 2.9
ΔH^0	2.5 ± 0.12	2.4 ± 0.21	3.3 ± 0.33	2.9 ± 0.11	2.7 ± 0.09
ΔS^0	34.8 ± 0.22	35.6 ± 0.01	40.7 ± 0.37	39.7 ± 0.98	38.9 ± 0.03

^a The values of K_{11} at a certain temperature are used for the calculation of Gibbs free energies Change by $\Delta G^0 = -RT \ln K_{11}$, where R is the gas constant and T the temperature expressed in Kelvin. The enthalpy of the association of n-alkylbenzenes with FA are calculated using the Van't Hoff equation: $\Delta H^0 = -R \ln K_{11}/(T)$. The entropy of the association is calculated by $\Delta S^0 = 1/T(\Delta H^0 - \Delta G^0)$.

4.5.2. Critical fulvic acid aggregation concentration (cfc): Effect of temperature

The average *cfc* was found to be 8.87 ± 0.06 , 8.23 ± 0.04 , and 6.21 ± 0.15 μM FA at temperatures 25⁰, 30⁰, and 40⁰ C, respectively, as shown in **Figures 14a, 25 a, and 25b**. Individually, the *cfc* values of these solute showed no systematic trend with respect to alkyl chain length or solute concentration, therefore, solute induced *cfc* formation is ruled out. The *cfc* appears to decrease with increasing temperature within experimental error. The decrease is most pronounced at 40 C by more than 2 μM FA. These observations show that there are minimum temperature T_{\min} and maximum temperature T_{\max} for aggregate formation. And that is backed up by studying the effect of temperature on the aggregation number of CTAB ¹¹¹. Similar to CTAB, this significant decrease in *cfc* at a higher temperature indicates a breakdown of aggregate pseudo-phase due to higher

mobility of individual FA molecules. Also, there could be enhanced accumulation of water inside the aggregate. Overall, the structural change of the aggregate after certain temperature could significantly affect K_{n1} , K_x and γ_m .

4.5.3. Effect of temperature on solute-aggregation association constant, K_{n1}

Figure 14a, **25a**, and **b** show the peak area ratio increases significantly as the concentration of FA increases and more solute associates with the aggregate. The K_{n1} values for the three different temperatures are summarized in **table 28**. K_{n1} values are highest at 30⁰ C and lowest at 40⁰C. These values indicate the hydrophobic domain is altered by the temperature.

Table 28. Values of K_{n1} from linear least-squares regression of A^0/A_i vs. $[FA]_t$ in the post-aggregation region at pH 5.5 and different temperatures.

Temperature	25.0 ⁰ C	30.0 ⁰ C	40.0 ⁰ C
Solute	K_{n1} ($10^3 \times M^{-1}$)	K_{n1} ($10^3 \times M^{-1}$)	K_{n1} ($10^3 \times M^{-1}$)
Benzene	1390 ± 1.2	6038 ± 4.2	2870 ± 3.2
Toluene	2372 ± 4.3	6716 ± 6.1	6562 ± 7.0
Ethylbenzene	8910 ± 5.5	11284 ± 8.1	10776 ± 7.3
n-Propylbenzene	11408 ± 7.1	18840 ± 10.3	17876 ± 9.9
n-Butylbenzene	13812 ± 3.9	28132 ± 14.2	22190 ± 11.1

4.5.4. Effect of temperature on solute-aggregate partition coefficient, K_x

Figure 15, 26a, and b show the relationship of K_x on the total [FA] concentration. They show the increase in [FA]_t increases the aggregates concentration and K_x values appear to level off to a constant value at the end. These **Figures** show that K_x values become constant above ca. 15, 17, and 18 μM [FA] at temperatures 25⁰, 30⁰, and 40⁰C, respectively. The average K_x values for all three temperatures are summarized in **table 29**. And as expected from the trend in K_{n1} values, the partition coefficients increase going from 25 to 30⁰C and decreases at higher temperatures. This decrease in K_x at a higher temperature could be due to the disturbance in the aggregates by the temperature of the solution.

Table 29. Partition coefficients of n-alkylbenzenes in FA at pH 5.5 and different temperatures.

Temperature	25.0 ⁰ C	30.0 ⁰ C	40.0 ⁰ C
Solute	$K_x (x10^7)$	$K_x (x10^7)$	$K_x (x10^7)$
Benzene	1.34	1.77	1.60
Toluene	2.13	3.89	3.21
Ethylbenzene	2.83	4.83	4.19
n-Propylbenzene	3.73	6.72	5.34
n-Butylbenzene	4.64	7.88	5.34

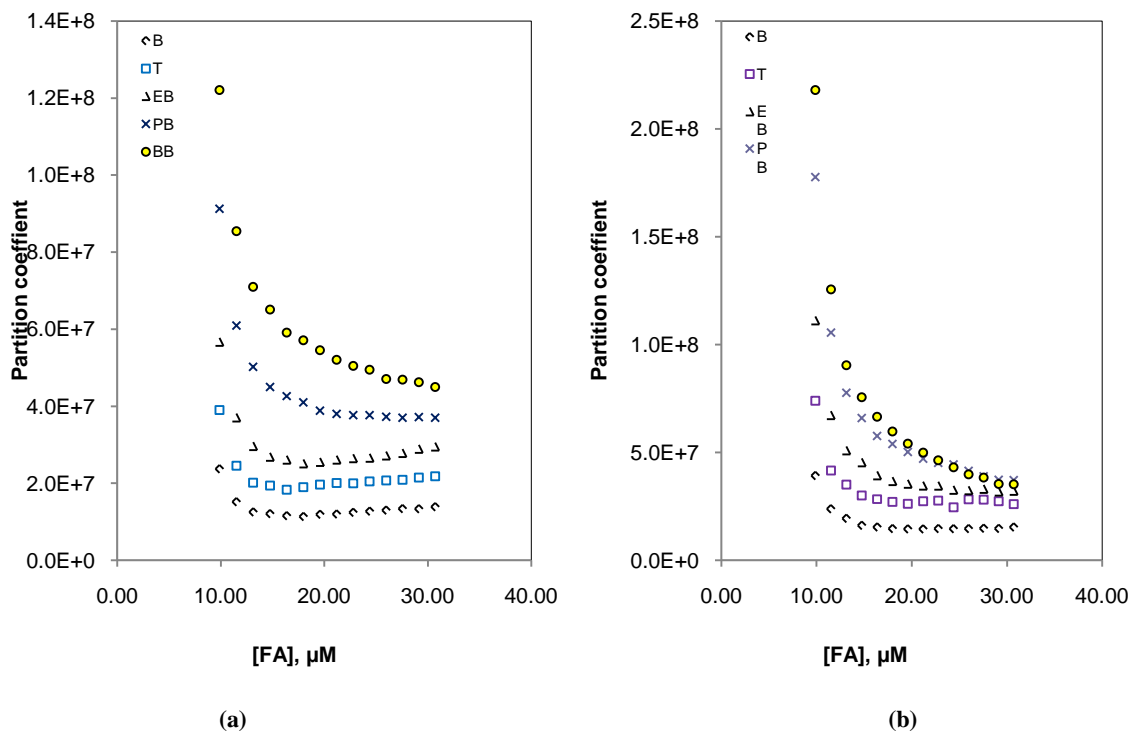


Figure 26. Effect of total FA concentration on water-aggregate pseudo-phase partition coefficient of n-alkylbenzenes at pH 5.5 and (a) 30.0⁰ C (b) 40.0⁰ C.

4.5.5. Effect of temperature on intra-aggregate activity coefficient

Figure 16, 27a, and b show the intra-aggregate activity coefficients (γ_m) of n-alkylbenzenes with increasing FA concentrations at 25⁰, 30⁰, and 40⁰C. The data shown here are for FA concentrations after the *cfc*. These γ_m values are lowest at 30⁰ C compared to the other temperatures. These can be explained by the fact that the environment inside the aggregates is optimum at 30⁰ C among temperatures covered in this study. Temperature affects the strength of the hydrophobic effect and subsequently the interaction with the solvent changes. This could mean there are stronger solvophobic and specific interactions between FA-aggregate and n-alkylbenzenes at the optimum

temperatures. The average γ_m values are shown in **table 30**. The variation of γ_m as a function of temperatures simply indicates the changing nature of the interior solvophobic microenvironment of the aggregate.

Table 30. Intra-aggregate activity coefficients of n-alkylbenzene at pH 5.5 and different temperatures.

Temperature	25.0 ⁰ C	30.0 ⁰ C	40.0 ⁰ C
Solute	$\gamma(x10^{-4})$	$\gamma(x10^{-4})$	$\gamma(x10^{-4})$
Benzene	1.83	1.41	1.55
Toluene	4.29	2.73	2.87
Ethylbenzene	11.40	6.78	7.81
n-Propylbenzene	36.70	20.20	25.5
n-Butylbenzene	123.00	71.90	107.0

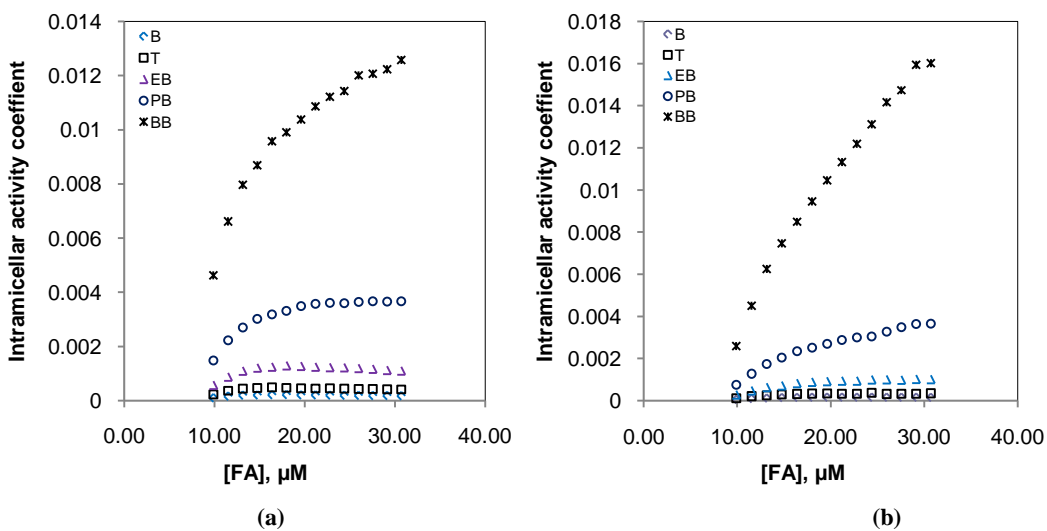


Figure 27. Effect of total FA concentration on intra-aggregate activity coefficients of n-alkylbenzene at pH 5.5 and (a) 30.0⁰ C and (b) 40.0⁰ C.

4.5.6. Effect of temperature on the transfer free energies of functional groups

The effect of the temperature on the transfer free energy of a methylene and aryl units of n-alkylbenzene from water to aggregate pseudo-phase is expected to be affected by the heat of the solution. The transfer free energy calculated as shown in **table 31** were -155 ± 6 , -193 ± 5 , and -119 ± 31 cal/mol per $-\text{CH}_2-$ at 25° , 30° , and 40°C , respectively. These values decrease from going from 25° to 30° C and then it increases considerably at 40° C. Also, the free energy of transfer of benzene were -9722 ± 17 , -9726 ± 32 , -9910 ± 15 cal/ mol at 25° , 30° , and 40°C , respectively. The values at 25° and 30° C are comparable and show insignificant effect, but the value at 40°C decreased considerably. These results again show the microenvironment is most stable at 30 and least stable at 40^oc.

Table 31. Thermodynamic transfer free energy of n-alkylbenzenes at pH 5.5 and different temperatures.

Temperature	25.0 ^o C	30.0 ^o C	40.0 ^o C
Transfer free energy of	cal/mol		
$-\text{CH}_2-$	-155 ± 6	-193 ± 5	-119 ± 31
	-9722 ± 17	-9726 ± 32	-9910 ± 15

APPLICATION OF AQUEOUS SDBS, HA, AND FA TO SOLUBILIZE AND EXTRACT PETROLUEM HYDROCARBONS

5.1. Introduction

Surfactants are widely used in tertiary oil recovery i.e., crude oil retained in the sand and the porous rocks, oil extraction during fracking, and also to mitigate oil spills in the environment. This study was performed to evaluate the treatability of sand contaminated with commercial diesel fuel by aqueous humic substances and compare them with that of the aqueous synthetic surfactant, SDBS. The study was conducted to mimic a primary natural condition where heavy hydrocarbons are spilled in the sand. The results shown here are only for the major composition of diesel fuel containing normal chain aliphatic hydrocarbons ($C_{10} - C_{22}$). Other branched aliphatic and aromatic compounds are not reported here. But the conclusions of this study may equally apply to those compounds.

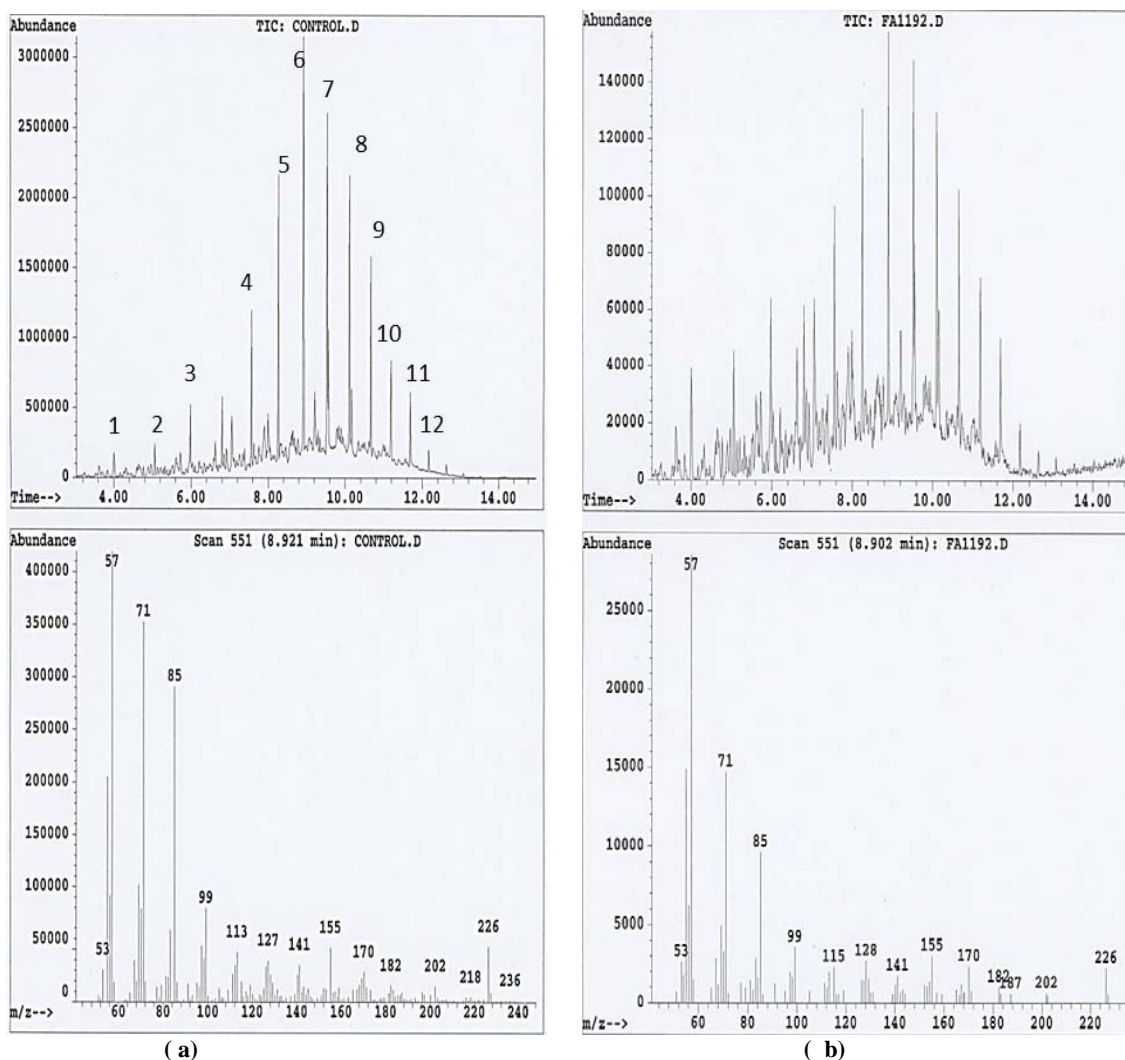


Figure 28. GC–MS of diesel fuel extracted from contaminated sand. Top: total ion chromatogram of diesel fuel and mass spectrum of hexadecane, m/e 226 (bottom). It shows the peaks caused by n-alkanes consecutively marked as 1-12 for C_{10} - C_{22} with carbon increments. (a) the control without FA and (b) after washing with FA at pH 11.9. The typical peak area was about 15 times smaller than the control showing extraction capability of FA.

5.2. Results and Discussion

The complexity of samples like diesel fuel requires the use of GC/MS analysis of organic extracts of sand deliberately contaminated with the fuel. First, the contaminated sand

was mixed with 1 mL of neat diesel fuel in 10 different sealed glass bottles (labeled 1-9) and equilibrate at 22 °C for 3 days. The first study involved washing the contaminated sand with 1.11 mM FA at pH 2.4, 4.3, 10.7 and 11.9. Secondly, a similar study was also performed using HA at pH 10.8 and 2.1. Finally, after adjusting the optimum pH for both HA and FA, they were compared that of SDBS without pH optimization. The optimum pH for FA and HA was found after extraction. The extraction solvent was chosen to be a 1:1 - dichloromethane and hexane after testing each solvent separately; the mixture showed the highest extraction performance. Each sample was carefully removed from the top and placed in a 2 mL screw top vial with septa and analyzed with a Hewlett Packard GC-MS (GC-HP 5890 + MS- HP5971) using a DB-1, fused silica capillary column. These studies provided the relative extraction efficiencies with respect to a control (blank). The control blank has sand, diesel, and the extraction solvent in the same proportions as others and treated the same as other samples. The blank has no surfactants. Therefore, the supernatant organic phase was sampled and analyzed by the GC-MS. The GC-MS profile of this petro-diesel fuel before and after washing with FA at pH 11.9 is depicted in **Figure 28**. This peak area was taken as the zero extraction value. The extraction efficiency is calculated from the mass balance by the equation: Total mols of i-th hydrocarbon present equals to moles washed off by surfactant solution + moles extracted by the mixed solvent. Assuming that the moles of solute are proportional to the total ion chromatographic peak area one can find the extraction efficiency of the surfactant as follows:

$$\% \text{ Extraction} = (1 - A_i / A^0) \times 100$$

Where A^i is the peak area of i -th hydrocarbon remained after washing off with surfactant and then extracting the hydrocarbons with mixed organic solvent and A^0 is the peak area of i -th hydrocarbon after extraction of the control with the same mixed organic solvent. It should be noted that only one washing and one extraction were performed throughout this work.

It is now clear from our previous studies that FA, HA, SDBS can associate, partition, and extract n -alkylbenzenes like hydrocarbons very efficiently. It is therefore possible that similar extraction efficiencies could be obtained for normal hydrocarbons, which are abundant in gasoline, diesel, or crude oils.

The extraction efficiency (or detergency) of FA at different pH is shown in **Figure 29**. The results in **table 32** show that FA exhibits the highest performance at pH 11.9 among pH values covered with an average of 65% removal efficiency for all the hydrocarbons. About 30 and 29 % removal efficiencies were also observed at pH 2.4 and 10.8 and these values are comparable. The least efficiency was seen at slightly acidic pH 4.3 where the removal efficiency averaged less than 20 %. Increasing the pH of FA results in structural expansion²⁴ and consequently enhancing its surface activity. It is consistent with our observation that the highest partitioning of n -alkylbenzenes takes place at elevated pH for FA.

Table 32. Removal efficiency extracted from the sand after sand washing with HA, FA, SDBS and water at different pH and at ambient conditions.

Surfactant	Water	SDBS	FA				HA	
pH	5.9	^a	2.4	4.3	10.8	11.9	2.1	10.8
% Average removal efficiency	1	5	31	16	28	65	4	30

^aNo pH adjustment was done.

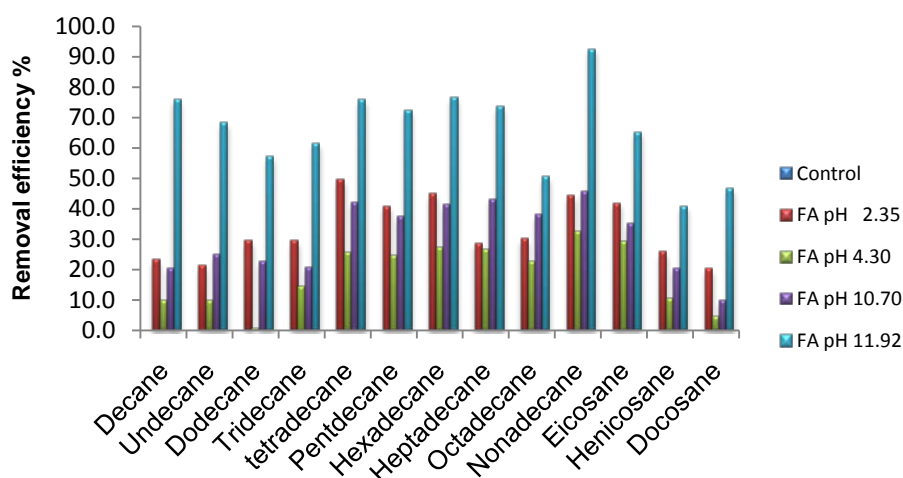


Figure 29. Percent retention of diesel hydrocarbons using fulvic acid at different pH and 22.0⁰ C.

The second study involving HA reveals much higher removal efficiency at basic pH 10.8 compare to that of the acidic medium as shown in **Figure 30**. As a matter of fact, HA showed very poor surface active (detergent) property in acidic pH. HA is known to precipitate out at $\text{pH} > 2$ ¹¹². This could reduce the solubilization ability of HA for hydrocarbons. However, we did not observe the precipitation of HA immediately after being transferred to the contaminated sand or during the mixing process. The effect of pH on HA and its active property was significantly greater than for FA. This might be due to

the presence of more ionizable functional groups in FA (910 –COOH and 330 –OH cmol/ kg) compared to HA (450 –COOH and 210 –OH cmol/ kg) that make FA more polar than HA. In HA, these functional groups are fewer and they start ionizing at high pH and this explained the aqueous solubility of HA at high pH.

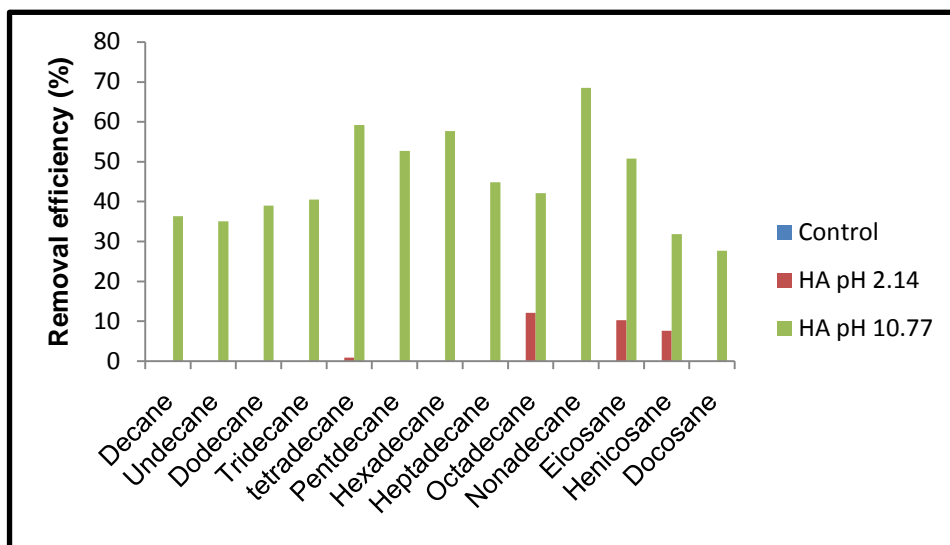


Figure 30. Removal efficiency of diesel hydrocarbons using humic acid at different pH values and 22.0⁰ C.

After optimizing the pH of FA and HA, another study was done to compare their washing abilities to that of SDBS. The evaluation of the percentage of diesel fuel removed from washed sand samples using HA, FA, water, and SDBS is shown in **Figure 31** and **table 32**. It is shown that SDBS, with an average of 2% removal efficiency, exhibits the least removal efficiency where very low concentration of hydrocarbons was recovered from the washed sand while FA at pH 11.9 showed the highest washing

efficiency with an average of 65 % compared to 30 % removal efficiency for HA. It shows that both humic and fulvic acids enhance the solubility of aliphatic hydrocarbons the same magnitude. As shown earlier, the *cmc* value of SDBS is two order of magnitude higher than both *chc* and *cfc* and that explains the low removal efficiency of SDBS. Humic acid is expected to perform better than FA, but only at the optimum pH.

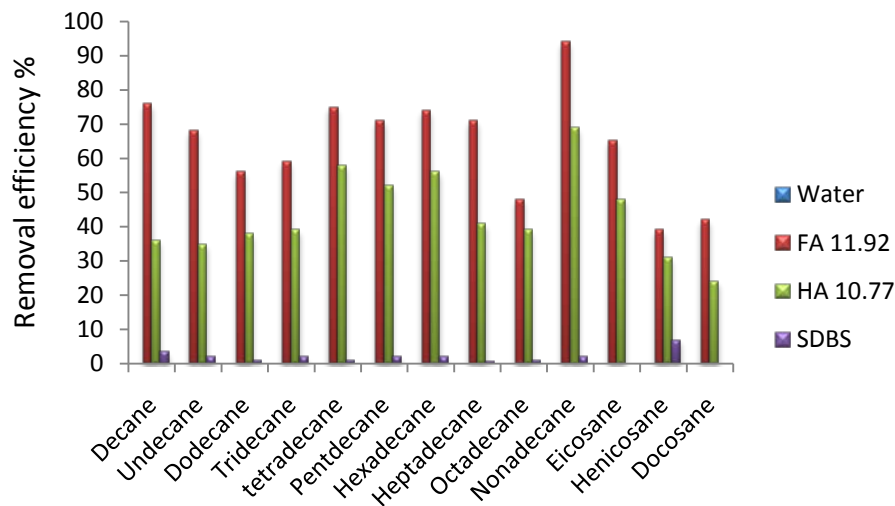


Figure 31. Removal efficiency of diesel hydrocarbons using fulvic acid, humic acid, SDBS and water at 22.0⁰ C.

The high solubilization and extractability of diesel fuel with surfactants prompted us to test its efficacy for crude oil extraction. The light crude was obtained directly from the Fula oil field, Sudan (appendix shows properties). The solubilization for visual

observation was done by adding 0.2540 g of crude oil in screw top vials with septa numbered 1, 2, 3, 4, and 5. Then, 30 ml of deionized water, 139 mg/L SDBS, 5.3 mg/L FA (pH 2.3), and 5.3 mg/L HA (pH 10.8), and a mixture of HA/FA (15 mL 5.3 mg/L each) were transferred to vial 1, 2, 3, 4, and 5, respectively. The solution was equilibrated for 3 days with occasional hand-shaking. **Figure 32** shows the photograph of the samples taken on the third day. The control shows no solubility of the crude in water followed by SDBS, FA, FA+HA, and HA. Obviously, HA shows the nearly complete solubilization of the crude in water while SDBS exhibits the lowest. FA and a mixture of FA and HA show good solubilization. This observation clearly demonstrates that humic substances are promising natural surfactants to extract crude oil.



Figure 32. Picture shows water (control) did not solubilize the crude oil, SDBS showed some solubility, FA and the mixture (FA/HA) show moderate solubility, and HA showed the highest solubility. Clearly, crude oil is very stable and hard to solubilize using high concentration of conventional surfactants.

We also observe that the color of FA becomes darker with decreasing pH as shown in **Figure 33**. This observation was investigated by recording the visible spectra of FA at different pH in the range of 400 - 900 nm (**Figure 34**) using a diode array spectrophotometer (Vernier Model SVIS-PL). It shows that at lower pH the absorbance is higher than that at higher pH. Also, at pH 11.9 and 10.8, a peak around 650 nm emerges in addition to the peaks around 450 nm for all. The pH of the medium can affect the ionization of $-\text{COOH}$, phenolic $-\text{OH}$, $-\text{NH}_2$ functional groups. And ionization of these functional groups could cause expanding or unfolding of FA molecules and a new

absorption band emerges toward the longer wavelength as a result of changing in the multiplicity of resonance structures.



Figure 33. Picture shows FA color change with changing pH. The color becomes darker with decreasing pH.

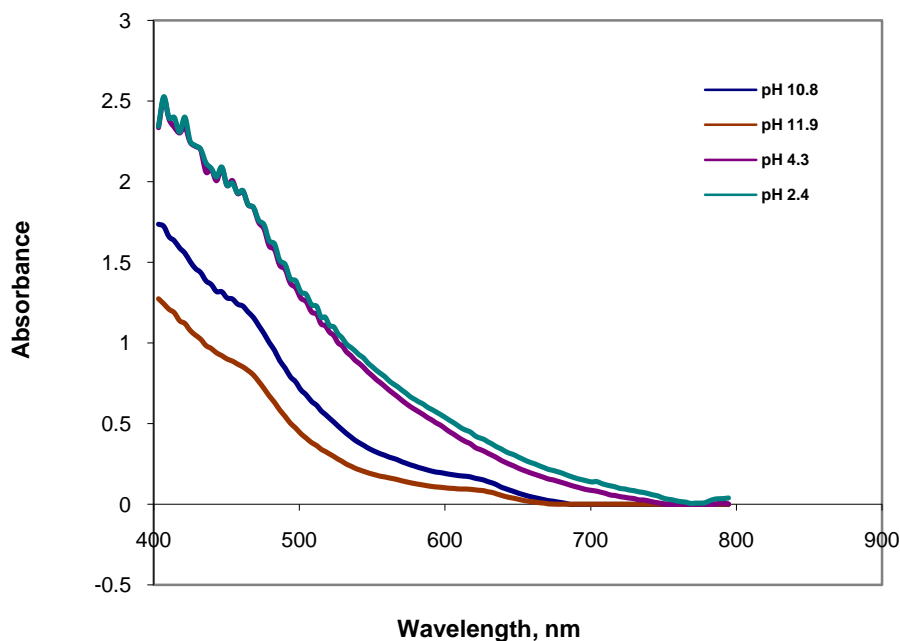
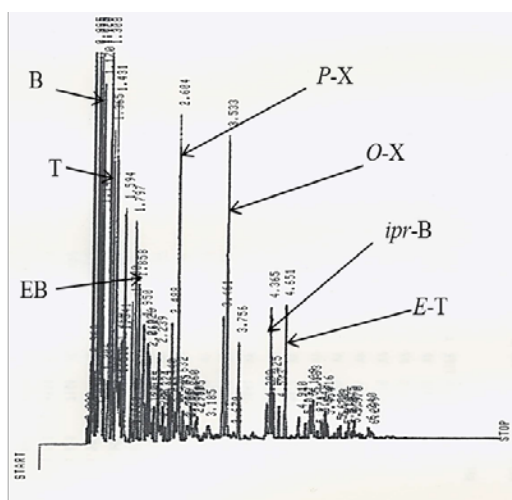


Figure 34. Changes in the UV-VIS spectra of aqueous FA solutions in the pH interval 2.4 - 11.92. The samples were darker at lower pH and lighter in color at higher pH correlates with relative magnitude of the absorbance.

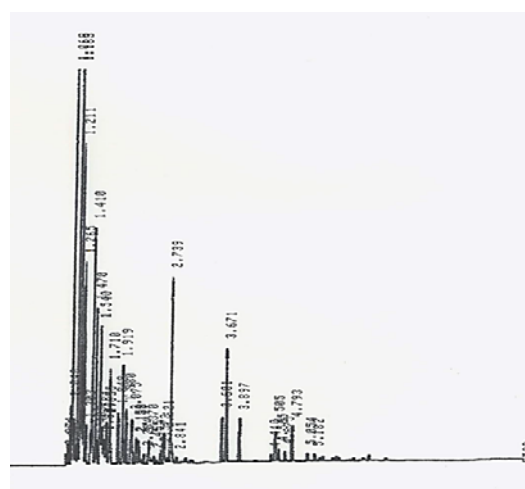
5.3. Solubilization and extraction of gasoline hydrocarbons with aqueous FA

We have shown that FA has very high affinity for the extraction of n-alkylbenzenes from aqueous media. We have tested this for the solubilization and partitioning of hydrocarbons from water containing 1 μ L gasoline (Shell 87) in 16 mL of water by adding FA solution at 0.534 μ M at each increment. **Figure 35** shows typical HSGC of gasoline vapor in equilibrium with the aqueous phase before and after the addition of FA. Clearly, there is a considerable decrease in vapor phase concentration of all the volatile solutes due to association and pseudo-phase partitioning with FA. The

peaks were identified from a separate GC-MS experiment and shown only for the volatile alkylbenzenes. **Figures 36 (a, b)** show the percent solubilization efficiency of the hydrocarbon calculated from the relative loss of vapor-phase concentration: % extraction = $(1 - A_i/A^0) \times 100$. The solubilization efficiency is 30-50% for all the alkylbenzenes. It appears that the smaller benzene has lower efficiency than that of the larger p-ethyltoluene. This is in agreement with our previous studies. The isomers of xylene (o, p) show no difference. It is noted that the solubilization efficiencies increase almost linearly with a slight deviation at 5-6 μM FA, which is close to the cfc. After this point one cannot rule out the possibility of mixed aggregate formation in presence of relatively large concentration of hydrocarbon in gasoline. However, the solubilization efficiencies are large enough to bind or solubilize petroleum hydrocarbons from contaminated water and reduce their volatility for further contamination.

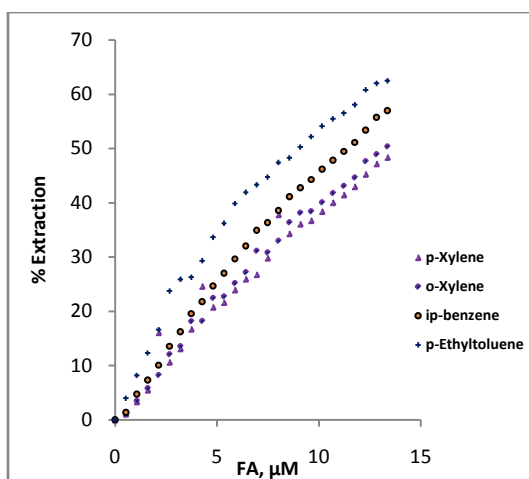


a. At 0th addition of FA in pure water

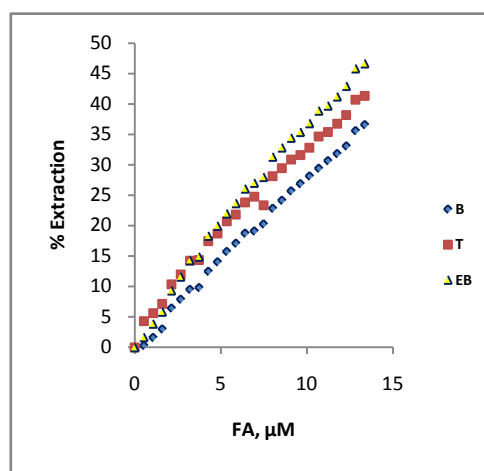


b. At 20th addition of FA (13.9μM)

Figure 35. A typical HSGC experiment run shows peaks for gasoline (Shell 87) in (a) absence and in (b) presence of 13.9 μM FA. HSGC was recorded for 24 addition of 0.534 μM FA each.



(a)



(b)

Figure 36. A plot of percent solubilization of (a) *o*-xylene, *p*-xylene, isopropylbenzene, and *p*-ethyltoluene and (b) B, T, and EB in FA and. About 35-60% of the compounds are extracted in FA as 1:1 or n:1 complex at 25.0⁰C.

STUDIES OF LIQUID-LIQUID EXTRACTION BY HSGC

6.1. Principle of liquid-liquid extraction (LLE)

Liquid-liquid extraction, LLE is one of the most used methods in chemistry laboratory to separate mixtures.¹¹³⁻¹¹⁵ LLE is done by using two immiscible solvents to give two phases, usually organic and aqueous phases, where the compound to be separated has high solubility in one of the phases. Thus there is a physicochemical transfer of solute from one phase to another. Any liquid hydrocarbon paired with water makes very good LLE solvents due to the difference in polarity, and the quality of the mixture gets better with increasing difference in their boiling points. The LLE between any two immiscible liquids such as water and liquid organic hydrocarbons, such as n-dodecane and 1-octanol is very important to many applications ranging from enhanced oil recovery to drug delivery¹¹⁶. Petrochemical industries utilize physicochemical properties such as partition coefficients of solutes in these two immiscible solvent phases to optimize technical and environmental conditions.¹¹⁷

Measuring the partition coefficient or extraction efficiency by using the minimum portions of solvent has always been a problem with LLE. What is the minimum concentration to effect an extraction is also not clear from theory or experiment? It has been shown that using large volumes of solvent is less efficient than small portions for single extraction¹¹³⁻¹¹⁵. This fact alone necessitates the study of LLE at molecular-scale if

possible. In practice, the LLE partition coefficient is measured by extracting the solute by a suitable solvent into a phase and measuring the concentration of the solute in both phases by a suitable analytical technique. This procedure could disturb the LL equilibrium and uses large quantities of solvents. The purpose of this work is to develop a HSGC procedure to test whether LLE partition coefficients can be measured by incrementally adding one of the solvents at extremely low volume (μL) into another solvent containing n-alkylbenzenes at infinite dilution. This experiment is very similar to experiments described above with SDBS, FA, and HA, except that we consider the formation of a neat phase with unit activity compared to that of a pseudo-phase aggregate. We also consider the formation of monomer solute: monomer solvent complex formation before the formation of the neat phase at some critical phase ratio (*cpr*). An equilibrium theory of the process is developed and applied for the extraction of aqueous n-alkylbenzenes with n-dodecane and 1-octanol as the immiscible solvents. We find almost no literature on the subject.

6.2. Theory of liquid-liquid extraction (LLE) with HSGC

In LLE an immiscible solvent, S, is added to water containing the solute, B, at very low concentrations. The solute is preferentially partitioned into S. In HSGC experiments the solvent, S (n-dodecane or 1-octanol) is incrementally added at the smallest possible volumes until it exceeds the solubility limit; this point is called the critical phase ratio (*cpr*). One may assume the formation of SB complex before *cpr*. The total moles of

solute, B in the system is conserved before and after the addition of solvent, S, in a dilute aqueous solution of B. Therefore, the mole balance can be expressed as follows:

$$(n_w + n_v)_0 = n_w + n_s + n_v \quad 26$$

Where, subscript 0 is the moles of solute in water, W and vapor, V (headspace vapor) before addition of the solvent, S (dodecane, octanol etc). Since the vapor/liquid (W) partition coefficient of B is independent of the addition of solvent, S, at all times, one can write:

$$K_{wv} = (n_w / n_v)_0 = n_w / n_v \quad 27$$

Here, K_{wv} is the mole fraction based partition coefficient, a constant for a very dilute solution. Dividing both sides of eq 27 by n_v , one can write:

$$(n_{v0}/n_v) + K_{wv} = 1 + K_{wv} + n_s/n_v \quad 28$$

In HSGC, the peak area is proportional to the number of moles of solute in the headspace vapor. Therefore,

$$A^0 / A_i = (1 + n_s / n_v) \quad 29$$

where, A^0 is the peak area at zero addition of S, and A_i is the peak area at i-th addition of S. Assuming, that both S and W are neat phases and define:

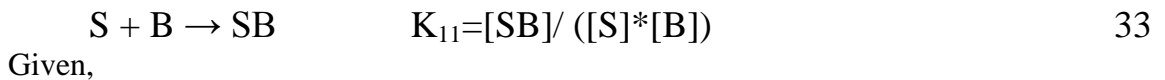
$$n_s/n_v = C_s * V_s / C_v * V_v = K_{sv} (V_s / V_v) \quad 30$$

where, K_{sv} is the molar concentration based partition coefficient. Equation 30 can be written as:

$$A^0 / A_i = (1 + K_{sv} (V_s / V_v)) \quad 31$$

$$A^0 / A_i = 1 + K_{sw} (V_s / V_w) \quad 32$$

Therefore, a plot of A^0 / A_i vs. V_s / V_w is a straight line with a slope K_{sw} and an intercept 1. Here, K_{sw} is the molar concentration based liquid-liquid partition coefficient. Here, V_s / V_w is the phase ratio. The solvent, S forms the neat phase almost immediately after it exceeds its solubility limit or the *cpr*. Before *cpr*, the solute, B binds to S, therefore we consider the equilibrium association constant for SB complex as follows:



$$K_{wv} = (B / B_v)_0 = B / B_v \quad 34$$

Here, the K_{11} is molar concentration based association constant. The subscript 0 indicates the distribution of B before the addition of S. Assuming vapor phase concentration of B_v is negligible compared to that of the total B_0 or that in solution and the total concentration of B is conserved, one can write.

$$B_0 = B + SB \quad 35$$

$$B_{v0} * K_{wv} = (K_{wv} + K_{11} * S * K_{wv}) B_v \quad 36$$

If the vapor phase concentrations are replaced by peak areas from HSGC measurement, one can write,

$$A^0/A_i = 1 + S K_{11} \quad 37$$

Assuming that the molar concentration of S is much larger than the concentration B, a plot of A^0 / A_i vs. S is linear with a slope of K_{11} in the pre-partition region and intercept of unity. This part of the derivation is similar to that of B-FA complex described in previous sections.

From the general theory discussed earlier, it states that under equilibrium condition, the thermodynamic activities of the solute are the same in two immiscible phases, i.e.

$$X_s \gamma_s = X_w \gamma_w \quad 38$$

Where, γ_w is the activity coefficient of solute, B, in the water phase and γ_s is the activity coefficient of solute, B, in the organic phase. Based on pure solute as the standard state, γ_s is also known as the intra-organic layer activity coefficient. Also, γ_s is calculated using the following equation:

$$\gamma_s = \gamma_w / K_x \quad 39$$

If the solute concentration is in the Henry's law region, then γ_w can be replaced by its infinite dilution activity coefficient, which can be obtained from the literature, or can be measured by the same HSGC technique. Equation 39 shows that measurements of γ_s can be obtained without a solute concentration.

The theory described above shows that one can get LLE partition coefficient for solute between two neat solvents from the same solution containing immiscible phases, the binding constants between two monomers, and the intra-organic layer activity coefficient. The theory did not consider any interfacial effect like water layer around polar and non-polar solvents and the effect of these pseudo-layers on the partitioning. The theory also shows that solute concentrations are not needed to separate the phases for later analysis. Similar studies were reported for solute-solvent pairs by Li and Carr⁸⁸ to

obtain bulk partition coefficients. However, no attempts were made to measure 1:1 association constant and the critical phase ratio, cpr.

6.3. Results and discussion

This work was done to understand the association equilibria partitioning of hydrophobic molecules dissolved in aqueous medium by the addition of extracting solvents such as n-dodecane and 1-octanol. All measurements were performed at 25.0⁰.

6.3.1. Liquid-liquid extraction, LLE with n-Dodecane (S) –water (W) system

For this study, we chose n-dodecane, because it is widely used as a solvent to extract alcohols from water by petrochemical companies. Also, it is a pure hydrocarbon that representative of the most nonpolar phase. The following measurements were obtained.

6.3.1.1. Association constant, K_{11} , and critical phase ratio (cpr)

In the beginning of the experiment, there was no addition of S. Therefore, the peak areas are proportional to the moles of solute present in the vapor phase in equilibrium with the liquid phase. The solvent, S was then added at 5.3 μL (or 4.3×10^{-3} g in 18.0 mL water) increments and the peak areas were measured after each addition. **Table 33** shows the data obtained from this experiment including the peak area from n-dodecane in the vapor phase.

Table 33. Table shows peak area ratio for the addition of n-dodecane in aqueous solution of n-alkylbenzenes at 25.0⁰ C. The n-dodecane peak area is also shown. Given the A⁰ one can calculate A_i for each entry.

Run #	Moles of n-C ₁₂ H ₂₆ added	Pure peak area, A ⁰ →	Benzene	Toluene	Ethyl benzene	n-Propyl benzene	n-Butyl benzene	Peak area of n-C ₁₂ H ₂₆
			2808	21017	54365	135153	150270	
			Phase Ratio, (V _d /V _w)					
0	0.00E+00	0.00E+00	1	1	1	1	1	134151
1	2.51E-05	3.17E-04	1.048	1.099	1.201	1.401	2.144	306240
2	5.02E-05	6.33E-04	1.12	1.197	1.274	1.476	2.219	317518
3	7.53E-05	9.50E-04	1.172	1.287	1.432	1.529	2.245	320798
4	1.00E-04	1.27E-03	1.246	1.414	1.571	1.703	2.396	319797
5	1.25E-04	1.58E-03	1.321	1.511	1.637	1.781	2.476	324734
6	1.51E-04	1.90E-03	1.371	1.625	1.796	1.928	2.6	323271
7	1.76E-04	2.22E-03	1.463	1.74	1.908	2.002	2.731	324657
8	2.01E-04	2.53E-03	1.523	1.86	2.03	2.148	2.751	328036
9	2.26E-04	2.85E-03	1.438	2.098	2.561	2.737	3.486	324384
10	2.51E-04	3.17E-03	1.632	2.467	3.26	3.809	4.875	328096
11	2.76E-04	3.48E-03	1.736	2.801	4	4.735	6.302	329058
12	3.01E-04	3.80E-03	1.834	3.147	4.637	5.717	7.681	331046
13	3.26E-04	4.12E-03	1.956	3.479	5.296	6.611	9.101	332025
14	3.51E-04	4.43E-03	2.077	3.848	5.871	7.766	10.301	331833
15	3.76E-04	4.75E-03	2.153	4.164	6.5	8.429	11.354	333967
16	4.02E-04	5.07E-03	2.275	4.522	7.062	9.346	12.448	333083
17	4.27E-04	5.38E-03	2.392	4.943	7.764	10.177	13.619	336528
18	4.52E-04	5.70E-03	2.531	5.224	8.464	11.342	14.769	337245
19	4.77E-04	6.02E-03	2.625	5.638	9.185	12.37	15.737	333393
20	5.02E-04	6.33E-03	2.757	5.993	9.329	12.784	17.16	337394

Figure 36 shows the peak area ratios as a function of n-dodecane/water phase ratio revealing the region before and after phase separation. **Figure 36** shows that the average *cpr* occurs at about $(3.4 \pm 0.3) \times 10^{-3}$ (volume of n-dodecane/volume of water). By using the solubility of n-dodecane in water which is 2.14×10^{-8} mols/L¹¹⁸, we calculate the expected phase ratio (n-dodecane/water) to be 3.21×10^{-3} , which is in

excellent agreement with our results. The n-dodecane peak area is a clear indication of the *cpr* and the onset of a neat phase formation with unit activity where the peak area remains unchanged within 0.72 % rsd. The fact that there is no systematic trend in the peak area after *cpr* is indicative of a reproducible gas sampling. Therefore, HSGC measurement of solubility at the *cpr* is meaningfully representative of a transition of S from SB complex into partitioning of B into neat solvent. Due to the high polarity of water and high non-polarity of n-dodecane, the two liquids are immiscible starting at the *cpr* resulting in two phases; water-rich and n-dodecane rich phases as dispersed micro-droplets (emulsion). The emulsion however was not observed visually.

Before the micro-droplets coalesce to form neat, clear and distinct phases, the solute could associate with S as SB complex. It is obvious that nonpolar and polarizable n-alkylbenzenes could associate with nonpolar solutes like n-dodecane or the hydrocarbon tail of 1-octanol. This is observed from the decrease in peak area ratio before *cpr*. These weak interactions are not generally measured or observed in other techniques. The solute-n-dodecane association constant value is expected to be low, because n-dodecane molecules are surrounded by water molecules. There is a distinct possibility for the formation of small clusters of n-dodecane and trap the n-alkylbenzene into the cluster. This could also happen in the transition region from cluster to neat solvent clusters like droplets. Equation 38 shows that a plot of A^0/A_i vs. S_t before reaching *cpr*, is linear with a slope of K_{11} and intercept of unity. **Table 34** shows that K_{11} values are relatively small and all members of the homologue show relatively weak interactions between a monomer solute and n-dodecane molecules. The values slightly

increase with increasing hydrophobicity of n-alkylbenzenes. The $-\text{CH}_2-$ of n-alkylbenzenes bring additional hydrophobic interactions.

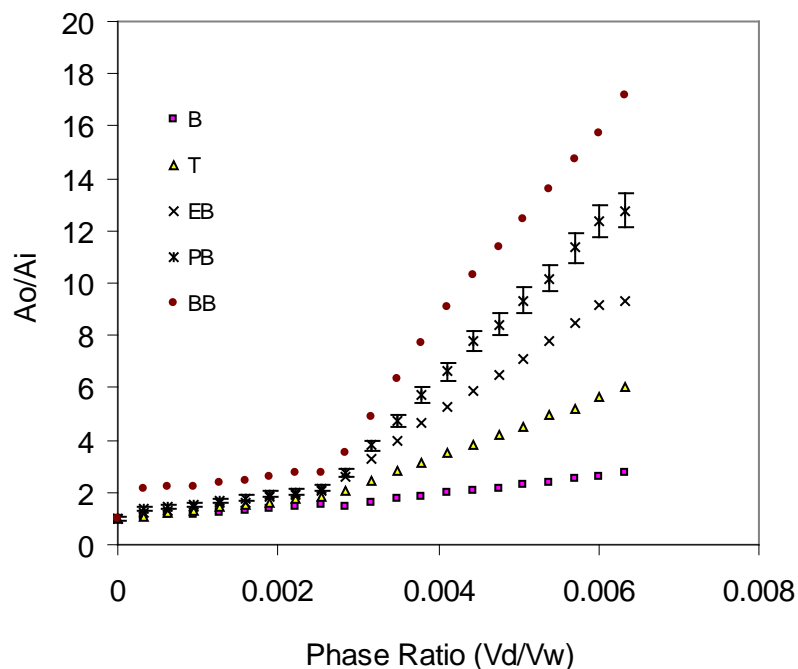


Figure 37. Peak area ratio as a function of n-dodecane/water phase ratio at 25.0⁰ C.

Table 34. Values of K_{11} from linear least-squares regression of A^0/A_i vs. $[\text{n-dodecane}]_t$ in the pre-phase separation at 25.0⁰C.

Solute	K_{11} (M^{-1})	Intercept	r^2
Benzene	79 ± 16	0.997 ± 0.005	0.9996
Toluene	153 ± 27	0.986 ± 0.006	0.9987
Ethylbenzene	225 ± 50	0.852 ± 0.011	0.9987
n-Propylbenzene	261 ± 60	0.974 ± 0.014	0.9946
n-Butylbenzene	296 ± 75	0.985 ± 0.010	0.9997

6.3.1.2. Solute partition coefficient between n-dodecane and water phases, K_x

According to **equation 32**, a plot of A^0 / A_i vs. V_s / V_w is a straight line with a slope K_{sw} and an intercept of 1. We note that K_{sw} is the molar concentration based liquid-liquid partition coefficient. This can be converted into mole fraction based LL partition coefficient, K_x . The K_{sw} and K_x values for n-alkylbenzenes in n-dodecane / water are shown in **table 35**. There are no literature values to compare with ours. However, our values are of the same order of magnitude with those of hydrocarbon/hydrocarbon partitioning in hydrocarbon/water system⁸⁸. The values indicate an increasing trend in K_x with increasing length of alkyl chain. The calculation of the free energy of transfer of a $-CH_2-$ unit from aqueous phase to n-dodecane was calculated from the linear relation between $\Delta G^0 (= -RT \ln K_x)$ vs. number in n-alkylbenzenes (excluding benzene). This yields an average of -406 ± 20 cal / mol $-CH_2-$ ($n=4$, $r^2 = 0.9953$). The free energy of transfer was linearly related to K_x and increases with increasing length of alkyl chain. This $-CH_2-$ increment shows affinity difference for the two phases. This indicates that microscopic phase of hydrocarbons (n-dodecane) in water is probably not like neat hydrocarbon phase.

Table 35. Partitioning of n-alkylbenzenes in n-dodecane / water at 25.0⁰ C.

Solute	K_{sw}	$\log K_{sw}$	K_x^a
Benzene	615 ± 7	2.78 ± 0.85	7724
Toluene	2110 ± 9	3.32 ± 0.95	26495
Ethylbenzene	4718 ± 11	3.67 ± 1.04	59258
n-Propylbenzene	9133 ± 14	3.96 ± 1.14	114711
n-Butylbenzene	16618 ± 18	4.22 ± 1.25	208722

^a $K_x = K_{sw} \times 12.56$, where the constant is molar volume ratio of n-dodecane/water

6.3.1.3. Estimation of Infinite dilution activity coefficient in n-dodecane micro-phase, γ^∞

The estimate of the activity coefficient of solutes inside the organic phase can be obtained by using **equation 39** and the literature values of the activity coefficient of n-alkylbenzenes in water, γ_w^∞ . The average γ_x^∞ values are shown in **table 36** along with UNIFAC values. Though UNIFAC is a computational technique based on neat solvent assumption unlike our system, but still there is some agreements for larger molecules in the series taking the experimental error into consideration. The mutual solubility of water and n-dodecane has affected the smaller molecules activity coefficients significantly. As shown later with 1-octanol the agreements are better when mutual solubility is considered.

Table 36. Infinite Dilution Activity Coefficients of n-alkylbenzenes in n-dodecane at 25.0⁰ C. UNIFAC activity coefficient calculator by Bruce Choy & Danny Reible, University of Sydney, Australia.

Solute	γ_s^∞	UNIFAC
Benzene	0.321 ± 0.022	1.00
Toluene	0.347 ± 0.111	1.85
Ethylbenzene	0.552 ± 0.217	2.09
n-Propylbenzene	1.19 ± 0.447	2.35
n-Butylbenzene	2.71 ± 0.559	2.61

6.3.2. Liquid-liquid extraction, LLE with 1-Octanol (S) –water (W) system

Extraction of organic compounds in 1-octanol (amphiphilic nature) is thought to mimic the absorption and partitioning of such molecules in tissue bio-membranes of living organisms¹¹⁹. For this reason the partitioning of a large number of molecules were studied in 1-octanol/water system¹²⁰. These data were then utilized to correlate molecular parameters and obtain relations between theory and experiment^{121,122, 123, 124}. The $K_{O/W}$ values were obtained with mutually saturated phases, often these phases are like emulsion or micro-droplets of 1-octanol in water. Experimental techniques such as batch shake-flask, generator column, slow stir method, filter probe method, centrifugal partition chromatography (CPC), and high performance liquid chromatography were used to find $K_{O/W}$ ^{120, 123, 125, 126}. Ideally, none of these techniques are equilibrium techniques because either they are phase separated, centrifuged, or measured as sorption (not partition) of solute on 1-octanol phase i.e., in LC and CPC. Here, we describe the equilibrium HSGC as a completely new method for the measurement of $K_{O/W}$. In addition

to $K_{O/W}$, the method allows measurement of 1-octanol-solute binding constant, critical phase ratio for LLE, and intra-solvent activity coefficient without knowing the solute concentrations.

6.3.2.1. Association constant, K_{11} , and critical phase ratio (*cpr*)

Similar to the n-dodecane/ water system, the experiment started with zero addition of 1-octanol to the n-alkylbenzene containing aqueous solution. The amount of 1-octanol, S added at 3.0 μL (or 2.5×10^{-3} g in 18.0 mL water) increments. The resulting data including the peak area from 1-octanol in the vapor phase are shown in **table 37**.

The peak area ratio as a function of 1-octanol/water phase ratio presented in **Figure 37** clearly shows the region before and after the phase separation. The average *cpr* occurs at about $(1.0 \pm 0.3) \times 10^{-3}$ (volume of 1-octanol/ volume of water). If we use the solubility of 1-octanol in water which is $4.5 \times 10^{-3} \text{ M}$ ¹²⁷, then the expected phase ratio of 1-octanol: water is 0.71×10^{-3} , which is in good agreement with our value within experimental error. The 1-octanol peak area after the *cpr* has not changed much (within 3 % rsd) indicating the formation of an organic phase saturated with water. The change in %rsd is relatively higher than that of n-dodecane due to the relatively higher mutual solubility of 1-octanol and water. Unlike n-dodecane, 1- octanol forms micro-emulsion, which was visually observed at the 9th addition after the *cpr* point. This shows that actual phase formation (almost like a pseudo-phase) takes place before any observation of phase separation or micro-emulsion formation. Before the *cpr*, an 1:1 complex of SB forms.

Table 37. Table shows peak area ratio for the addition of 1-octanol in aqueous solution of n-alkylbenzenes at 25.0^o C. The 1-octanol peak area is also shown. Given the A⁰ one can calculate A_i for each entry.

Run #	Moles of C ₈ H ₁₇ OH added	Pure peak area, A ⁰	Benzene	Toluene	Ethyl benzene	n-Propyl benzene	n-Butyl benzene	Peak area of C ₈ H ₁₇ OH
			12440	30731	72862	71755	23341	
		Phase Ratio, (V _d /V _w)	↓ Peak area ratio, A ⁰ /A _i					
0	0	0.00E+00	1.00	1.00	1.00	1.00	1.00	241460
1	1.88E-08	1.67E-04	1.01	1.04	1.04	1.04	1.03	232886
2	3.75E-08	3.33E-04	0.84	0.92	0.92	1.10	1.10	235213
3	5.63E-08	5.00E-04	0.85	0.88	0.93	1.16	1.12	228846
4	7.51E-08	6.67E-04	0.88	0.95	1.04	1.33	1.18	226960
5	9.38E-08	8.33E-04	0.95	1.05	1.43	1.53	1.24	220590
6	1.13E-07	1.00E-03	1.22	1.43	1.71	1.67	1.79	225427
7	1.31E-07	1.17E-03	1.13	1.68	1.85	2.73	2.56	216934
8	1.50E-07	1.33E-03	1.07	2.18	2.69	3.59	4.16	215928
9	1.69E-07	1.50E-03	0.98	2.77	3.53	4.74	5.80	210684
10	1.87E-07	1.67E-03	0.96	3.31	4.46	5.83	6.92	206228
11	2.06E-07	1.83E-03	0.97	4.05	5.42	6.59	8.20	207696
12	2.25E-07	2.00E-03	0.90	4.89	6.20	7.48	9.73	202978
13	2.44E-07	2.17E-03	0.90	5.80	7.31	8.96	11.07	201837
14	2.62E-07	2.33E-03	0.89	6.34	8.26	10.06	12.21	204636
15	2.81E-07	2.50E-03	0.88	6.96	9.03	11.26	13.67	196961
16	3.00E-07	2.67E-03	0.88	7.57	9.89	12.68	15.46	202096
17	3.18E-07	2.83E-03	0.89	8.23	10.67	13.85	16.58	196192
18	3.37E-07	3.00E-03	0.88	8.84	11.51	15.25	17.84	197112
19	3.56E-07	3.17E-03	0.89	9.54	12.21	16.47	18.87	187871

The hydrophobic interaction due to the presence of –OH in 1-octanol is expected to be weak due to the intra and inter hydrogen bonds with water. The results from the linear least-squares regression of A⁰/A_i vs. [1-octanol] before *cpr* are shown in **table 38**. It shows that K₁₁ value increases with increasing –CH₂- of the solute and the overall

values indicate weaker interactions than that of n-dodecane. This observation is attributed to the amphiphilic nature of 1-octanol.

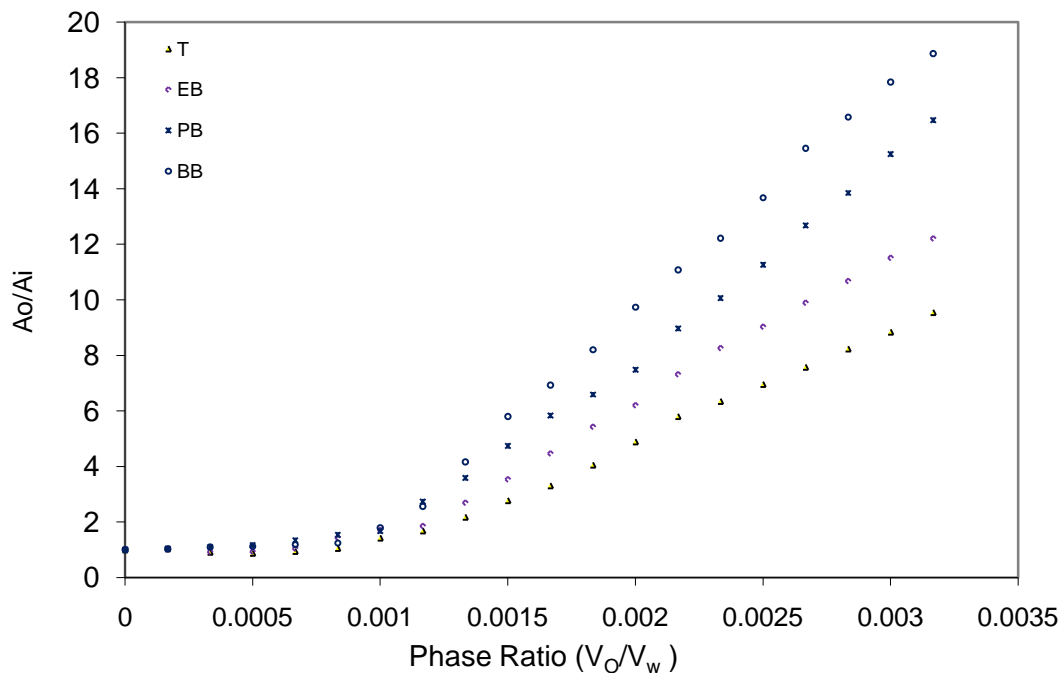


Figure 38. Peak area ratio as a function of 1-octanol /water phase ratio at 25.0⁰ C.

Table 38. Values of K_{11} from linear least-squares regression of A^0/A_i vs. $[1\text{-octanol}]_t$ in the pre-aggregation region at 25.0⁰ C.

Solute	K_{11} (M^{-1})	Intercept	r^2
Toluene	45 ± 2	0.9906 ± 0.006	0.9995
Ethylbenzene	104 ± 12	0.9866 ± 0.013	0.9982
n-propylbenzene	111 ± 6	0.9789 ± 0.015	0.9895
n-butylbenzene	118 ± 9	0.9825 ± 0.013	0.9993

6.3.2.2. Solute partition coefficient between 1-octanol and water phases, K_x

The plot of A^0 / A_i vs. V_s / V_w gave a straight line with a slope K_{sw} and an intercept of 1. Then mole fraction and molar-based solute partition coefficient (K_x and K_{sw}) are shown in **table 39**. The values of our data (Log K) are in good agreement with the literature values within the experimental error. The free energy of transfer of the $-CH_2-$ from aqueous phase to the neat organic phase was -136.7 ± 15 cal/mol which is higher than that into n-dodecane phase. This could be explain by the fact that the 1-octanol phase is saturated with water and becomes an emulsion 1-octanol in water. This could make the organic pseudo-phase more polar, very hydrophobic, and larger in size. Therefore, the transfer of the solute into the organic phase becomes more difficult.

Table 39. Partition coefficient for n-alkylbenzene in 1-octanol/ water system at 25.0 °C.

Solute	K_{sw}	logK	logK ^a	K_x
Toluene	4046 ± 12	3.60 ± 0.003	2.80	35402
Ethylbenzene	5351 ± 14	3.73 ± 0.14	3.28	46821
n-propylbenzene	6279 ± 19	3.80 ± 0.27	3.90	54941
n-butylbenzene	8279 ± 21	3.92 ± 0.47	4.44	72442

^a from reference number 128.

6.3.2.3. Estimation of Infinite dilution activity coefficient in 1- octanol micro-phase

The estimate of the activity coefficient of solutes inside the organic phase in equilibrium with the water phase can be obtained by using **equation 39** and the literature values of the activity coefficient of solute in water, γ_x^{83} are possible. Here, γ_s^∞ values are

calculated from $K_{sw} = 0.151 \gamma_w / \gamma_s$, where the constant is a correction factor for the mutual solubility of phases ¹²⁷. The average γ_s^∞ values are shown in **table 40** along with theoretical values. These values show an excellent agreement within the experimental error. Obviously, the mutual solubility of 1-octanol and water plays an important role in activity and partition coefficients.

Table 40. Infinite Dilution Activity Coefficients in 1-octanol at 25.0⁰ C.

Solute	γ_s^∞ <i>exp</i>	γ_s^∞ <i>calc</i>
Toluene	0.259 ± 0.092	0.343
Ethylbenzene	0.698 ± 0.126	0.922
n-propyl benzene	2.48 ± 0.270	3.27
n-butylbenzene	7.81 ± 2.239	10.32

γ_s^∞ values are calculated using, $K_{sw} = 0.151 \gamma_w / \gamma_s$ by reference ¹²⁷.

CONCLUSION AND FUTURE OUTLOOK

Natural organic matter (NOM) in soils and sediments plays an important role in transportation of substances between soil and water. It consists of both humic and non-humic fractions and the former includes humic acids (HA), fulvic acids (FA), and humin. These compounds are responsible for partitioning, binding, and transport of organics and metal ions in nature. Here, we have studied FA and HA for the association, binding and partitioning of small n-alkylbenzenes (benzene, toluene, ethylbenzene, n-propylbenzene, and n-butylbenzene) to understand the basic chemical equilibria. The n-alkylbenzenes were chosen because they are the major constituents of gasoline and also very toxic to the environment. Our studies were extended to synthetic surfactant sodium dodecylbenzene sulphonate (SDBS) for comparative purpose. Almost no such studies could be found in the literature and, therefore, constitute a fundamental contribution in this field ¹²⁹. The studies were applied to examine the solubilization of hydrocarbons in gasoline, diesel, and crude oil with FA, HA, and SDBS.

A self-made high precision equilibrium headspace gas chromatographic technique (HSGC) was used to measure the peak area (proportional to vapor pressure) of the monomer solute in the vapor phase in equilibrium with the liquid phase and calculate the association equilibria of n-alkylbenzenes solutes at about 10^{-6} mole fraction. This

approach allowed determination of solute - monomer surfactant (S), association constants (K_{II}), solute- aggregate, S_n , association constant (K_{nI}), critical aggregation constant (critical fulvic acid aggregation concentration cfc , critical humic acid aggregation concentration, chc , and critical micelles concentration, cmc), mole fraction based partition coefficients (K_x), infinite dilution activity coefficients of solute inside the aggregate pseudo-phase (γ_m), and transfer free energies of alkyl chain $-CH_2-$ from aqueous to aggregate pseudo-phase. The parameter values were obtained at infinite dilution where solute-solute interactions are nonexistent. Theory of equilibria applied to HSGC shows that solute concentration is not needed to extract these parameters and this is one of the most important analytical advantages compared all other techniques. The HSGC can be used to measure many solutes simultaneously at very low concentrations for extremely complex samples like gasoline, diesel, and crude oil.

For surfactants like compounds there is a critical concentration where the molecules start to aggregate with hydrophobic inner core and hydrophilic outer layer. This is known as the critical aggregation concentration (cac). We found the average critical concentrations were 7.85 ± 0.06 , 4.81 ± 0.02 , and 1038 ± 200 mg/L, for FA, HA and SDBS, respectively. The cfc value decreases slightly with increasing pH and temperature of the reaction mixture indicating a change in the ionization of FA molecules. The typical K_{II} values for benzene to n-butylbenzene ($6.9 \times 10^4 \text{ M}^{-1}$ to $3.6 \times 10^5 \text{ M}^{-1}$) are about 2-3 orders of magnitude higher than that for SDS and SDBS and 2 order of magnitude lower than that for HA. This indicates the size of the surfactant

molecule plays a direct role in association of smaller n-alkylbenzenes with HA being the largest and SDS is the smallest. The K_{11} value increases with increasing the pH and temperature of the reaction mixture. The effect of the temperature on K_{11} values is a sign of an endothermic association process driven by entropy. Similarly, K_{n1} values for benzene to n-butylbenzene ($1.4 \times 10^6 \text{ M}^{-1}$ to $1.4 \times 10^7 \text{ M}^{-1}$) are also 3-4 orders of magnitude higher than that for SDS and SDBS and 2 orders of magnitude lower than that for HA. Increasing the pH of the solution causes FA molecules to become more ionic, and like ionic surfactants, form an aggregate (or micelles) with an inner hydrocarbon like pseudo-phase and hydrophilic (or ionic) outer layer oriented towards water for favorable solution stability. As the aggregation pseudo-phase becomes more hydrophobic, the hydrophobic interaction (K_{11} and K_{n1}) gets stronger.

In the post aggregation region the solute partition into the pseudo-phase. The average K_x values are of the order of 10^7 above the cac and much higher than that with SDS, SDBS, and HA. This indicates that the partitioning of n-alkylbenzenes in FA is more favored than that in HA, SDBS and SDS. This indicates the aggregate pseudo-phase for HA and FA acids are different. The K_x values for FA system increases considerably with increasing pH and temperature. Because, increasing the pH of the solution ionizes the functional groups (-COOH, phenolic-OH and $-\text{NH}_2$) of FA molecules resulting in higher repulsion between these groups, therefore, the size of the aggregate increases impart the maximum stability. Our model allows the calculation of inter-aggregate activity coefficient, which is a measure of non-ideality of the pseudo-phase environment. The n-alkylbenzenes in FA pseudo-phase shows the lowest γ_m

among the three systems studied. And it also shows that benzene has the lowest γ_m (0.0001) and n-butylbenzene has the highest (0.01) value. These values are 8-10 orders of magnitude lower than γ in bulk water thereby indicating a strong specific binding and partitioning processes in the pseudo-phase. The very low (0.0001) intra-aggregate activity coefficients found here are one the lowest found in solution chemistry. Most importantly, the transfer free energy of partitioning of a $-\text{CH}_2-$ group were -155, -194, and -236 cal/mol, compared to that of benzene, -9722, -8013, and -6426 cal/mol for FA, HA, and SDBS, respectively, this indicates that the aggregate pseudo-phase for all of them is more polarizable benzene-like and less n-alkane aliphatic-like. Clearly, a π - π attractive interaction between benzene rings is a predominant force for binding these molecules. For FA, the transfer free energy decreases (energetically favorable) with increasing pH due to the formation of a stable pseudo-phase.

This study shows that there is strong binding and partitioning of n-alkylbenzenes in FA and HA present as single molecule or as aggregates. These findings are used to evaluate the treatability of sand contaminated with commercial diesel fuel by aqueous humic substances and compare them with that of the aqueous synthetic surfactant, SDBS. This study was performed by using a Hewlett Packard GC-MS. The diesel contaminated sand was washed with HA or FA and then extracted with 1:1 mixture of hexane/ DCM to find out the removal efficiency. The FA exhibits the highest removal efficiency at pH 11.9 with an average of 65% for all the hydrocarbons. The removal efficiencies were about 28 and 30 % at pH 10.8 and 2.4, respectively. Similarly, HA reveals much higher

removal efficiency (35 %) at pH 10.8 compare to that of pH 2.14, where it reaches only an average of 2 % efficiency. And SDBS, with an average of 2% removal efficiency, exhibits the least removal efficiency. The *cmc* value of SDBS is 3 orders of magnitude higher than both *chc* and *cfc* and that explains the low removal efficiency of SDBS. Humic acid is expected to remove slightly better than FA, but only at the optimum pH. Visual inspection of solubilization of crude oil shows the hydrocarbon extraction efficiency in the following order: HA > FA > SDBS. Finally, the hydrocarbons in gasoline samples tested for their extraction into FA. The extraction efficiency was found to be 30-60% for identified n-alkylbenzenes and probably the same for all other volatile hydrocarbons present in gasoline.

The theory of association equilibria developed here was successfully applied to the partitioning of hydrocarbons in immiscible phases such as n-dodecane-water and 1-octanol-water. If a solute partition from one phase to another due their enhanced solubility in one of the phases then adding that phase in very small increments could be monitored by the change in its concentration in the vapor phase. This concept was tested for water-n-dodecane and water- 1-octanol systems with n-alkylbenzenes as solutes at infinite dilution. These experiments allowed us to obtain the association constant, K_{II} , and critical phase ratio (*cpr*) for solvent extraction, solute partition coefficient between organic and water phases, K_x , and infinite dilution activity coefficient in organic phase, γ_s^∞ . The results show that the average *cpr* occurs at about $(3.4 \pm 0.3) \times 10^{-3}$ (volume of n-dodecane/volume of water) which is in excellent agreement with the solubility of n-dodecane in water (3.21×10^{-3} v/v). This is indicative of nearly neat pseudo-phase. And

that for 1-octanol the average *cpr* occurs at about $(1.0 \pm 0.3) \times 10^{-3}$ (volume of 1-octanol/volume of water) and it is in a good agreement with the expected value (0.71×10^{-3}). The K_{II} values for toluene to n-butylbenzene are (153 M^{-1} to 296 M^{-1}) and (45 M^{-1} to 118 M^{-1}) for n-dodecane and 1-octanol, respectively. These values are relatively small and all members of the homologue show relatively weak interactions between a monomer solute and n-dodecane and 1-octanol. The values slightly increase with increasing hydrophobicity of n-alkylbenzenes. The partitioning of n-alkylbenzenes in n-dodecane, $\log K$ for toluene to n-butylbenzenes are (3.32 to 4.22) and are in a fair agreement with literature values¹²³. The value of $\log K$ for toluene to n-butylbenzene is 3.60 to 3.92 for 1-octanol/water are also in good agreement with the literature values.

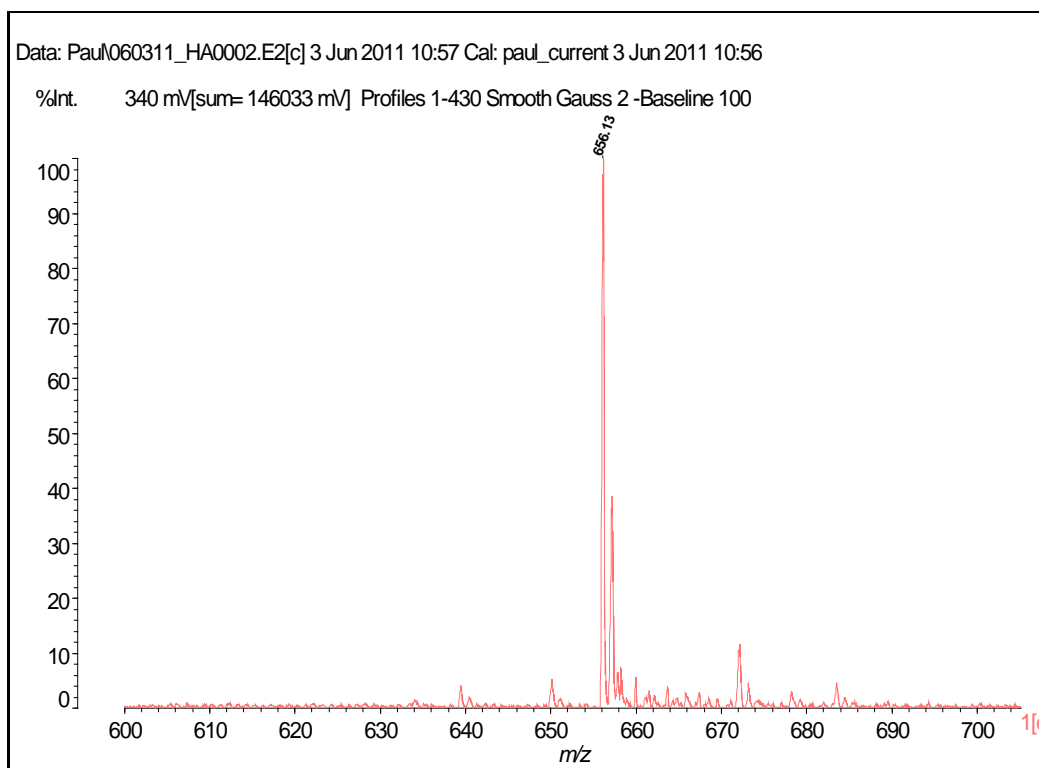
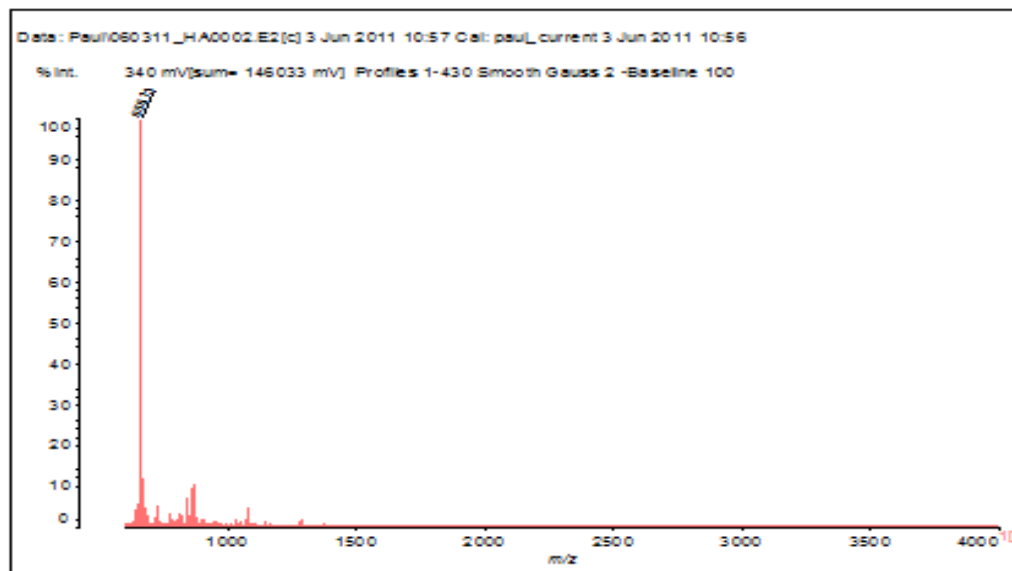
Clearly, we have established the HSGC experimental methodology and the theoretical basis to study association and partitioning of nonpolar volatile solutes from one phase to another phase. The system could be as simple as two immiscible solvents, synthetic and very complex natural surfactants such as FA and HA. Volatile solutes from any source can be studied. Future studies should include polar volatile solutes in homologous series, methylated fulvic acid, and humic acids from other sources. Since the basic theory is applicable to any system where binding association and partitioning of small volatile solutes are expected one can extend this work to complex macromolecules, proteins, and functionalized nano-particles. We believe such studies could contribute to the fundamental understanding of molecular interactions in such complex systems.

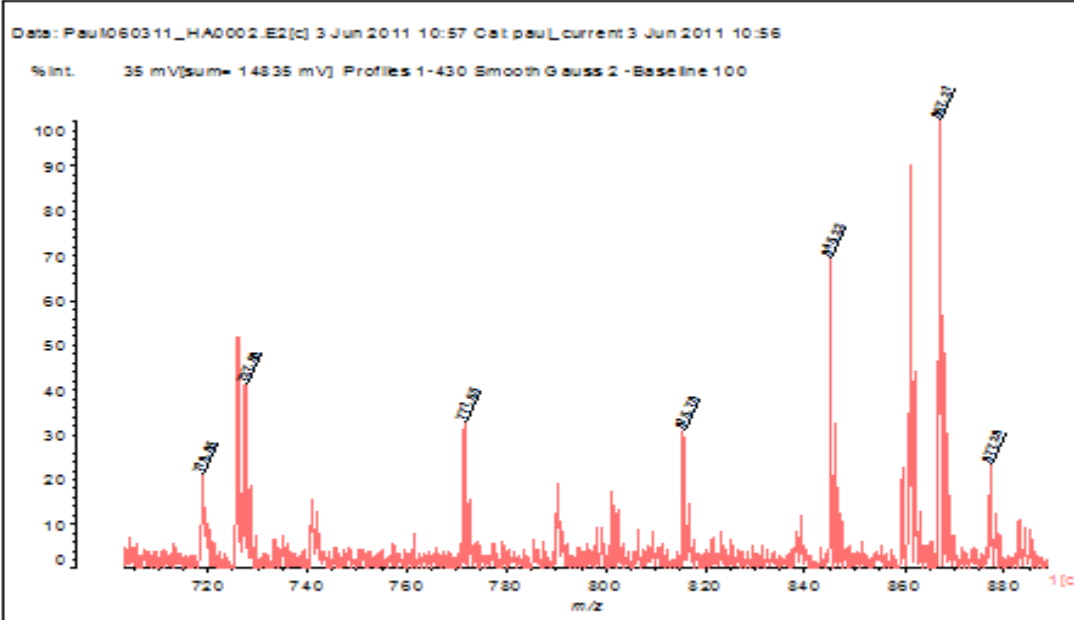
APPENDIX

Table 41. Analysis of crude oil from Fula field, Sudan using wellhead sampling

Physical Property			
Color:	Colourless	Transparency:	Transparent
Sediment:	None	pH	7.54
Content of Ion			
Item	Content		
	mg/L	mmol/L	
OH ⁻	0.00	0.00	
CO ₃ ²⁻	0.00	0.00	
HCO ₃ ⁻	329.51	5.40	
Cl ⁻	322.60	9.10	
SO ₄ ²⁻	14.41	0.15	
K ⁺ +Na ⁺	315.10	13.70	
Ca ²⁺	15.03	0.37	
Mg ²⁺	4.25	0.17	
Salinity	836.15		
Water Type:	NaHCO ₃		
Oil in water mg/L	17		

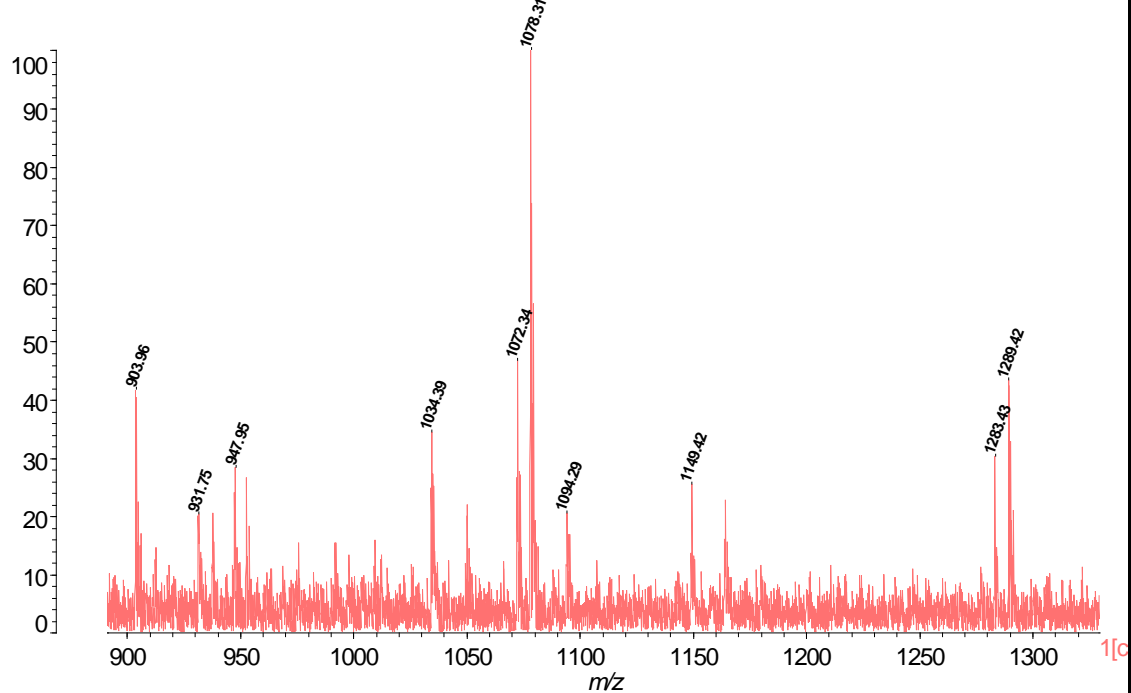
Figure 39. Matrix-assisted laser desorption/ionization time-of-flight mass spectrometry, MALDI-TOF-MS. The following spectra are taken for HA sample used in this work





Data: Pau\060311_HA0002.E2[c] 3 Jun 2011 10:57 Cal: paul_current 3 Jun 2011 10:56

%Int. 15 mV[sum= 6445 mV] Profiles 1-430 Smooth Gauss 2 -Baseline 100



REFERENCES

1. Schwarzenbach, R.P.; Gschwend, P.M., Imboden, D.M. Environmental organic chemistry. John Wiley and Sons, Inc., New York, 1993.
2. Corvasce, M.; Zsolnay, A.; D'Orazio, V.; Lopez, R.; Miano, T.M. Characterization of water extractable organic matter in a deep soil profile. *Chemosphere*. 2006, 62, 1583–1590.
3. Lam, B.; Baer, A.; Alae, M.; Lefebvre, B.; Moser, A.; Williams, A.; Simpson, A.J. Major structural components in freshwater dissolved organic matter. *Environ. Sci. Technol.* 2007, 41, 8240–8247.
4. Zafiriou, O.C.; Jousset-Dubien, J.; Zepp, R.G.; Zika, R.G. Photochemistry of natural waters. *Environ. Sci. Technol.* 1984, 18, 358A–371A.
5. Schulten, H.R.; Schnitzer, M. Chemical model structures for soil organic matter and soils. *Soil Sci.* 1997, 162, 115–130.
6. Daniel E. Martire. Lattice model for nonrandom pairing and the determination of “sociation” constants of organic complexes. *The Journal of Physical Chemistr.* 1983, 87, 13.
7. Johnson, W.P.; Amy, G.L. Facilitated transport and enhanced desorption of polycyclic aromatic hydrocarbons by natural organic matter in aquifer sediments. *Environ. Sci. Technol.* 1995, 29, 807–817.
8. Conte, P.; Agretto, A.; Spaccini, R.; Piccolo, A. Soil remediation: humic acids as natural surfactants in the washing of highly contaminated soils. *Environ. Pollut.* 2005, 515–522.
9. Guetzlhoff, T.F.; Rice, J.A. Does humic acid form a micelle?. *Sci. Total Environ.* 1994, 152, 31–35.
10. Reid, P. M.; Wilkinson, A. E.; Tipping, E.; Jones, M. N. Aggregation of humic substances in aqueous media as determined by light-scattering methods. *Journal of Soil Science.* 1991, 42, 259–270.
11. Ferreira, J.A.; Nascimento, O.R.; Martin-Neto, L. Hydrophobic interactions between spin-label 5-SASL and humic acid as revealed by ESR spectroscopy. *Environ. Sci. Technol.* 2001, 35, 761–765.

12. Simpson, A.J.; Kingery, W.L.; Shaw, D.R.; Spraul, M.; Humpfer, E.; Dvortsak, P. The application of ^1H HR-MAS NMR spectroscopy for the study of structures and associations of organic components at the solid-aqueous interface of a whole soil. *Environ. Sci. Technol.* 2001, 35, 3321–3325.
13. Kerner, M.; Hohenberg, H.; Ertl, S.; Reckermann, M.; Spitzzy, A. Self-organization of dissolved organic matter to micelle-like microparticles in river water. *Nature.* 2003, 422, 150–154.
14. Wandruszka, R. von. The micellar model of humic acid: evidence from pyrene fluorescence measurements. *Soil Sci.* 1998, 163, 921–930.
15. Chien, Y. -Y.; Kim, E. -G.; Bleam, W. F. Paramagnetic relaxation of atrazine solubilized by humic micellar solutions. *Environ. Sci. Technol.* 1997, 31, 3204–3208.
16. Simpson, A.J.; Kingery, W.L.; Hayes, M.H.B.; Spraul, M.; Humpfer, E.; Dvortsak, P.; Kerssebaum, R.; Godejohann, M.; Hofmann, M. Molecular structures and associations of humic substances in the terrestrial environment. *Naturwissenschaften.* 2002, 89, 84–88.
17. Ram, N.; Raman, K. V. Stability constants of complexes of metals with humic and fulvic acids under non-acid-conditions. *Zeitschrift für Pflanzenernährung und Bodenkunde.* 1984, 147, 171–176.
18. Wershaw, R. L.; Burcar, P. L.; Goldberg, M. C. Interaction of pesticides with natural organic material Interaction of pesticides with natural organic material. *Environ. Sci. Technol.* 1969, 3, 271–273.
19. Chiou, C.T.; Malcolm, R.L.; Brinton, T.I.; Kile, D.E. Water solubility enhancement of some organic pollutants and pesticides by dissolved humic and fulvic acids. *Environ. Sci. Technol.* 1986, 20, 502–508.
20. Chiou, C.T.; Kile, D.E.; Brinton, T.I.; Malcolm, R.L.; Leenheer, J.A. A comparison of water solubility enhancements of organic solutes by aquatic humic materials and commercial humic acids. *Environ. Sci. Technol.* 1987, 21, 1231–1234.
21. Chakravarty, M.; Amin, P.M.; Singh, H.D.; Baruah, J.N.; Iyengar, M.S. A kinetic model for microbial growth on solid hydrocarbons. *Biotechnol. Bioeng.* 1972, 14, 61–73.

22. Ogram, A.V.; Jessup, R.E.; Ou, L.T.; Rao, P.S.C. Effects of sorption on biological degradation rates of (2,4-dichlorophenoxy) acetic acid in soils. *Appl. Environ. Microbiol.* 1985, 49, 582–587.
23. Backhus, D.A.; Gschwend, P.M. Fluorescent polycyclic aromatic hydrocarbons as probes for studying the impact of colloids on pollutant transport in groundwater. *Environ. Sci. Technol.* 1990, 24, 1214–1223.
24. Jones, K.D.; Tiller, C.L. Effect of solution chemistry on the extent of binding of phenanthrene by a soil humic acid: a comparison of dissolved and clay bound humic. *Environ. Sci. Technol.* 1999, 33, 580–587.
25. Steinberg, C.E.W.; Xu, Y.; Lee, S.K.; Freitag, D.; Kettrup, A. Effect of dissolved humic material (DHM) on bioavailability of some organic xenobiotics to *Daphnia magna*. *Chem. Spec. Bioavailab.* 1993, 5, 1–9.
26. Johnsen, S.; Kukkonen, J.; Grande, M. Influence of natural aquatic humic substances on the bioavailability of benzo[a]-pyrene to Atlantic salmon. *Sci. Total. Environ.* 1989, 81, 691–702.
27. Fujimura, Y.; Kuwatsuka, S.; Katayama, A. Bioavailability and biodegradation rate of DDT by *Bacillus* sp. B75 in the presence of dissolved humic substances. *Soil Sci. Plant Nutr.* 1996, 42, 375–381.
28. Fava, F.; Piccolo, Al. Effects of humic substances on the bioavailability and aerobic biodegradation of polychlorinated biphenyls in a model soil. *Biotechnol. Bioeng.* 2002, 77, 204–211.
29. Georgi, A. Sorption of hydrophobic organic compounds on dissolved humic substances. *Umweltforschungszentrum Leipzig-Halle.* 1998, 22, 1–8.
30. Gauthier, T.D.; Seitz, W.R.; Grant, C.L. Effects of structural and compositional variations of dissolved humic materials on pyrene Koc values. *Environ. Sci. Technol.* 1987, 21, 243–248.
31. McCarthy, J.F.; Roberson, L.E.; Burris, L.W. Association of benzo(a)pyrene with dissolved organic matter: prediction of K_{dom} from structural and chemical properties of the organic matter. *Chemosphere.* 1989, 19, 1911–1920.
32. Kukkonen, J.; Oikari, A. Bioavailability of organic pollutants in boreal waters with varying levels of dissolved organic material. *Water Res.* 1991, 25, 455–463.

33. Paolis, F.; Kukkonen, J. Binding of organic pollutants to humic and fulvic acids: influence of pH and the structure of humic material. *Chemosphere*. 1997 34, 1693–1704.
34. Chin, Y.P.; Aiken, G.R.; Danielsen, K.M. Binding of pyrene to aquatic and commercial humic substances: the role of molecular weight and aromaticity. *Environ. Sci. Technol.* 1997, 31, 1630–1635.
35. Perminova, I.V.; Grechishcheva, N.Y.; Petrosyan, V.S. Relationships between structure and binding affinity of humic substances for polycyclic aromatic hydrocarbons: relevance of molecular descriptors. *Environ. Sci. Technol.* 1999, 33, 3781–3787.
36. Gschwend, P.M.; Wu, S. On the constancy of sedimentwater partition coefficients of hydrophobic organic pollutants. *Environ. Sci. Technol.* 1985, 19, 90–96.
37. Schlautman, M.A.; Morgan, J.J. Effects of aqueous chemistry on the binding of polycyclic aromatic hydrocarbons by dissolved humic materials. *Environ. Sci. Technol.* 1993 27, 961–969.
38. Morra, M.J.; Corapcioglu, M.O.; von Wandruszka, R.M.A.; Marshall, D.B.; Topper, K. Fluorescence quenching and polarization studies of naphthalene and 1-naphthol interaction with humic acid. *J. Soil Sci. Soc.* 1990, 54, 1283–1289.
39. Chen, S.; Inskeep, W.P.; Williams, S.A.; Callis, P.R. Fluorescence lifetime measurements of fluoranthene, 1-naphthol, and napropamide in the presence of dissolved humic acid. *Environ. Sci. Technol.* 1994, 28, 1582–1588.
40. Gauthier, T.D., Shane, E.C., Guerin, W.F., Seitz, W.R., Grant, C.L. Fluorescence quenching method for determining equilibrium constants for polycyclic aromatic hydrocarbons binding to dissolved humic materials. *Environ. Sci. Technol.* 1986, 20, 1162–1166.
41. Engebretson, R.R.; von Wandruszka, R. Microorganization in dissolved humic acids. *Environ. Sci. Technol.* 1994, 28, 1934–1941.
42. Engebretson, R.R.; von Wandruszka, R. Kinetic aspects of cation-enhanced aggregation in aqueous humic acids. *Environ. Sci. Technol.* 1998, 32, 488–493.
43. Engebretson, R.R.; Amos, T.; von Wandruszka, R. Quantitative approach to humic acid associations. *Environ. Sci. Technol.* 1996, 30, 990–997.

44. Ragle, C.S.; Engebretson, R.R.; von Wandruszka, R. The sequestration of hydrophobic micropollutants by dissolved humic acids. *Soil Sci.* 1997, 162, 106–114.
45. Von Wandruszka, R. The micellar model of humic acid: evidence from pyrene fluorescence measurements. *Soil Issues.* 1998, 163, 921–930.
46. Yates, L.M.; Engebretson, R.R.; Haakenson, T.J.; von Wandruszka, R. Immobilization of aqueous pyrene by dissolved humic acid. *Anal. Chim. Acta.* 1997, 356, 295–300.
47. Nanny, M.A.; Bortiatynski, J.M.; Hatcher, P.G. Noncovalent interactions between acenaphthenone and dissolved fulvic acid as determined by ¹³C NMR T1 relaxation measurements. *Environ. Sci. Technol.* 1997, 35, 530–534.
48. Simpson, M.J.; Simpson, A.J.; Hatcher, P.G. Noncovalent interactions between aromatic compounds and dissolved humic acid examined by nuclear magnetic resonance spectroscopy. *Environ. Toxicol. Chem.* 2004, 23, 355–362.
49. Shinozuka, N.; Lee, C.; Hayano, S. Solubilizing Action of Humic Acid from Marine Sediments. *The Science of the Total Environment.* 1987; 62; 311-314.
50. Shinozuka, N.; Lee, C. Aggregate formation of humic acids from marine sediments. *Mar. Chem.* 1991; 33; 229–241.
51. Chiou, C.T.; Porter, P.E.; Schmedding, D.W. Partition equilibria of nonionic organic compounds between soil organic matter and water. *Environ. Sci. Technol.* 1983, 17, 227.
52. Chiou, C.T.; Malcolm, R.L.; Brinton, T.I.; Kile, D.E. Water solubility enhancement of some organic pollutants and pesticides by dissolved humic and fulvic acids. *Environ. Sci. Technol.* 1986, 20, 502–508.
53. Smith, E.H.; Tseng, S.K.; Weber Jr., W.J. Modeling the adsorption of target compounds by GAC in the presence of background dissolved organic matter. *Environ. Prog.* 1987, 6, 18–25.
54. Summers, R.S.; Haist, B.; Koehler, J.; Ritz, J.; Zimmer, G.; Sontheimer, H. The influence of background organic matter on GAC adsorption. *J. Am. Water Works Assoc.* 1989, 81, 66–74.
55. Carter, M.C.; Weber Jr., W.J. Modeling adsorption of TCE by activated carbon preloaded by background organic matter. *Environ. Sci. Technol.* 1994, 28, 614–623.

56. Matsui, Y.; Knappe, D.R.U.; Iwaki, K.; Ohira, H. Pesticide adsorption by granular activated carbon adsorbers. 2. Effects of pesticide and natural organic matter characteristics on pesticide breakthrough curves. *Environ. Sci. Technol.* 2002, 36, 3432–3438.
57. Zhang, Y.; Zhou, J.L. Removal of estrone and 17 β -estradiol from water by adsorption. *Water Res.* 2005, 39, 3991–4003.
58. Buffle, J.; Greter, F. L.; Haerdi, W. Measurement of complexation properties of humic and fulvic acids in natural waters with lead and copper ion-selective electrodes. *Anal. Chem.* 1977, 49, 216- 222.
59. Schnitzer, M.; Khan, S. U. Humic substances in the environment. Marcel Dekker, New York, 1972, p. 327.
60. Schulten, H. R.; Schnitzer, M. A state of the art structural concept for humic substances. *Naturwiss.* 1993, 80, 29-30.
61. Schnitzer, M. "A lifetime perspective on the chemistry of soil organic matter." *Advances in Agronomy.* 1999: 1-30, 30A, 30B, 31-58.
62. Chen, Y.; Schnitzer.; M. Water adsorption on humic substances. *Can. J. Soil Sci.* 1976, 56, 521-524.
63. Gressel, N.; McGrath, A. E.; McColl, J.C.; Power, R.F. Spectroscopy of aqueous extract of forest litter: I: Suitability of methods. *Soil Sci. Soc. Am. J.* 1995, 59, 1715– 1723.
64. Jerry A. L.; Colleen E. R.; Paul M. G.; Edward T. F.; Imma Ferre. Molecular resolution and fragmentation of fulvic acid by electrospray ionization/multistage tandem mass spectrometry. *Anal. Chem.* 2001, 73, 1461-1471.
65. Laub, R.J.; Pecsok, R.L. Physicochemical applications of gas chromatography, Wiley, New York, 1978.
66. Condor, J.R.; Young, C.L. Physicochemical measurement by gas chromatography, Wiley, Chichester, 1979.
67. Atkinson, D.; Curthoys, G. Determination of heats of adsorption by gas-solid chromatography. *J. Chem. Educ.* 1978, 55, 564.
68. Davis, S.S.; Higuchi, T.; Rytting, J.H. "Determination of thermodynamics of functional groups in solutions of drug molecules. A critical evaluation of the

- thermodynamic properties of organic compounds using the "Group Contribution" approach. Its application to solution behaviour drug absorption and distribution and structure-activity relationships". *Advances in Pharmaceutical Sciences*. 1974, 4, 73-261.
69. Joseph O . Carnali.; Frederick M. Fowkes. Microemulsions of methyl methacrylate in aqueous sodium lauryl sulfate: structure and interaction energetics by SAXS, NMR spectroscopy and GC headspace analysis. *Langmuir*. 1985, 1, 5-577-587.
 70. Vitha, M.F.; Dallas, A.J.; Carr, P.W. Study of water-sodium dodecyl sulfate micellar solubilization thermodynamics for several solute homolog series by headspace gas chromatography. *J. Phys. Chem*. 1996, 100, 5050-5062.
 71. Hussam, A.; Basu, S.C.; Hixon, M.; Olumee, Z. General method for the study of solute-surfactant association equilibria of volatile solutes by headspace gas chromatography. *Anal. Chem*. 1995, 67, 1459-1464.
 72. Bruno, K.; Leslie, S. Static Headspace-Gas Chromatography: Theory and Practice, 2nd Edition. *John Wiley & Sons*. 2006.
 73. Hussam , A. Carr, W. A study of rapid and precise methodology for the measurement of vapor/liquid equilibria by headspace gas chromatography. *Anal. Chem*. 1985, 57, 793-801.
 74. Alvarez-Pueblaa, R.A.; Valenzuela-Calahorrob, C.; Garridoa, J. J. Theoretical study on fulvic acid structure, conformation and aggregation: A molecular modeling approach. *Science of the Total Environment*. 2006, 358, 243– 254.
 75. Bruce, C. F. Fused quartz diaphragm-type pressure transducer. *Journal of Physics E Scientific Instruments*. 2001, 4(10), 790. DOI:10.1088/0022-3735/4/10/024.
 76. Kōzō Shinoda.; Eric Hutchinson. Pseudo-phase separation model for the thermodynamic calculations on micellar solutions, *J. Phys. Chem*. 1962 66 (4), 577-582.
 77. Robbins, G.A.; Wang, S.; Stuart, J.D., Using the headspace method to determine Henry's law constants. *Anal. Chem*. 1993, 65, 3113-3118.
 78. Hussam, A.; Park, J. H.; Carr, P. W. Use of homologous series of liquids for the study of the linearity and relative response factors for methyl and methylene groups in flame ionization detectors by headspace gas chromatography. *Microchemical Journal*. 1987, 36, 107-111.

79. Park, J. H.; Hussam, A.; Couasnon, P.; Fritz, D.; Carr, P. W. Experimental reexamination of selected partition coefficients from rohrschneider's data set. *Anal. Chem.* 1987, 59, 1970-1976.
80. Park, J. H.; Hussam, A.; Cousnon, P. Carr, P. W. The precision of area and height measurement with flame ionization detector in temperature programmed capillary gas chromatography. *Microchemical Journal.* 1987, 35, 232-239.
81. Ogner. G.; Schnitzer, M. Chemistry of fulvic acid, a soil humic fraction and its relation to lignin. *Can. J. Chem.* 1971, 49, 1053-1063.
82. Hansen, E. H. Schnitzer, M. Molecular weight measurements of polycarboxylic acids in water by vapor pressure osmometry. *Anal Chim. Acta.* 1969, 46, 247-254.
83. Kurt Kosswig. Surfactants in Ullmann's encyclopedia of industrial chemistry. Wiley-VCH, Weinheim. 2005.
84. Grossman, P. D.; Colburn, J. C. (Eds.), Capillary Electrophoresis, Theory and Practice, Academic Press, San Diego, CA 1992, pp. 3-43.
85. Bruno, K.; Leslie, S. Static Headspace-Gas Chromatography: Theory and Practice, 2nd Edition. *John Wiley & Sons.* 2006.
86. Hait, S. K.; Majhi, P. R.; Blume, A.; Moulik, S. P. critical assessment of micellization of sodium dodecyl benzene sulfonate (SDBS) and its interaction with poly(vinyl pyrrolidone) and hydrophobically modified polymers. *The Journal of Physical Chemistry B.* 2003, 107, 3650-3658.
87. Daniel, C.; Erdogan G. Micellization and intermicellar interactions in aqueous sodium dodecyl benzene sulfonate solutions. *Journal of Colloid and Interface Science.* 1982, 90, 410-423.
88. Li, J.; Carr, P. W. Measurement of water-hexadecane partition coefficients by headspace gas chromatography and calculation of limiting activity coefficients in water. *Anal. Chem.* 1983, 55, 1443.
89. Tanford, Charles. The Hydrophobic effect: Formation of micelles and biological membranes. New York, NY: John Wiley & Sons Inc. 1973.
90. Remediation of LNAPL-contaminated sand by using Humic acid as a surfactant.(light non-aqueous phase liquids)(Report). *Journal of the Alabama Academy of Science,* 01-JAN-08.

91. Paul, P. M.; Seitz, W. R. Fluorescence Polarization Studies of Perylene-Fulvic Acid Binding. *Environ. Sci. Technol.* 1982, 16, 613-616.
92. Young, C.; von Wandruszka, R. Comparison of aggregation behavior in aqueous humic acids. *Geochem. Trans.*, **2001**, 2, A DOI: 10.1039/b100038l.
93. Yonebayashi, K.; Hattori, T. Surface active properties of soil humic acids. *Sci. Total Environ.* 1987, 62, 55–64.
94. Hayano, S., Shinozuka, N., Hyakutake, M. Surface active properties of marine humic acids. *Yukagaku.* 1982, 31, 357–362.
95. Tombacz, E. Colloidal properties of humic acids and spontaneous changes of their colloidal state under variable solution conditions. *Soil Sci.* 1999, 164, 814–824.
96. Pan, B.; Ghosh, S.; Xing, B. Nonideal binding between dissolved humic acids and polyaromatic hydrocarbons. *Environ. Sci. Technol.* 2007, 41, 6472-6478.
97. Zhu, D. Q.; Hyun, S. H.; Pignatello, J. J.; Lee, L. S. Evidence for π - π electron donor acceptor interactions between π -donor aromatic compounds and π -acceptor sites in soil organic matter through pH effects on sorption. *Environ. Sci. Technol.* 2004, 38, 4361-4368.
98. Simon, S. A.; McDaniel, R. V.; McIntosh, T. J. Interaction of benzene with micelles and bilayers. *J. Phys. Chem.* 86:1449- 1456.
99. Jung, A.V.; Frochet, C.; Villieras, F.; Lartiges, B.S.; Parant, S.; Viriot, M.L.; Bersillon, J.L. Interaction of pyrene fluoroprobe with natural and synthetic humic substances: Examining the local molecular organization from photophysical and interfacial processes. *Chemosphere.* 2010, 80, 228–234.
100. Thurman, E.M., Organic geochemistry of natural water. Kluwer academic publishers, Dordrecht, Massachusetts, 1985.
101. Thurman, E. M., Wershaw, R. L., Malcolm, R. L., and Pinckney, D. J. Molecular size of aquatic humic substances. *Org. Geochem.* 1982,4, 27-35.
102. Kučerík J., Šmejkalová D., Čechovská H., Pekař M. New insights into conformational behaviour of humic substances: Application of high resolution ultrasonic spectroscopy, *Organic Geochemistry.* 2007, 38, 2098-2110.
103. Silvia, G.; Gabriella, P.; Fabrizio, A. Perspective on the use of humic acids from biomass as natural surfactants for industrial applications. *Biotechnology Advances.* 2011, 29, 913–922.

104. Adani, F.; Tambone, F.; Davoli, E.; Scaglia, B. Surfactant properties and tetrachloroethene (PCE) solubilisation ability of humic acid-like substances extracted from maize plant and from organic wastes: a comparative study. *Chemosphere*. 2010,78, 1017.
105. Quadri, G.; Chen, X.; Jawitz, J. W.; Tambone, F.; Genevini, P.; Faoro, F. Biobased surfactant like molecules from organic wastes: the effect of waste composition and composting process on surfactant properties and on the ability to solubilize tetrachloroethene (PCE). *Environ Sci Technol*. 2008, 42, 2618.
106. Gadad P.; Lei, H.; Nanny, M. A. Influence of cations on noncovalent interactions between 6-propionyl-2-dimethylaminonaphthalene (PRODAN) and dissolved fulvic and humic acids. *Water Res*. 2007, 41, 4488.
107. Alvarez-Puebla, A. R.; Garrido, J. J.; Aroca, R. F. Surface-enhanced vibrational microspectroscopy of fulvic acid micelles. *Anal. Chem*. 2004,76, 7118–7125.
108. Zhao, J.; Nelson, D. J. Fluorescence study of the interaction of Suwannee River fulvic acid with metal ions and Al_3^+ -metal ion competition. *J. Inorg. Biochem*.2005,99, 383-396.
109. Alizadeh, N.; Ranjbar, B.; Mahmodian, M. Electrochemical study of the thermodynamics of interaction of lysozyme, with sodium dodecyl sulfate in binary ethanol – water mixtures. *J. Colloid Interf. Sci*. 2003, 212, 211.
110. Bai, G.; Wang, Y.; Yan, H. Thermodynamics of interaction between cationic gemini surfactants and hydrophobically modified polymers in aqueous solutions. *The Journal of Physical Chemistry B*. 2002, 06, 2153-2159.
111. Malliaris, A.; Le Moigne, J.; Sturm, J.; Zana, R. Temperature dependence of the micelle aggregation number and rate of intramicellar excimer formation in aqueous surfactant solutions. *J. Phys. Chem*. 1985, 89, 2709.
112. Brum, M.C.; Oliveira, J.F. Removal of humic acid from water by precipitate flotation using cationic surfactants. *Minerals Engineering*. 2007, 20, 945–949.
113. Furniss, B. S.; Hannaford. A. J.; Smith. P. W S.; Tatchell. A. R. Vogel's textbook of Practical organic chemistry, 5th ed.; Longman: New York, 1989; 158-160.
114. Skoog. D. A; West .D. Analytical Chemistry. 4th ed.: Saunders: Philadelphia, 1986; 484-486.

115. Kennedy, J. H. Analytical Chemistry Principles: Harcourt Brace Jovanovich: San Diego, 1984: pp 614-618.
116. Shain, S. A.; Prausnitz, J. M. Thermodynamics and interfacial tension of multicomponent liquid–liquid interfaces. *AIChE J.* 1964, 10 (5), 766–773.
117. Perry, R.H.; Green, D.W. Perry’s Chemical Engineers Handbook, seventh ed., McGraw-Hill, New York, 1997.
118. Nelson, T. M.; Jurs, P. C. Prediction of Aqueous Solubility of Organic Compounds. *J. Chem. Inf. Comput. Sci.* 1994, 34, 601-609.
119. Cramb, D. T.; Wallace, S. C. Structure and Biomembrane Mimetic Behavior of the Water–Octanol Interface. *J. Phys. Chem. B.* 1997, 101, 15.
120. Leo, A.J.; Hansch, C.; Elkins, D. Partition coefficients and their uses. *Chem. Rev.* 1971, 71, 525-621.
121. Doucette, W. J.; Andren, A. W. Estimation of octanol/water partition coefficients: evaluation of six methods for highly hydrophobic aromatic hydrocarbons. *Chemosphere* .1988, 17, 334-359.
122. Meylan, W. M.; Howard, P. H.; Boethling, R. S.. Improved Method for Estimating Water Solubility from Octanol/Water Partition Coefficient. *Environmental toxicology and chemistry.* 1996,15, 100-106.
123. Shuo, G.; Chenzhong, C. A new approach on estimation of solubility and n-octanol/water partition coefficient for organohalogen compounds. *Int J Mol Sci.* 2008, 9, 962–977.
124. Bodor, N.; Huang, M. J. A new method for the estimation of the aqueous solubility of organic compounds. *J. Pharm. Sci.* 1992;81, 954–960.
125. Karickhoff, S.W.; Brown, D.S. Determination of octanol/water distribution coefficients, water solubilities, and sediment/water partition coefficients for hydrophobic organic pollutants. U.S. EPA-600/4-79-032, 1979.
126. McCall, J. M. Liquid-liquid partition coefficients by high-pressure liquid chromatography. *J. Med. Chem.* 1975, 18, 549.
127. Lyman, W. J.; Reehl, W. F.; Rosenblatt, D. H. Handbook of chemical property estimation methods: environmental behavior of organic compound. American Chemical Society, Washington DC. 1990, 47-49.

128. Sangster, J. octanol- water partition coefficients of simple organic compounds. J. Phys. chem. ref. data, 18, 3, 1989.
129. Eljack, M.; Hussam, A.; Khan, U. S. Association of n-alkylbenzenes with fulvic acid in aqueous media. *Environmental Science & Technology*. (submitted in October, 2013).

BIOGRAPHY

Mahmoud Eljack graduated from Abdelmajid High School, Karkoug, Sudan, in 2001. He received his Bachelor of Science (first class honors) from University of Khartoum in 2006. He received his Master of Science in Chemistry from George Mason University in 2011.